

**Dynamics of subnuclear chromatin organization during
C. elegans development: a role for H3K9 methylation**

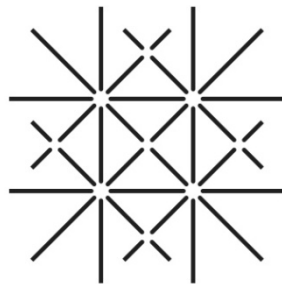
Inauguraldissertation

zur
Erlangung eines Doktors der Philosophie
vorgelegt der
philosophisch-Naturwissenschaftlichen Fakultät
der Universität Basel

von

Benjamin Daniel Towbin

aus
Basel, Basel-Stadt



**U N I
B A S E L**

Basel, 2012

Genehmigt von der Philosophisch-Naturwissenschaftlichen
Fakultät auf Antrag von

Prof. Dr. Susan M. Gasser
Prof. Dr. Peter Askjaer

Basel, den 21.2.2012

Prof. Dr. Martin Spiess
Dekan



Namensnennung-Keine kommerzielle Nutzung-Keine Bearbeitung 2.5 Schweiz

Sie dürfen:



das Werk vervielfältigen, verbreiten und öffentlich zugänglich machen

Zu den folgenden Bedingungen:



Namensnennung. Sie müssen den Namen des Autors/Rechteinhabers in der von ihm festgelegten Weise nennen (wodurch aber nicht der Eindruck entstehen darf, Sie oder die Nutzung des Werkes durch Sie würden entlohnt).



Keine kommerzielle Nutzung. Dieses Werk darf nicht für kommerzielle Zwecke verwendet werden.



Keine Bearbeitung. Dieses Werk darf nicht bearbeitet oder in anderer Weise verändert werden.

- Im Falle einer Verbreitung müssen Sie anderen die Lizenzbedingungen, unter welche dieses Werk fällt, mitteilen. Am Einfachsten ist es, einen Link auf diese Seite einzubinden.
- Jede der vorgenannten Bedingungen kann aufgehoben werden, sofern Sie die Einwilligung des Rechteinhabers dazu erhalten.
- Diese Lizenz lässt die Urheberpersönlichkeitsrechte unberührt.

Die gesetzlichen Schranken des Urheberrechts bleiben hiervon unberührt.

Die Commons Deed ist eine Zusammenfassung des Lizenzvertrags in allgemeinverständlicher Sprache: <http://creativecommons.org/licenses/by-nc-nd/2.5/ch/legalcode.de>

Haftungsausschluss:

Die Commons Deed ist kein Lizenzvertrag. Sie ist lediglich ein Referenztext, der den zugrundeliegenden Lizenzvertrag übersichtlich und in allgemeinverständlicher Sprache wiedergibt. Die Deed selbst entfaltet keine juristische Wirkung und erscheint im eigentlichen Lizenzvertrag nicht. Creative Commons ist keine Rechtsanwaltsgesellschaft und leistet keine Rechtsberatung. Die Weitergabe und Verlinkung des Commons Deeds führt zu keinem Mandatsverhältnis.

Contents

Chapter 1: Introduction.....	7
Chromatin as a regulated barrier to DNA associated processes	9
Large scale chromatin structure within the nucleus and gene regulation.....	14
Thesis overview	19
 Chapter 2: The nuclear envelope - a scaffold for silencing?.....	27
 Chapter 3: Repetitive transgenes in <i>C. elegans</i> accumulate heterochromatic marks and are sequestered at the nuclear envelope in a copy-number and lamin-dependent manner	37
 Chapter 4: Step-wise methylation of histone H3K9 positions chromosome arms at the nuclear envelope in <i>C. elegans</i> embryos	51
 Chapter 5: Concluding remarks and future prospects.....	81
 List of abbreviations	84
Acknowledgements	85
Curriculum Vitae	86

Chapter 1: Introduction

Heritable organismal traits are encoded in the DNA sequence. The information within DNA is transcribed into RNA and subsequently translated into proteins. These ultimately confer the structural, sensory, and regulatory functions of cellular metabolism. However, the DNA sequence (or genotype) is not sufficient to define the physical appearance (or phenotype) of an organism or cell. All cell types of a multicellular organism share identical DNA sequence, but differ substantially in their macroscopic characteristics. This heterogeneity is the basis for the formation of tissues with fundamentally different functions such as skin, muscle or bone from cells of identical genotype.

Cellular heterogeneity is not restricted to multicellular organisms, for the genome of unicellular organisms similarly does not encode for a single phenotypic state. Within isogenic bacterial populations, cell-to-cell variability is ubiquitous and can range from minor adaptations of the metabolic machinery to substantial remodeling of gross physical appearance, such as the switch from vegetative growth to spore formation (Veening et al., 2008).

Hence, an organism's DNA may be conceived as a description of all possible phenotypic states that are defined by the differential activity of distinct sets of genes rather than a deterministic floor plan. In principle, thousands of gene expression states are possible, but biological systems have evolved such that only a very small fraction of states ever occurs. Typically, a core set of genes conferring house-keeping functions is active in all cell types, but a subset of genes are specifically expressed in defined cell types. Cell-type specific expression patterns are tightly controlled, such that for example an epidermal cell never starts to express a neuron-specific gene. This apparently trivial characteristic is common to all forms of life. A core aspect for understanding cellular differentiation and tissue homeostasis is therefore to understand how defined gene expression states are acquired, and maintained over time and through cell division.

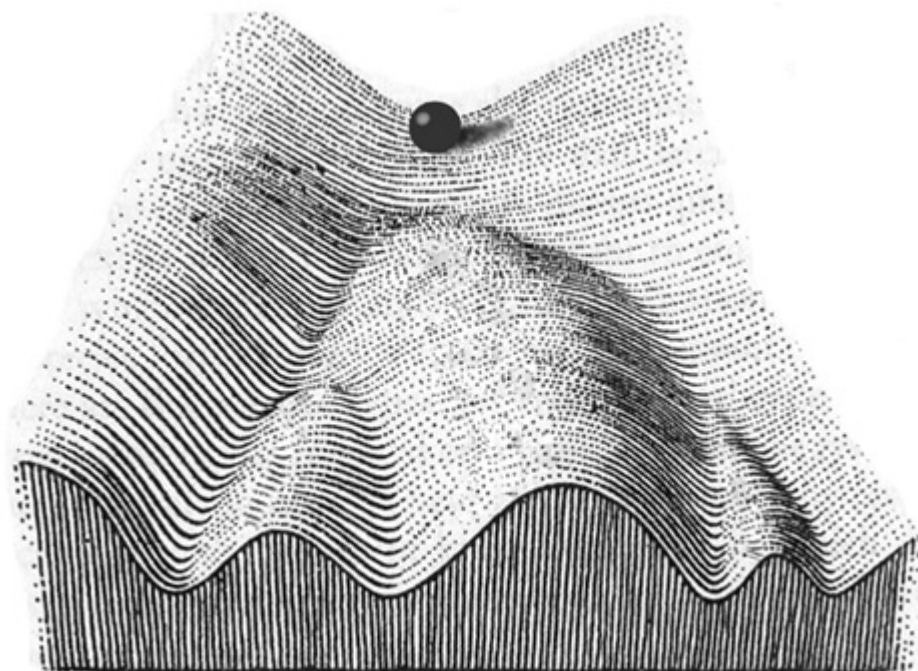


Figure 1. The epigenetics landscape. Waddington's famous drawing describes a probability landscape of cellular states. Transitions between cell states are unlikely to occur spontaneously, since these would imply a temporary existence of a state with low probability (reprinted from, Waddington, 1957).

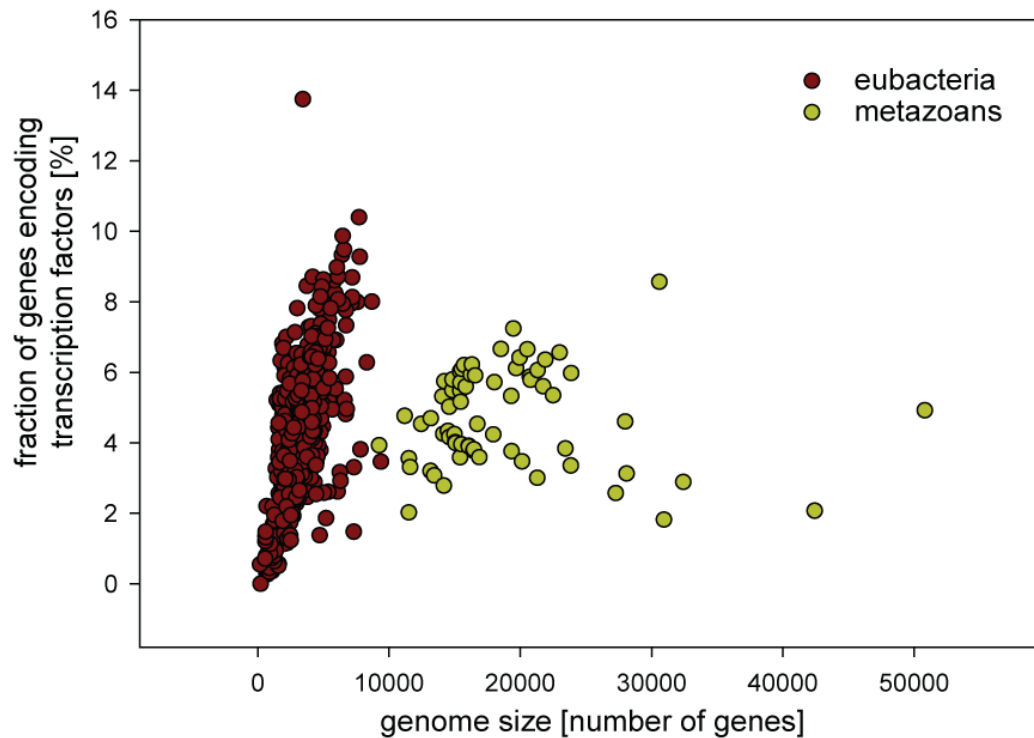


Figure 2. The fraction of transcription factors encoded by the genome increases with genome complexity in bacteria. The fraction of all genes encoding transcription factors (TFs) is plotted against the total gene number for 449 bacterial species (red) 68 metazoans (yellow). Relative TF content strongly increases with genomic complexity. Metazoan genomes do not follow this trend, although their genomes encode a much larger number of genes (data reanalyzed from Charoensawan et al., 2010)

In 1957, Conrad Waddington pioneered a simplistic, but illustrative, representation of this concept which he called the *epigenetic landscape* (Waddington, 1957). In a modern day interpretation of this graph, each theoretically possible cellular expression state is denoted as a point in a multidimensional landscape. Similar expression states are located next to each other, and the z-axis reflects the likelihood of a given state to occur. Depressions correspond to (semi-) stable gene expression states, whereas mountains describe expression states that occur only transiently or never at all. Natural cellular differentiation pathways are depicted as valleys connecting local depressions.

When Conrad Waddington coined the terminology and concept of the epigenetic landscape molecular insights on the regulation of genes were only about to emerge. Nevertheless, he predicted that the stable establishment of diverse cell types from a single fertilized oocyte must require a highly interconnected regulation of individual genes that includes regulatory feed-back mechanisms. This prediction has stood the test of time and has been validated in today's era of systems biology, which has shown that auto- and cross-regulation of genes is a ubiquitous feature of transcription factor networks (for review see Alon, 2007; Huang, 2009).

Apart from the initial establishment of defined cell types, a major question has been how cellular identity can be maintained throughout mitosis and cell division. Although classic transcription factor networks have the potential to transmit cell fate choices across cell division (Alon, 2007), regulation that is uniquely based on transcription factors becomes substantially more complex for larger genomes (Figure 2; Charoensawan et al., 2010; van Nimwegen, 2003). This augmented regulatory cost may be a reason why additional means to control gene expression have evolved in eukaryotes, where essentially every step involved in the production of functional proteins is tightly regulated.

The characterization of covalent modifications on histones and DNA as a mode of gene regulation has created a wave of excitement over the past 20 years and has led to the proposal that they act as a

regulatory code that carries heritable information on gene expression states (Jenuwein and Allis, 2001; Strahl and Allis, 2000). However, despite enormous research efforts that provide increasingly detailed insights into the regulation of chromatin modifications, the existence of such a heritable histone code remains controversial (Henikoff and Shilatifard, 2011).

The specific aim of this thesis was to investigate how post-translational histone modifications control the three dimensional architecture of chromatin within the nucleus and how subnuclear chromatin architecture contributes to tissue-specific gene regulation. The following section reviews aspects of chromatin biology that are most relevant for the experimental work presented in this thesis. A focus is therefore placed on the regulatory functions of histone methylation and acetylation, whereas the implications of DNA methylation and other chromatin modifications are not reviewed in detail. The second half of this introduction discusses the role of histone modifications in shaping the large scale organization of chromatin in the nucleus.

Chromatin as a regulated barrier to DNA associated processes

Virtually all DNA in the eukaryotic nucleus is wrapped around an octameric complex consisting of the four histone proteins H2A, H2B, H3 and H4, which form the core nucleosome. Each nucleosome is enwrapped by 147bp of DNA and individual nucleosomes are spaced by 20-50bp of linker DNA. In higher eukaryotes, this linker can be bound by H1, a fifth histone protein. Hence, DNA-based reactions, such as replication, repair and transcription must entail the recognition of DNA sequence within the context of a nucleosome or require the temporary displacement of histones from DNA. The packaging of DNA into chromatin therefore imposes a potential barrier to genetic processes, while at the same time offering the means for tight control.

As early as in the 1960s it has been suggested that posttranslational modification (PTM) of histone proteins by acetylation and methylation (Allfrey et al., 1964; Murray, 1964) may “*affect the capacity of the histones to inhibit ribonucleic acid synthesis in vivo*” (Allfrey et al., 1964). Since then, numerous covalent posttranslational histone modifications have been identified, culminating in a recent study describing 130 different PTMs, including acetylation, methylation, phosphorylation, ubiquitylation, sumoylation, propionylation, ADP ribosylation, butyrylation, formylation, citrullination and crotonylation (Tan et al., 2011).

Differential chromatin modification of active and inactive genes

Histone lysine acetylation and methylation are among the best studied histone PTMs and their presence on chromatin is tightly linked to transcriptional activity. Histone acetylation is generally associated with transcribed genes (Wang et al., 2008). In contrast, histone lysine methylation is correlated with both transcriptionally active and silent chromatin, depending on which lysine residue is methylated (Bannister and Kouzarides, 2011). Adding to this complexity, lysines can occur in a mono-, di-, or tri-methylated state.

Chromatin immunoprecipitation has been a powerful tool to associate specific histone marks with distinct genome functions (Orlando and Paro, 1993; Solomon et al., 1988). In brief, chromatin is cross-linked by formaldehyde and the DNA is fragmented mechanically or enzymatically into stretches of one or several nucleosomes. This is followed by immunoprecipitation of chromatin fragments using antibodies directed against specific histone marks, histone variants or non-histone chromatin proteins and quantification of the precipitated DNA. First applied in 1988 (Solomon et al., 1988), this method has been continuously improved and adapted. An important technological step was the quantification of precipitated DNA by DNA microarrays (ChIP-chip, Ren et al., 2000) or deep-sequencing (ChIP-seq, Robertson et al., 2007), which has allowed the characterization of histone modification states along the complete genome at the resolution of individual nucleosomes (Barski et al., 2007). The mapping of histone marks on the genome has revealed a remarkable association of specific modifications with distinct genome functions. For example, H3K4me3 occurs predominantly at active gene promoters or on promoters with poised RNA polymerase (Guenther et al., 2007; Mikkelsen et al., 2007; Zhou et al.,

2011). Similarly, H3K36me3 is associated with gene activity, but is found throughout the transcribed region (Barski et al., 2007; Bell et al., 2007; Mikkelsen et al., 2007). In contrast to H3K4me3 and H3K36me3, methylation on H3K9, H3K27 and H4K20 occurs predominantly on silent chromatin (Zhou et al., 2011). H3K27me3 is enriched on promoters of inactive tissue- or stage specific genes that are silenced by the Polycomb pathway (Mohn et al., 2008; Sawarkar and Paro, 2010), whereas H3K9me3 and H4K20me3 have been mapped to silent repetitive DNA, such as transposons, telomeric repeats and satellite sequences (Mikkelsen et al., 2007). Similarly, non repetitive genes occupied by H3K9me3 tend to be transcriptionally inactive (Mikkelsen et al., 2007), although some highly transcribed genes have been reported to carry this mark as well (Kim et al., 2007; Vakoc et al., 2005b; van Steensel, 2011).

Direct modulation of chromatin structure by histone acetylation

The correlation of specific histone modifications with gene expression states strongly suggests a function in gene regulation, and a role for post-translational histone modifications in transcription is supported by ample evidence (Henikoff and Shilatifard, 2011). However, the molecular mechanism of chromatin mediated gene regulation has remained largely unclear. Two distinct models have been proposed, both of which are likely to play an important role. First, histone modifications can directly alter the molecular contacts between neighboring nucleosomes or between histones and the DNA. Second, PTMs regulate interactions between histones and other proteins, which are thereby recruited to chromatin.

Histone acetylation has long been predicted to directly affect chromatin structure, given that this modification neutralizes the positive charge of lysine residues (van Holde, 1989). Perhaps the best evidence for this effect exists for H4K16 acetylation, which was shown to inhibit the formation of higher order chromatin structures *in vitro* (Shogren-Knaak et al., 2006). Acetylation of H3K56 has also been shown to alter the physical properties of chromatin. In contrast to H4K16, which lies on the flexible N terminal tail of histone H4, H3K56 is positioned on the globular domain of H3 and lies on the core of the nucleosome. Specifically, H3K56 is located exactly at the entry/exit point of DNA (Luger et al., 1997), making its acetylation likely to modulate nucleosome-DNA interaction. Using nucleosomes homogenously acetylated at H3K56, the laboratory of Jason Chin showed that, in contrast to H4K16ac, H3K56ac does not affect the formation of higher order nucleosome assembly. However, as may be expected from its location, H3K56ac affected the local interaction of DNA with the nucleosome, leading to an enhancement of transient unwrapping of the DNA (nucleosome breathing, Neumann et al., 2009). So far, acetylation of H4K16 and H3K56 are the only two residues that have been studied in isolation, but it is likely that most acetylation on histones will alter their structure, and that multiple acetylation events have cumulative effects.

Recruitment of chromatin modifying enzymes by histone PTMs

In addition to direct modulation of chromatin structure, methylation and acetylation, are thought to act via the recruitment of non-histone proteins to chromatin. Indeed, numerous factors interacting with histones in a modification dependent manner have been identified (Suganuma and Workman, 2011) and proteomic approaches indicate that hundreds of proteins dynamically associate with chromatin (Bartke et al., 2010; Ohta et al., 2010; Vermeulen et al., 2010). Histone binding proteins tend to have a modular architecture and several protein domain classes have been characterized to recognize specific histone modification marks. Bromo domain proteins recognize histone lysine acetylation (Dhalluin et al., 1999), whereas methylated histone lysines are bound by various folds, including Chromo-, MBT-, Tudor- and PHD domains (Bannister et al., 2001; Kim et al., 2006; Lachner et al., 2001; Yun et al., 2011).

Domains recognizing modified histones frequently occur in enzymes that catalyze the deposition or removal of chromatin marks (i.e. histone (de)methylases or histone (de)acetylases). Enzymes that bind directly, or through an interacting protein, to the same modification that they deposit have the potential to confer spreading of a chromatin mark in *cis*, or reinstall the mark after cell division on newly

incorporated unmodified histones (Figure 3A & 3B). Evidence for such a mechanism exists for the propagation of H3K9me3 at centromeres in mouse and fission yeast (Bannister et al., 2001; Lachner et al., 2001; Nakayama et al., 2001), and for the inheritance of the H3K27me3 mark at Polycomb-repressed loci (Hansen et al., 2008). Experiments described in Chapter 4 of this thesis suggest the existence of a similar mechanism for the maintenance of H3K9 methylation at perinuclear chromatin in *C. elegans*.

Chromatin modifying enzymes that are recruited by a histone mark that differ from their reaction product can mediate cross-talk between histone modifications. For example, the *C. elegans* protein

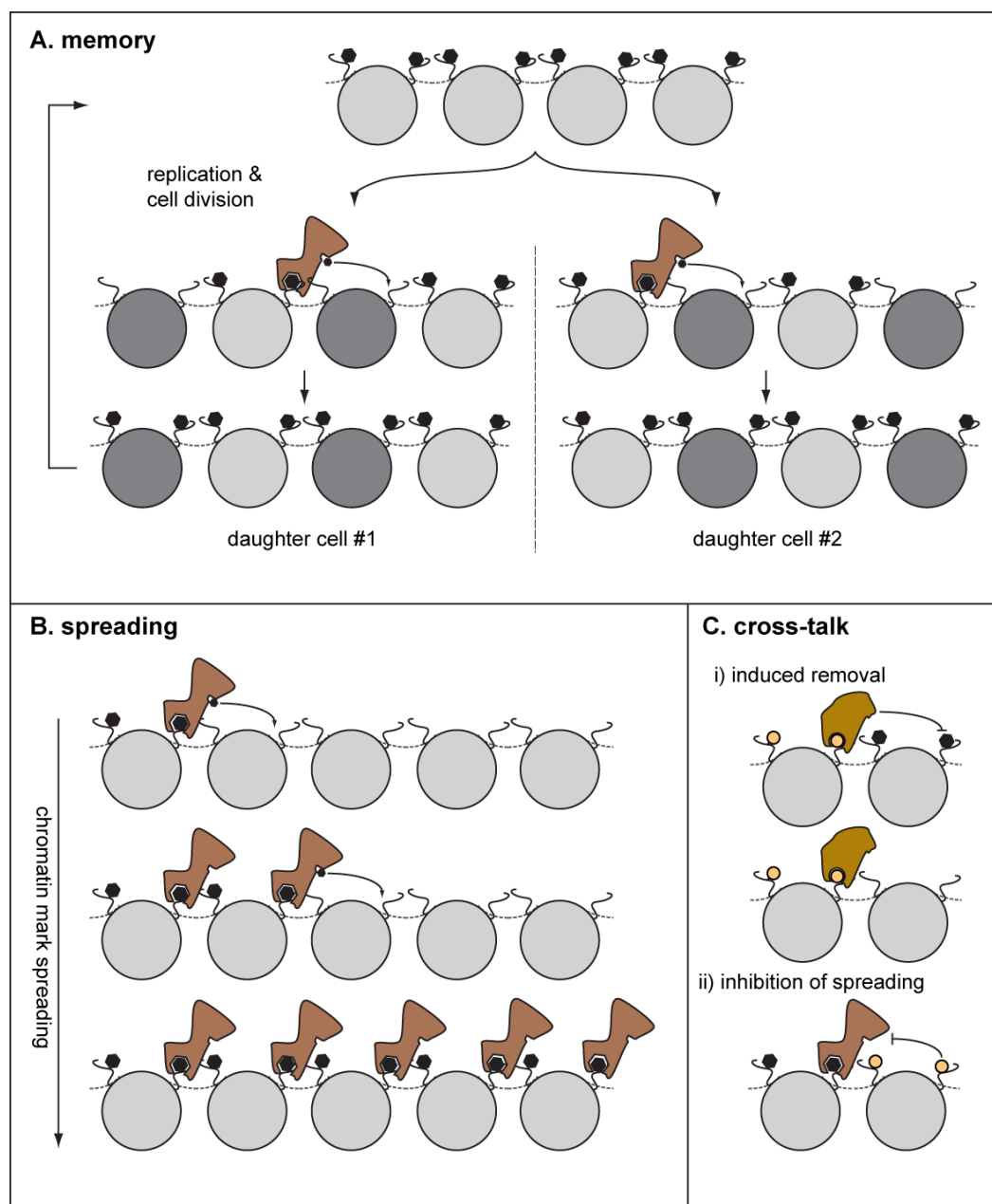


Figure 3. Inheritance, spreading, and cross-talk of histone modifications. The occurrence of histone mark binding domains in chromatin modifying enzymes implies several modes histone modification cross-talk. (A) Enzymes recruited by the same mark as they deposit can ensure the propagation of a methylation state to unmodified nucleosomes incorporated during replication (dark grey). A similar mechanism may act to propagate a modification in *cis* along the chromosome (B). The best studied mammalian examples include the recruitment of the H3K9 histone methyltransferase (HMT) Suv39h to chromatin via interaction with HP1 (Bannister et al., 2001; Lachner et al., 2001) and the inheritable propagation of H3K27me3 by Ezh2, which gets recruited via the H3K27me3 binding protein EED (Hansen et al., 2008). (C) The modular architecture of HMTs also mediates cross-talk between distinct histone modifications as explained in the main text.

ceKDM7A contains a PHD domain that binds specifically to H3K4me3, whereas its JmjC domain demethylates H3K9me1, H3K9me2, and H3K27me2 (Lin et al., 2010). Conversely, the presence of a histone mark can prevent the deposition of another one, as is the case for the inhibition of the Polycomb Repressive Complex 2 (PRC2) by H3K4me3 (Schmitges et al., 2011). In this function, these enzymes may sharpen the boundaries between active and silent chromatin domains, or prevent an ambiguous modification status (Figure 3C).

Combinatorial functions of histone modifications

An early hypothesis that emerged with the discovery of the complexity of post-translational histone modification was that histone marks act as a combinatorial code that complements the genetic code of the DNA (Jenuwein and Allis, 2001; Strahl and Allis, 2000). This concept predicted that histone modifications would be recognized by a set of proteins that trigger downstream events controlling DNA associated processes. Additionally, the histone-code hypothesis proposed that histone modifications are interpreted in a combinatorial manner, such that a histone concurrently carrying two modifications would invoke a different response than the sum of the consequences of either mark alone.

The combinatorial analysis of many histone modification maps generated for several different cell types has recently been used to seek evidence for such a histone code (Ernst and Kellis, 2010; Ernst et al., 2011; Wang et al., 2008). To this end, computational algorithms were applied that classify chromatin domains into distinct states based on their combinatorial histone modification profiles without human supervision. In all studies, distinct chromatin states corresponding to defined functional categories have been extracted that would not be obvious from the profiles of individual marks. Maybe the best example for a combinatorial presence of different histone marks is the co-occurrence of H3K4me3 and H3K27me3 at inactive promoters with poised polymerase, which is particularly prevalent in embryonic stem cells (Bernstein et al., 2006; Ernst et al., 2011). Similarly, enhancers and promoters share largely similar modification profiles, but are distinguished by the relative abundance of H3K4me1 and H3K4me3 (Ernst et al., 2011; Heintzman et al., 2007). These experiments do not prove the existence of a histone code, but they at least show that the combined analysis of histone modifications can be used to identify distinct functional elements of the genome. For now, it remains unclear if multiple histone modifications truly reside on the same nucleosome or if the concurrent enrichment of two modifications at one genomic site reflects the occurrence of two populations of nucleosomes with each of them carrying a single mark. Similarly, only few examples of proteins have been reported that recognize specific combinations of histone marks (Moriniere et al., 2009; Ruthenburg et al., 2011; Wang and Patel, 2011) and thereby could elicit a cellular response caused by the co-occurrence of two modifications. It will be crucial to further characterize this type of behavior to evaluate the existence of a histone code that is interpreted by the cell.

Gene regulation by histone modification induced recruitment of factors to chromatin

How can histone modification control gene expression by the recruitment of non-histone factors? For histone marks associated with transcribed genes, at least two modes of action have been proposed. H3K4me3 has been shown to directly interact with the basal transcription factor TFIID via the PHD domain of its subunit TAF3 (Vermeulen et al., 2007). In this scenario, H3K4me3 could enhance the recruitment of RNA polymerase II by direct interaction with the basal transcription machinery. Alternatively, acetylated histones, as well as H3K4me3 have been shown to recruit chromatin remodelers (Erdel et al., 2011; Hassan et al., 2002; Ruthenburg et al., 2011). These large multi-subunit complexes have the potential to control transcription at the initiation, as well as the elongation step by catalyzing the removal, sliding or replacement of nucleosomes (reviewed in Flaus and Owen-Hughes, 2011). In this context, it is important to note that enzymes depositing H3K4me3 and H3K36me3, as well as histone acetylation, are recruited to chromatin via molecular interaction with RNA Polymerase II (reviewed in Sims et al., 2004). Consequently, the modification of histones at active genes is an intrinsic part of transcription and often occurs downstream of transcriptional activation. Nevertheless,

these modifications likely conduct important functions in gene regulation by the recruitment of factors to chromatin. For example, the deposition of H3K4me3 may facilitate repeated transcriptional initiation, whereas H3K36me3 has been proposed to prevent cryptic initiation events in the gene body (Carrozza et al., 2005; Keogh et al., 2005).

To assay how histone modifications negatively influence transcription *in vivo* has remained technically challenging. A classic model is that chromatin occurs in an “open” state that is accessible for DNA binding proteins such as transcription factors and in a “closed” state that is refractory to soluble proteins, thereby preventing transcription. This view was initially inspired by cytological preparations of chromatin within the nucleus visualized by light or electron microscopy (Heitz, 1928). Based on DNA staining patterns, the nucleus was divided into two compartments: A dense staining compartment, termed heterochromatin is enriched at the nuclear periphery and around the nucleolus, whereas a lighter staining compartment termed euchromatin covers the rest of the nucleus. The dense staining of heterochromatin is generally interpreted to reflect a higher compaction of DNA, and this dense staining region is enriched for histone modifications characteristic for silent chromatin (H3K9me3 and H4K20me3).

At the molecular level, DNA accessibility has been probed by the efficiency of enzymes to process DNA within the context of native chromatin structure. For this purpose, chromatin is either exposed to DNase I (Weintraub and Groudine, 1976), or to DNA methylating enzymes (Bell et al., 2010; Gottschling, 1992) and inaccessible chromatin is identified as regions that are protected from DNase digestion or methylation. The main determinant for successful DNase I cleavage is the presence or absence of nucleosomes. DNase hypersensitivity assays have therefore been a powerful tool to identify genomic regions that lack nucleosomes or where nucleosomes are partially unfolded. These regions occur predominantly at regulatory regions and transcriptional start sites and, to a lesser extent, in the transcribed region of active genes (Boyle et al., 2008). However, it is difficult to determine whether nucleosome depletion is a consequence of transcriptional activity, or if opening of chromatin structure occurs upstream of transcription factor binding (Henikoff and Shilatifard, 2011). Protection from DNase I digestion in inactive chromatin regions in dependence of histone modifications on the other hand has not been very informative, maybe due to the low dynamic range of this method in nucleosome occupied regions (Bell et al., 2011).

The alternative strategy of using the efficacy of DNA methylating enzymes on chromatin was first applied by Daniel Gottschling in 1992 (Gottschling, 1992). By expression of the *E. coli* DNA methyltransferase *dam* in yeast he found that a reporter gene was methylated less efficiently when placed in a silenced subtelomeric region than at a euchromatic site. More recently, Bell and co-workers similarly used a bacterial CpG methylase, to probe chromatin accessibility genome-wide in cultured *Drosophila* cells (Bell et al., 2010). In this study, genes carrying the Polycomb repressive mark H3K27me3 were methylated slightly less efficiently than H3K27me3 free, but nevertheless inactive control genes. However, no difference in accessibility was apparent for H3K9me2 domains. It is unclear whether the apparent independence of DNA accessibility on H3K9me2 is of technical nature, or if H3K9me2 does indeed not confer a closed chromatin state. This would be in contrast to classic models, which implied that H3K9me2 inhibits transcription by the recruitment of auxiliary factors such as HP1 that condense chromatin and thereby reduce its accessibility (Bannister et al., 2001; Lachner et al., 2001).

The overall value of DNA accessibility to explain chromatin mediated repression has been questioned, given that protection from methylation or cleavage in heterochromatin is rarely more than two-fold better than in euchromatin (Chen and Widom, 2005; Filion et al., 2010; Sha et al., 2010; van Steensel, 2011). However, small effects on DNA accessibility could have a cumulative effect, given that for a productive transcription many factors need to be recruited. Moreover, accessibility of DNA modifying enzymes to chromatin may underestimate the sequestration from larger complexes, such as the RNA polymerase holocomplex. Nevertheless, the exact mechanism of how post-translational histone

modifications contribute to gene silencing remains an open question. One important step towards a better understanding will be the identification and *in vivo* characterization of proteins recruited to specific histone marks. Recent efforts to map chromatin associated non-histone proteins indicate that the bimodal classification into eu- and heterochromatin is too simplistic, and that several distinct chromatin based silencing mechanisms are likely to exist (Filion et al., 2010; Ram et al., 2011). A provocative model emerging from these studies is that combinations of chromatin proteins may directly recruit defined subsets of TFs by specific molecular interactions, rather than by a general mechanism of modulating chromatin structure and accessibility (Filion et al., 2010; van Steensel, 2011).

Large scale chromatin structure within the nucleus and gene regulation

Increasing evidence suggests that models depicting chromatin as a linear template for transcription do not capture all of its regulatory potential, but that higher order folding of chromatin also has important functions. Molecular characterization of chromatin structure beyond the scale of the nucleosome is poor, but at a macroscopic level chromatin structure has been intensively studied and yielded strong evidence for a non-random organization of chromatin within the nucleus (reviewed in Rajapakse and Groudine, 2011).

A predominant theme is the spatial segregation of chromatin within the nucleus into domains with high transcriptional activity in the nuclear center, and silent domains associated with the nuclear periphery or the nucleolus. This model is supported by several fundamentally distinct experimental approaches that range from chromosome conformation capture methods to DamID and ChIP, as well as microscopy. The following section summarizes this evidence and compares insights gained from the different techniques.

Chromosome territory formation

One of the most apparent organizational features of the mammalian nucleus is the spatial separation of individual chromosomes, which leads to the formation of chromosome territories (CTs). This was first demonstrated by Thomas Cremer and colleagues in 1988 by the use of fluorescence *in situ* hybridization (FISH) probes targeting an entire chromosome (Cremer et al., 1988; Lichter et al., 1988). Several studies reported on defined patterns of CT organization relative to each other and with respect to the nuclear periphery (Bridger et al., 2000; Cremer et al., 2001; Sun et al., 2000), culminating in the concurrent visualization of all chromosomes in human fibroblasts using a combinatorial chromosome labeling scheme (Bolzer et al., 2005). A conclusion common to most of these studies is that gene poor and large chromosomes tend to locate close to the nuclear envelope.

Reproducible subnuclear localization was also found for the position of individual genes with respect to the bulk of their chromosome. A well studied example concerns the position of the Hox B cluster (*Hoxb*) relative to its CT in mouse cells. In embryonic stem cells, where all *Hoxb* genes are inactive, the locus is condensed and preferentially positioned inside its chromosome territory. However, during differentiation, when the *Hoxb* genes are consecutively activated, the cluster decondenses and the active *Hoxb* genes loop out of their territory (Chambeyron and Bickmore, 2004; Chambeyron et al., 2005; Morey et al., 2007). Originally described by FISH, these results were recently confirmed by high-resolution chromosome conformation capture (see below, Noordermeer et al., 2011b). Using this approach, a strong correlation was observed between the temporal change in structural organization of the Hox B cluster and the expression of individual *Hoxb* genes, as well as with the transition from a H3K27me3 to H3K4me3 modification state. These studies propose chromatin compaction and loop formation as a mode of developmental gene regulation. An important question will be if the change in local chromatin architecture contributes to *Hox* gene regulation, or whether it is merely a consequence of transcriptional activation.

Enhancer-promoter looping: regulation of gene expression through higher order chromatin architecture

A potential mechanism describing how gene movement or chromatin unfolding could influence transcription is by facilitating or inhibiting the interaction of gene promoters with distal regulatory elements (enhancers). In 2002, Job Dekker and colleagues developed chromosome conformation capture (3C) as a powerful method to detect such DNA-DNA contacts *in vivo* (Dekker et al., 2002). In a 3C experiment, chromatin is chemically cross-linked by formaldehyde in its native three dimensional conformation. Thereby, two genomic sites that are in spatial proximity can be covalently connected even when they are far away from each other *in cis*. Restriction digest followed by re-ligation is then used to generate linear DNA fragments from cross-linked interacting segments, which can subsequently be quantified by PCR using a primer pair specific for each of the ligated DNA elements.

3C has been extensively used to characterize enhancer-promoter looping at several complex mammalian loci, including the α - and β -globin loci (Palstra et al., 2003; Tolhuis et al., 2002; Vernimmen et al., 2007), the H19-Igf2 locus (Murrell et al., 2004), and the interleukin T_H2 locus (Spilianakis et al., 2005). These initial studies demonstrated that local DNA-DNA contacts are tissue-specifically controlled and that transcription factor binding is important for their establishment (Drissen et al., 2004; Splinter et al., 2006; Vakoc et al., 2005a). More recent data suggests that downstream of transcription factors, DNA looping is at least in part mediated by the cohesin complex (Hadjur et al., 2009; Nativio et al., 2009; Seitan et al., 2011). Cohesin has long been characterized to connect sister chromatids after replication by forming ring structures around the two replicated strands (reviewed in Peters et al., 2008). However, via the interaction with the sequence specific DNA binding protein CTCF (for CCCTC-binding factor), cohesin is also recruited to specific sites during G1 phase (Parelho et al., 2008; Rubio et al., 2008; Wendt et al., 2008), when no sister strand cohesion is required. CTCF has been described to mediate insulation of promoters from distal enhancer elements already in the 1990s (Bell et al., 1999) and is long known to control gene expression (reviewed in Phillips and Corces, 2009). These experiments suggest that CTCF regulates gene expression by initiating DNA loop formation via cohesin recruitment. In support of this model, inactivation of cohesin in post-mitotic cells demonstrated a replication independent function of the complex for gene expression and neuronal development in flies (Pauli et al., 2008; Pauli et al., 2010; Schuldiner et al., 2008) and T-cell receptor recombination in mice (Seitan et al., 2011). Whether these developmental defects are due to impaired DNA looping, or reflect other regulatory functions of cohesin remains to be determined.

Characterization of large scale chromosome architecture by genome-wide chromosome conformation capture

After the initial development of 3C in 2002, this technology has been continuously adapted to allow for a more open search for DNA-DNA contacts (reviewed in de Wit and de Laat, 2012). The nomenclature of these methods has been equally creative as confusing and is summarized here for reasons of clarity: In 4C, the interaction between a single site (called the anchor or view point) and the rest of the genome is measured using microarrays or deep sequencing (one against all, Simonis et al., 2006). 5C is an adapted version of 3C where many putative interaction pairs are examined at once using a large (but nevertheless restricted) set of primer pairs (many against many, Dostie et al., 2006). By exploiting deep-sequencing technology, the Hi-C method can theoretically measure interactions of all genomic loci with each other (all against all, Lieberman-Aiden et al., 2009), but with current sequencing technology, its use has been limited to a maximal resolution of 1Mb for mammalian genomes. Finally, ChIA-PET combines chromatin immunoprecipitation (ChIP) with Hi-C and is aimed at identifying DNA-DNA contacts that occur in the presence of a specific protein of interest (Fullwood et al., 2009).

In principle, genome-wide adaptations of 3C (such as 4C and Hi-C) can be used to identify specific DNA-DNA contacts without prior knowledge. However, in reality, due to the lack of resolution and a low signal-to-noise ratio most of the observed chromatin cross-linking events do not reflect stable interactions. Instead, a high 4C or Hi-C signal is more often explained by an increased frequency of

random collisions of two loci that is caused by other constraints. Nevertheless, chromosome conformation capture techniques have proven a powerful tool to study large scale chromosome folding, as outlined below.

Evidence for active and silent subnuclear compartments from 4C and Hi-C experiments

Given the arrangement of the genome in chromosome territories, two genomic loci on the same chromosome are expected to be more often in close proximity than two loci on distinct chromosomes. It is therefore not surprising that interactions detected by 4C predominantly occur within one chromosome (Simonis et al., 2006; Zhao et al., 2006). Interestingly, however, interaction frequencies along the chromosome cannot simply be explained by proximity in *cis*, but instead appear to be regulated in a tissue specific manner. 4C interactions of the β -globin locus for example, differ strongly when assayed in liver and in brain. In liver cells, where β -globin is highly transcribed, it preferentially interacts with other active genes, whereas it mostly contacts inactive loci in brain cells (Simonis et al., 2006). One interpretation of these results is that chromatin is segregated into spatial subnuclear compartments and that tissue specific genes occupy distinct regions in different cell types, in a manner that is correlated with gene activity.

This proposal was assessed more generally by measuring contact frequencies among all loci using Hi-C in human lymphoblasts. Again, CTs were an obvious feature of the contact maps, as interacting loci were mostly located on the same chromosome (Lieberman-Aiden et al., 2009). Two independent studies have applied distinct algorithms to analyze Hi-C data at a finer scale than CT formation (Lieberman-Aiden et al., 2009; Yaffe and Tanay, 2011). In agreement with 4C data (Simonis et al., 2006; Zhao et al., 2006), both approaches describe a classification of the genome into active and silent compartments within which interactions occur more frequently than across compartments. However, the exact identity of these compartments remains somewhat controversial. Whereas Lieberman-Aiden et al. propose the existence of two large subnuclear compartments (active and silent), Yaffe and Tanay suggest a further separation of the silent compartment into a centromere proximal and a centromere distal domain. Higher resolution contact maps and optimized normalization schemes will be required to fully characterize the subnuclear chromatin interaction space. Nevertheless, already at the resolution currently available, Hi-C studies corroborate the evidence for functional nuclear subcompartments.

Microscopic visualization of subnuclear compartments

Perhaps the most direct evidence for subnuclear compartments stems from fluorescence and electron microscopy (reviewed in Lanctot et al., 2007; Taddei et al., 2004). For example, the clustering of silent chromatin in DNA dense staining foci at the nuclear envelope and around the nucleolus is an obvious feature of nearly all cell types. More specifically, using FISH and live imaging, numerous loci have been reported to be associated with these peripheral or perinucleolar heterochromatic compartments when silent, and relocate away from them upon activation (Brown et al., 1997; Dernburg et al., 1996; Francastel et al., 2001; Grogan et al., 2001; Hewitt et al., 2004; Kosak et al., 2002; Meister et al., 2010; Williams et al., 2006). Similarly, many transcribed genes are non-randomly positioned in the nucleus and co-regulated loci are often spatially clustered in assemblies of multiple active RNA Polymerases (Osborne et al., 2004; Schoenfelder et al., 2010). Importantly, although correlated with transcription, the movement of genes away from heterochromatic compartments is unlikely to be a necessary consequence of transcriptional activation, since promoters of housekeeping genes can be highly active, but remain localized at the nuclear periphery (Meister et al., 2010; Chapter 4).

The nuclear lamina: a scaffold for silent chromatin

The visualization of genetic loci in living cells has shown that chromatin is undergoing constant Brownian-like motion in the nucleus (Heun et al., 2001; Marshall et al., 1997). Interestingly, silent genes that are associated with the nuclear periphery are much more constrained in their movement than active genes in the nuclear center (Chubb et al., 2002; Heun et al., 2001). This indicates that perinuclear genes are molecularly tethered to a relatively immobile nuclear landmark. Two structures have been

proposed to serve as such nuclear a scaffold. The nuclear lamina, which directly underlies the nuclear membrane is thought to interact with silent chromatin (reviewed in Dechat et al., 2010). In contrast, the nuclear pore complex (NPC) has been reported to serve as a binding platform for active genes, in addition to its well described role in nuclear transport (reviewed in Liang and Hetzer, 2011). Since the experimental scope of this thesis concerns the spatial organization of silent chromatin, this introduction focuses on the nuclear lamina, whereas scaffold functions of the NPC are not discussed in detail.

The central components of the nuclear lamina are the lamin proteins, which form a meshwork of intermediate filaments along the nuclear periphery (Aebi et al., 1986). Additionally, an increasing number of proteins is reported to directly or indirectly contact lamins and form a complex network of interacting proteins at the nuclear envelope (Figure 4; reviewed in Prokocimer et al., 2009). Interestingly, several nuclear envelope proteins can directly bind to chromatin. For example the chromatin binding protein BAF binds to the lamin associated transmembrane proteins Emerin, MAN1 and LAP2b (reviewed in Margalit et al., 2007) and lamin B receptor (LBR) interacts with the H3K9me2/3 binder HP1 (Ye and Worman, 1996). Lamins have also been shown to directly interact with histones (Goldberg et al., 1999) and DNA (Luderus et al., 1992) *in vitro*, but it is unclear if these direct interactions also occur *in vivo*. Importantly, a function of lamins as scaffold for perinuclear chromatin is also supported by genetic data since peripheral loci relocate to the nuclear center upon lamin depletion (Mattout et al., 2011; Shevelyov et al., 2009; Towbin et al., 2011).

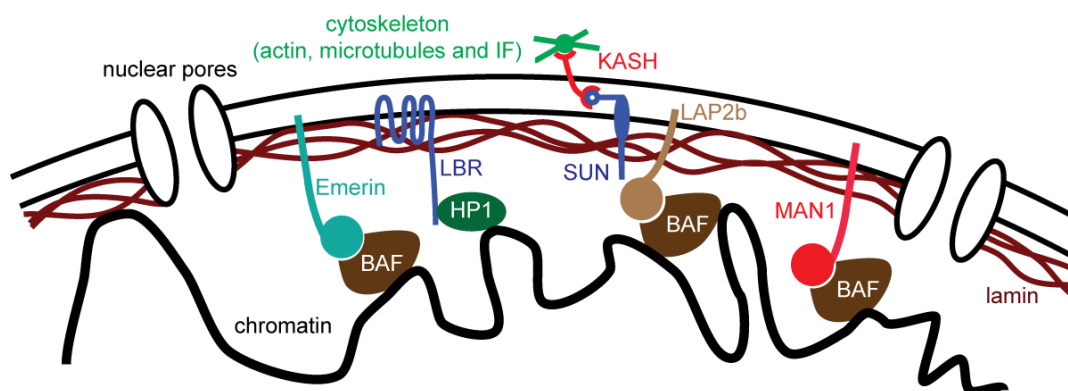


Figure 4. Schematic view of the nuclear envelope (not comprehensive). Lamins form a meshwork of intermediate filament proteins underlying the nuclear envelope. They interact with several distinct classes of transmembrane proteins. i) Nuclear envelope associated LEM domain proteins (Emerin, LAP2b and MAN1) interact via their LEM domain with the small protein BAF, which has affinity for chromatin. ii) Lamin B receptor (LBR) contains seven transmembrane domains that span the inner nuclear membrane (INM). It interacts directly with the chromatin binding protein HP1. iii) SUN domain proteins span the INM. They interact with lamins at the nucleoplasmic side and with KASH domain proteins in the perinuclear space. KASH domain proteins (called Nesprins in human) pass the outer nuclear membrane where they contact the cytoskeleton. Different types of Nesprins exist, for which interactions with actin, microtubules, as well as the intermediate filament (IF) cytoskeleton have been reported (adapted from Prokocimer et al., 2009; Towbin et al., 2009).

Further evidence for a role of lamins in perinuclear gene targeting stems from DamID and ChIP experiments (Guelen et al., 2008; Handoko et al., 2011; Ikegami et al., 2010; Peric-Hupkes et al., 2010; Pickersgill et al., 2006). In a pioneering study, Pickersgill et al. reported the specific lamin interaction of 500 genes in *Drosophila* Kc cells. As expected, lamin association correlated with low expression, and with the absence of H3K4me3 and H4K16ac chromatin marks. Moreover, lamin interaction was shown to be dynamic since distinct changes in lamin binding were observed upon induction of differentiation by ecdysone treatment: Loss of lamin interaction correlated with gene activation, whereas repression was accompanied by gain in lamin binding (Pickersgill et al., 2006). Subsequent studies in mouse and human cells showed that the characteristics of lamin bound loci are conserved in mammals (Guelen et al., 2008; Peric-Hupkes et al., 2010) and consistent results have also been obtained from studies in *C. elegans* (Ikegami et al., 2010). Additionally, the higher mapping resolution of these studies revealed that lamin bound regions form large clusters in *cis* that often span multiple genes and

can be up to 10 Mb in size. An interesting feature of these mammalian lamin associated domains (LADs) is that their boundaries are correlated with the occurrence of CTCF binding (Guelen et al., 2008).

The influence of lamin attachment on large scale chromatin folding and the regulation of DNA-DNA contacts

The correlation of LAD boundaries and CTCF binding sites was revisited by a study that mapped CTCF associated chromatin loops genome-wide using ChIA-PET. CTCF mediated loops were seen strongly enriched at the border of LADs, whereas regions inside LADs were generally depleted from CTCF loops (Handoko et al., 2011). This suggests an intimate link between the anchoring of chromatin to the nuclear lamina, and the establishment of specific DNA contacts. Acting as an insulator protein, CTCF may control the spreading of lamin attachment in *cis*. On the other hand, lamin attachment and the resulting segregation of chromatin into subnuclear compartments may influence the formation of DNA loops by CTCF and thereby control interactions of promoters with distal regulatory elements. Existing Hi-C contact maps indicate that attachment to the nuclear lamina could have a major impact on the interaction space of a locus with the rest of the genome. At least at the resolution of 1Mb, DNA contacts within LADs or within non-LAD regions are substantially more frequent than interactions between lamin bound and unbound loci (Yaffe and Tanay, 2011). It remains to be determined whether this trend will also hold true at higher resolution, but these data indicate that among other mechanisms the attachment of genes to lamins may contribute to gene regulation by the physical spatial separation of distant enhancer elements and gene promoters. In support of such a model, it has been shown that large scale subnuclear chromatin organization constrains the ability of an ectopically integrated enhancer element to exclusively activate target genes located in its spatial proximity (Noordermeer et al., 2011a).

What is the mechanism for perinuclear chromatin anchoring?

The correlative studies summarized above strengthen the hypothesis that large scale chromatin architecture could influence gene expression. However, to functionally test this model one needs to interfere with chromatin organization and study the consequences on gene expression (Taddei et al., 2004). One approach has been to artificially tether a chromosomal domain to the nuclear periphery that is usually located internally. Inspired by experiments initially done in budding yeast (Andrulis et al., 1998), three groups have inducibly targeted genomic loci to the nuclear envelope in mammalian cells (Finlan et al., 2008; Kumaran and Spector, 2008; Reddy et al., 2008). These studies indicate that artificial relocation of chromatin to the periphery can restrict gene repression, at least for some promoters. Consistently, perinuclear tethering of several transgenes was also shown to cause repression in *Drosophila* (Dialynas et al., 2010). Chapter 2 of this thesis contains an in depth discussion of perinuclear targeting experiments and potential pitfalls in their interpretation.

Although targeting experiments support a function for artificial perinuclear gene targeting in gene repression, they do not address how endogenous chromatin is positioned at the nuclear envelope. Sequence analysis of mammalian and fly LADs did not reveal strongly enriched sequence motifs (Kind and van Steensel, 2010), indicating that perinuclear chromatin positioning is not directly determined by the DNA sequence. However, LADs are strongly correlated with specific histone modifications. LAD boundaries show high levels of H3K27me3 (Guelen et al., 2008; Peric-Hupkes et al., 2010) and H3K9me2 is enriched throughout 80% of all lamin bound regions (Peric-Hupkes et al., 2010; Wen et al., 2009).

Perhaps the most obvious correlation of perinuclear chromatin anchoring with histone modifications was observed in *C. elegans*. Here, chromatin associated with the nuclear envelope was determined by ChIP using antibodies raised against LEM-2, a lamin interacting transmembrane protein homologous to human MAN1 (see Figure 4, Ikegami et al., 2010). On all chromosomes, LEM-2 domains were consistently located on the outer segments of chromosomes (chromosome arms), whereas the central chromosomal regions were not associated with the nuclear envelope. Strikingly, all three methylation

states of H3K9 (me1, me2 and me3) showed a very similar pattern, as they were depleted from the chromosome center and enriched in LEM-2 domains (Liu et al., 2011). In addition to an enrichment of H3K9 methylation, chromosome arms also share other characteristics with mammalian lamin associated domains: As in LADs, genes density is lower on chromosome arms, whereas repetitive sequences are enriched (The *C. elegans* Sequencing Consortium, 1998). Furthermore, highly conserved and essential genes are enriched in chromosome centers (Kamath et al., 2003), indicating that genes on chromosome centers tend to be required for core metabolism.

In this thesis, evidence for a causal relationship between the perinuclear localization of *C. elegans* chromosome arms and H3K9 methylation is presented (see Chapter 4). Given the strong parallels between peripheral chromatin in *C. elegans* and in mammals it is likely that the concepts learnt from this study will also apply for other organisms, although some aspects of regulation may be more complex in mammals.

Thesis overview

This thesis comprises two experimental sections. In Chapter 3, I describe the establishment and use of repetitive transgenes as an experimental system to study perinuclear chromatin anchoring *in vivo* and throughout development of *C. elegans*. I find that repetitive transgenes accumulate high levels of histone modifications characteristic for silent chromatin (H3K9me3 and H3K27me3) in a copy number dependent manner. Transgenes with high repeat copy number (250 copies) become methylated at much higher levels than smaller transgenes insertions (50-70 copies), on which no enrichment of H3K9me3 is apparent. The accumulation of silent chromatin marks on large transgene arrays is correlated with a change in the subnuclear distribution of the transgenes. Small arrays are randomly distributed throughout nuclear space, whereas big arrays of identical sequence composition are enriched at the nuclear envelope. This indicates that histone modification status may influence perinuclear chromatin localization (Meister et al., 2010; Towbin et al., 2011). Furthermore, evidence is presented that depletion of lamin from *C. elegans* embryos by RNAi causes a partial detachment of arrays from the nuclear envelope, and genetic mutation of lamin leads to a stochastic derepression of array borne promoters in adult worms (Mattout et al., 2011).

The experiments described in Chapter 4, make use of transgene arrays as a tool to search for factors involved in perinuclear chromatin attachment. The main result of this study is the identification of the two major H3K9 histone methyltransferases in the worm that are essential for the anchoring of chromatin at the nuclear envelope. Importantly, this is not only true for gene arrays, but also for endogenous peripheral chromatin located on the chromosome arms. Interestingly, the enzyme required for the deposition of H3K9me3 associates with its own product, and thereby becomes enriched at the nuclear envelope as well. This generates a nuclear subcompartment with an increased concentration of H3K9 histone methyltransferase activity at the nuclear envelope. Based on these results, I propose a self-reinforcing mechanism that ensures high levels of H3K9 methylation on perinuclear chromatin.

The results described here support a mechanistic understanding of subnuclear chromatin organization in higher eukaryotes. Nevertheless, many questions remain unanswered. How is H3K9 methylated chromatin recognized and targeted to the nuclear envelope? Does H3K9 methylation and perinuclear chromatin sequestration contribute to gene silencing in the worm and if so, how? How does chromatin association with nuclear landmarks influence the constraints on DNA-DNA contact formation?

Genetic experiments presented in this thesis also indicate that H3K9 methylation is not required for viability of the worm, at least for development up to the first larval stage, although minor developmental defects may occur (see Chapter 5 for discussion). This opens the possibility to study the implications of complete loss of this chromatin modification on gene expression, which is not possible in many other metazoan model systems, where H3K9 methylation is essential. This thesis presents the establishment of important tools that will strengthen the worm as a powerful system to decipher the

mechanism and function of subnuclear chromatin organization in the developmental regulation of gene expression.

References

- Aebi, U., Cohn, J., Buhle, L., and Gerace, L. (1986). The nuclear lamina is a meshwork of intermediate-type filaments. *Nature* 323, 560-564.
- Allfrey, V.G., Faulkner, R., and Mirsky, A.E. (1964). Acetylation and methylation of histones and their possible role in the regulation of RNA synthesis. *Proceedings of the National Academy of Sciences* 51, 786-794.
- Alon, U. (2007). Network motifs: theory and experimental approaches. *Nat Rev Genet* 8, 450-461.
- Andrulis, E.D., Neiman, A.M., Zappulla, D.C., and Sternglanz, R. (1998). Perinuclear localization of chromatin facilitates transcriptional silencing. *Nature* 394, 592.
- Bannister, A.J., and Kouzarides, T. (2011). Regulation of chromatin by histone modifications. *Cell Res* 21, 381-395.
- Bannister, A.J., Zegerman, P., Partridge, J.F., Miska, E.A., Thomas, J.O., Allshire, R.C., and Kouzarides, T. (2001). Selective recognition of methylated lysine 9 on histone H3 by the HP1 chromo domain. *Nature* 410, 120-124.
- Barski, A., Cuddapah, S., Cui, K., Roh, T.-Y., Schones, D.E., Wang, Z., Wei, G., Chepelev, I., and Zhao, K. (2007). High-Resolution Profiling of Histone Methylations in the Human Genome. *Cell* 129, 823-837.
- Bartke, T., Vermeulen, M., Xhemalce, B., Robson, S.C., Mann, M., and Kouzarides, T. (2010). Nucleosome-Interacting Proteins Regulated by DNA and Histone Methylation. *Cell* 143, 470-484.
- Bell, A.C., West, A.G., and Felsenfeld, G. (1999). The Protein CTCF Is Required for the Enhancer Blocking Activity of Vertebrate Insulators. *Cell* 98, 387-396.
- Bell, O., Schwaiger, M., Oakeley, E.J., Lienert, F., Beisel, C., Stadler, M.B., and Schubeler, D. (2010). Accessibility of the *Drosophila* genome discriminates PcG repression, H4K16 acetylation and replication timing. *Nat Struct Mol Biol* 17, 894-900.
- Bell, O., Tiwari, V.K., Thomä, N.H., and Schubeler, D. (2011). Determinants and dynamics of genome accessibility. *Nat Rev Genet* 12, 554-564.
- Bell, O., Wirbelauer, C., Hild, M., Scharf, A.N.D., Schwaiger, M., MacAlpine, D.M., Zilbermann, F., van Leeuwen, F., Bell, S.P., Imhof, A., *et al.* (2007). Localized H3K36 methylation states define histone H4K16 acetylation during transcriptional elongation in *Drosophila*. *Embo J* 26, 4974-4984.
- Bernstein, B.E., Mikkelsen, T.S., Xie, X., Kamal, M., Huebert, D.J., Cuff, J., Fry, B., Meissner, A., Wernig, M., Plath, K., *et al.* (2006). A Bivalent Chromatin Structure Marks Key Developmental Genes in Embryonic Stem Cells. *Cell* 125, 315-326.
- Bolzer, A., Kreth, G., Solovei, I., Koehler, D., Saracoglu, K., Fauth, C., Uml, S., Eils, R., Cremer, C., *et al.* (2005). Three-Dimensional Maps of All Chromosomes in Human Male Fibroblast Nuclei and Prometaphase Rosettes. *PLoS Biology* 3, e157.
- Boyle, A.P., Davis, S., Shulha, H.P., Meltzer, P., Margulies, E.H., Weng, Z., Furey, T.S., and Crawford, G.E. (2008). High-Resolution Mapping and Characterization of Open Chromatin across the Genome. *Cell* 132, 311-322.
- Bridger, J.M., Boyle, S., Kill, I.R., and Bickmore, W.A. (2000). Re-modelling of nuclear architecture in quiescent and senescent human fibroblasts. *Current Biology* 10, 149.
- Brown, K.E., Guest, S.S., Smale, S.T., Hahn, K., Merkenschlager, M., and Fisher, A.G. (1997). Association of Transcriptionally Silent Genes with Ikaros Complexes at Centromeric Heterochromatin. *Cell* 91, 845.
- Carrozza, M.J., Li, B., Florens, L., Suganuma, T., Swanson, S.K., Lee, K.K., Shia, W.-J., Anderson, S., Yates, J., Washburn, M.P., *et al.* (2005). Histone H3 Methylation by Set2 Directs Deacetylation of Coding Regions by Rpd3S to Suppress Spurious Intragenic Transcription. *Cell* 123, 581-592.
- Chambeyron, S., and Bickmore, W.A. (2004). Chromatin decondensation and nuclear reorganization of the HoxB locus upon induction of transcription. *Genes Dev* 18, 1119-1130.
- Chambeyron, S., Da Silva, N.R., Lawson, K.A., and Bickmore, W.A. (2005). Nuclear re-organisation of the Hoxb complex during mouse embryonic development. *Development* 132, 2215-2223.
- Charoensawan, V., Wilson, D., and Teichmann, S.A. (2010). Genomic repertoires of DNA-binding transcription factors across the tree of life. *Nucleic Acids Research* 38, 7364-7377.
- Chen, L., and Widom, J. (2005). Mechanism of Transcriptional Silencing in Yeast. *Cell* 120, 37-48.

- Chubb, J.R., Boyle, S., Perry, P., and Bickmore, W.A. (2002). Chromatin Motion Is Constrained by Association with Nuclear Compartments in Human Cells. *Current Biology* 12, 439.
- Cremer, M., von Hase, J., Volm, T., Brero, A., Kreth, G., Walter, J., Fischer, C., Solovei, I., Cremer, C., and Cremer, T. (2001). Non-random radial higher-order chromatin arrangements in nuclei of diploid human cells. *Chromosome Res* 9, 541-567.
- Cremer, T., Lichter, P., Borden, J., Ward, D.C., and Manuelidis, L. (1988). Detection of chromosome aberrations in metaphase and interphase tumor cells by in situ hybridization using chromosome-specific library probes. *Hum Genet* 80, 235-246.
- de Wit, E., and de Laat, W. (2012). A decade of 3C technologies: insights into nuclear organization. *Genes & Development* 26, 11-24.
- Dechat, T., Adam, S.A., Taimen, P., Shimi, T., and Goldman, R.D. (2010). Nuclear Lamins. *Cold Spring Harbor Perspectives in Biology* 2.
- Dekker, J., Rippe, K., Dekker, M., and Kleckner, N. (2002). Capturing Chromosome Conformation. *Science* 295, 1306-1311.
- Dernburg, A.F., Broman, K.W., Fung, J.C., Marshall, W.F., Philips, J., Agard, D.A., and Sedat, J.W. (1996). Perturbation of Nuclear Architecture by Long-Distance Chromosome Interactions. *Cell* 85, 745.
- Dhalluin, C., Carlson, J.E., Zeng, L., He, C., Aggarwal, A.K., and Zhou, M.-M. (1999). Structure and ligand of a histone acetyltransferase bromodomain. *Nature* 399, 491-496.
- Dialynas, G., Speese, S., Budnik, V., Geyer, P.K., and Wallrath, L.L. (2010). The role of *Drosophila* Lamin C in muscle function and gene expression. *Development* 137, 3067-3077.
- Dostie, J., Richmond, T.A., Arnaout, R.A., Selzer, R.R., Lee, W.L., Honan, T.A., Rubio, E.D., Krumm, A., Lamb, J., Nusbaum, C., *et al.* (2006). Chromosome Conformation Capture Carbon Copy (5C): A massively parallel solution for mapping interactions between genomic elements. *Genome Research* 16, 1299-1309.
- Drissen, R., Palstra, R.-J., Gillemans, N., Splinter, E., Grosveld, F., Philipsen, S., and de Laat, W. (2004). The active spatial organization of the β -globin locus requires the transcription factor EKLF. *Genes & Development* 18, 2485-2490.
- Erdel, F., Krug, J., Langst, G., and Rippe, K. (2011). Targeting chromatin remodelers: Signals and search mechanisms. *Biochimica et Biophysica Acta (BBA) - Gene Regulatory Mechanisms* 1809, 497-508.
- Ernst, J., and Kellis, M. (2010). Discovery and characterization of chromatin states for systematic annotation of the human genome. *Nat Biotech* 28, 817-825.
- Ernst, J., Kheradpour, P., Mikkelsen, T.S., Shores, N., Ward, L.D., Epstein, C.B., Zhang, X., Wang, L., Issner, R., Coyne, M., *et al.* (2011). Mapping and analysis of chromatin state dynamics in nine human cell types. *Nature* 473, 43-49.
- Filion, G.J., van Bommel, J.G., Braunschweig, U., Talhout, W., Kind, J., Ward, L.D., Brugman, W., de Castro, I.s.J., Kerkhoven, R.M., Bussemaker, H.J., *et al.* (2010). Systematic Protein Location Mapping Reveals Five Principal Chromatin Types in *Drosophila* Cells. *Cell* 143, 212-224.
- Finlan, L.E., Sproul, D., Thomson, I., Boyle, S., Kerr, E., Perry, P., Ylstra, B., Chubb, J.R., and Bickmore, W.A. (2008). Recruitment to the Nuclear Periphery Can Alter Expression of Genes in Human Cells. *PLoS Genetics* 4, e1000039.
- Flaus, A., and Owen-Hughes, T. (2011). Mechanisms for ATP-dependent chromatin remodelling: the means to the end. *FEBS Journal* 278, 3579-3595.
- Francastel, C., Magis, W., and Groudine, M. (2001). Nuclear relocation of a transactivator subunit precedes target gene activation. *Proceedings of the National Academy of Sciences* 98, 12120-12125.
- Fullwood, M.J., Liu, M.H., Pan, Y.F., Liu, J., Xu, H., Mohamed, Y.B., Orlov, Y.L., Velkov, S., Ho, A., Mei, P.H., *et al.* (2009). An oestrogen-receptor-alpha-bound human chromatin interactome. *Nature* 462, 58-64.
- Goldberg, M., Harel, A., Brandeis, M., Rechsteiner, T., Richmond, T.J., Weiss, A.M., and Gruenbaum, Y. (1999). The tail domain of lamin Dm0 binds histones H2A and H2B. *Proceedings of the National Academy of Sciences* 96, 2852-2857.
- Gottschling, D.E. (1992). Telomere-proximal DNA in *Saccharomyces cerevisiae* is refractory to methyltransferase activity in vivo. *Proceedings of the National Academy of Sciences of the United States of America* 89, 4062-4065.
- Grogan, J.L., Mohrs, M., Harmon, B., Lacy, D.A., Sedat, J.W., and Locksley, R.M. (2001). Early Transcription and Silencing of Cytokine Genes Underlie Polarization of T Helper Cell Subsets. *Immunity* 14, 205.

- Guelen, L., Pagie, L., Brasset, E., Meuleman, W., Faza, M.B., Talhout, W., Eussen, B.H., de Klein, A., Wessels, L., de Laat, W., *et al.* (2008). Domain organization of human chromosomes revealed by mapping of nuclear lamina interactions. *Nature* **453**, 948-951.
- Guenther, M.G., Levine, S.S., Boyer, L.A., Jaenisch, R., and Young, R.A. (2007). A Chromatin Landmark and Transcription Initiation at Most Promoters in Human Cells. *Cell* **130**, 77-88.
- Hadjur, S., Williams, L.M., Ryan, N.K., Cobb, B.S., Sexton, T., Fraser, P., Fisher, A.G., and Merkenschlager, M. (2009). Cohesins form chromosomal cis-interactions at the developmentally regulated *IFNG* locus. *Nature* **460**, 410-413.
- Handoko, L., Xu, H., Li, G., Ngan, C.Y., Chew, E., Schnapp, M., Lee, C.W.H., Ye, C., Ping, J.L.H., Mulawadi, F., *et al.* (2011). CTCF-mediated functional chromatin interactome in pluripotent cells. *Nat Genet* **43**, 630-638.
- Hansen, K.H., Bracken, A.P., Pasini, D., Dietrich, N., Gehani, S.S., Monrad, A., Rappsilber, J., Lerdrup, M., and Helin, K. (2008). A model for transmission of the H3K27me3 epigenetic mark. *Nat Cell Biol* **10**, 1291-1300.
- Hassan, A.H., Prochasson, P., Neely, K.E., Galasinski, S.C., Chandy, M., Carrozza, M.J., and Workman, J.L. (2002). Function and Selectivity of Bromodomains in Anchoring Chromatin-Modifying Complexes to Promoter Nucleosomes. *Cell* **111**, 369-379.
- Heintzman, N.D., Stuart, R.K., Hon, G., Fu, Y., Ching, C.W., Hawkins, R.D., Barrera, L.O., Van Calcar, S., Qu, C., Ching, K.A., *et al.* (2007). Distinct and predictive chromatin signatures of transcriptional promoters and enhancers in the human genome. *Nat Genet* **39**, 311-318.
- Heitz, E. (1928). Das Heterochromatin der Moose. *Jahrb Wiss Botanik*, 762-818.
- Henikoff, S., and Shilatifard, A. (2011). Histone modification: cause or cog? *Trends in Genetics* **27**, 389-396.
- Heun, P., Laroche, T., Shimada, K., Furrer, P., and Gasser, S.M. (2001). Chromosome Dynamics in the Yeast Interphase Nucleus. *Science* **294**, 2181-2186.
- Hewitt, S.L., High, F.A., Reiner, S.L., Fisher, A.G., and Merkenschlager, M. (2004). Nuclear repositioning marks the selective exclusion of lineage-inappropriate transcription factor loci during T helper cell differentiation. *Eur J Immunol* **34**, 3604-3613.
- Huang, S. (2009). Non-genetic heterogeneity of cells in development: more than just noise. *Development* **136**, 3853-3862.
- Ikegami, K., Egelhofer, T., Strome, S., and Lieb, J. (2010). *Caenorhabditis elegans* chromosome arms are anchored to the nuclear membrane via discontinuous association with LEM-2. *Genome Biology* **11**, R120.
- Jenuwein, T., and Allis, C.D. (2001). Translating the Histone Code. *Science* **293**, 1074-1080.
- Kamath, R.S., Fraser, A.G., Dong, Y., Poulin, G., Durbin, R., Gotta, M., Kanapin, A., Le Bot, N., Moreno, S., Sohrmann, M., *et al.* (2003). Systematic functional analysis of the *Caenorhabditis elegans* genome using RNAi. *Nature* **421**, 231-237.
- Keogh, M.-C., Kurdistani, S.K., Morris, S.A., Ahn, S.H., Podolny, V., Collins, S.R., Schuldiner, M., Chin, K., Punna, T., Thompson, N.J., *et al.* (2005). Cotranscriptional Set2 Methylation of Histone H3 Lysine 36 Recruits a Repressive Rpd3 Complex. *Cell* **123**, 593-605.
- Kim, A., Kiefer, C.M., and Dean, A. (2007). Distinctive Signatures of Histone Methylation in Transcribed Coding and Noncoding Human beta-Globin Sequences. *Molecular and Cellular Biology* **27**, 1271-1279.
- Kim, J., Daniel, J., Espejo, A., Lake, A., Krishna, M., Xia, L., Zhang, Y., and Bedford, M.T. (2006). Tudor, MBT and chromo domains gauge the degree of lysine methylation. *EMBO Rep* **7**, 397-403.
- Kind, J., and van Steensel, B. (2010). Genome-nuclear lamina interactions and gene regulation. *Current Opinion in Cell Biology* **22**, 320-325.
- Kosak, S.T., Skok, J.A., Medina, K.L., Riblet, R., Le Beau, M.M., Fisher, A.G., and Singh, H. (2002). Subnuclear Compartmentalization of Immunoglobulin Loci During Lymphocyte Development. *Science* **296**, 158-162.
- Kumaran, R.I., and Spector, D.L. (2008). A genetic locus targeted to the nuclear periphery in living cells maintains its transcriptional competence. *J Cell Biol* **180**, 51-65.
- Lachner, M., O'Carroll, D., Rea, S., Mechtler, K., and Jenuwein, T. (2001). Methylation of histone H3 lysine 9 creates a binding site for HP1 proteins. *Nature* **410**, 116-120.
- Lancot, C., Cheutin, T., Cremer, M., Cavalli, G., and Cremer, T. (2007). Dynamic genome architecture in the nuclear space: regulation of gene expression in three dimensions. *Nat Rev Genet* **8**, 104.
- Liang, Y., and Hetzer, M.W. (2011). Functional interactions between nucleoporins and chromatin. *Current Opinion in Cell Biology* **23**, 65-70.

- Lichter, P., Cremer, T., Borden, J., Manuelidis, L., and Ward, D.C. (1988). Delineation of individual human chromosomes in metaphase and interphase cells by in situ suppression hybridization using recombinant DNA libraries. *Hum Genet* 80, 224-234.
- Lieberman-Aiden, E., van Berkum, N.L., Williams, L., Imakaev, M., Ragoczy, T., Telling, A., Amit, I., Lajoie, B.R., Sabo, P.J., Dorschner, M.O., *et al.* (2009). Comprehensive Mapping of Long-Range Interactions Reveals Folding Principles of the Human Genome. *Science* 326, 289-293.
- Lin, H., Wang, Y., Wang, Y., Tian, F., Pu, P., Yu, Y., Mao, H., Yang, Y., Wang, P., Hu, L., *et al.* (2010). Coordinated regulation of active and repressive histone methylations by a dual-specificity histone demethylase ceKDM7A from *Caenorhabditis elegans*. *Cell Res* 20, 899-907.
- Liu, T., Rechtsteiner, A., Egelhofer, T.A., Vielle, A., Latorre, I., Cheung, M.-S., Ercan, S., Ikegami, K., Jensen, M., Kolasinska-Zwiercz, P., *et al.* (2011). Broad chromosomal domains of histone modification patterns in *C. elegans*. *Genome Research* 21, 227-236.
- Luderus, M.E.E., de Graaf, A., Mattia, E., den Blaauwen, J.L., Grande, M.A., de Jong, L., and van Driel, R. (1992). Binding of matrix attachment regions to lamin B1. *Cell* 70, 949.
- Luger, K., Mader, A.W., Richmond, R.K., Sargent, D.F., and Richmond, T.J. (1997). Crystal structure of the nucleosome core particle at 2.8 Å resolution. *Nature* 389, 251-260.
- Margalit, A., Brachner, A., Gotzmann, J., Foisner, R., and Gruenbaum, Y. (2007). Barrier-to-autointegration factor - a BAFfling little protein. *Trends in Cell Biology* 17, 202-208.
- Marshall, W.F., Straight, A., Marko, J.F., Swedlow, J., Dernburg, A., Belmont, A., Murray, A.W., Agard, D.A., and Sedat, J.W. (1997). Interphase chromosomes undergo constrained diffusional motion in living cells. *Current Biology* 7, 930.
- Mattout, A., Pike, Brietta L., Towbin, Benjamin D., Bank, Erin M., Gonzalez-Sandoval, A., Stadler, Michael B., Meister, P., Gruenbaum, Y., and Gasser, Susan M. (2011). An EDMD Mutation in *C. elegans* Lamin Blocks Muscle-Specific Gene Relocation and Compromises Muscle Integrity. *Current biology : CB* 21, 1603-1614.
- Meister, P., Towbin, B.D., Pike, B.L., Ponti, A., and Gasser, S.M. (2010). The spatial dynamics of tissue-specific promoters during *C. elegans* development. *Genes & Development* 24, 766-782.
- Mikkelsen, T.S., Ku, M., Jaffe, D.B., Issac, B., Lieberman, E., Giannoukos, G., Alvarez, P., Brockman, W., Kim, T.-K., Koche, R.P., *et al.* (2007). Genome-wide maps of chromatin state in pluripotent and lineage-committed cells. *Nature* 448, 553-560.
- Mohn, F., Weber, M., Rebhan, M., Roloff, T.C., Richter, J., Stadler, M.B., Bibel, M., and Schübeler, D. (2008). Lineage-Specific Polycomb Targets and *De Novo* DNA Methylation Define Restriction and Potential of Neuronal Progenitors. *Molecular Cell* 30, 755-766.
- Morey, C., Da Silva, N.R., Perry, P., and Bickmore, W.A. (2007). Nuclear reorganisation and chromatin decondensation are conserved, but distinct, mechanisms linked to Hox gene activation. *Development* 134, 909-919.
- Moriniere, J., Rousseaux, S., Steuerwald, U., Soler-Lopez, M., Curtet, S., Vitte, A.-L., Govin, J., Gaucher, J., Sadoul, K., Hart, D.J., *et al.* (2009). Cooperative binding of two acetylation marks on a histone tail by a single bromodomain. *Nature* 461, 664-668.
- Murray, K. (1964). The Occurrence of Epsilon-N-Methyl Lysine in Histones. *Biochemistry* 3, 10-15.
- Murrell, A., Heeson, S., and Reik, W. (2004). Interaction between differentially methylated regions partitions the imprinted genes *Igf2* and *H19* into parent-specific chromatin loops. *Nat Genet* 36, 889-893.
- Nakayama, J.-i., Rice, J.C., Strahl, B.D., Allis, C.D., and Grewal, S.I.S. (2001). Role of Histone H3 Lysine 9 Methylation in Epigenetic Control of Heterochromatin Assembly. *Science* 292, 110-113.
- Nativio, R., Wendt, K.S., Ito, Y., Huddleston, J.E., Uribe-Lewis, S., Woodfine, K., Krueger, C., Reik, W., Peters, J.-M., and Murrell, A. (2009). Cohesin Is Required for Higher-Order Chromatin Conformation at the Imprinted *IGF2-H19* Locus. *PLoS Genet* 5, e1000739.
- Neumann, H., Hancock, S.M., Buning, R., Routh, A., Chapman, L., Somers, J., Owen-Hughes, T., van Noort, J., Rhodes, D., and Chin, J.W. (2009). A Method for Genetically Installing Site-Specific Acetylation in Recombinant Histones Defines the Effects of H3 K56 Acetylation. *Molecular Cell* 36, 153-163.
- Noordermeer, D., de Wit, E., Klous, P., van de Werken, H., Simonis, M., Lopez-Jones, M., Eussen, B., de Klein, A., Singer, R.H., and de Laat, W. (2011a). Variegated gene expression caused by cell-specific long-range DNA interactions. *Nat Cell Biol* 13, 944-951.
- Noordermeer, D., Leleu, M., Splinter, E., Rougemont, J., De Laat, W., and Duboule, D. (2011b). The Dynamic Architecture of Hox Gene Clusters. *Science* 334, 222-225.

- Ohta, S., Bukowski-Wills, J.-C., Sanchez-Pulido, L., Alves, F.d.L., Wood, L., Chen, Z.A., Platani, M., Fischer, L., Hudson, D.F., Ponting, C.P., *et al.* (2010). The Protein Composition of Mitotic Chromosomes Determined Using Multiclassifier Combinatorial Proteomics. *Cell* 142, 810-821.
- Orlando, V., and Paro, R. (1993). Mapping polycomb-repressed domains in the bithorax complex using in vivo formaldehyde cross-linked chromatin. *Cell* 75, 1187-1198.
- Osborne, C.S., Chakalova, L., Brown, K.E., Carter, D., Horton, A., Debrand, E., Goyenechea, B., Mitchell, J.A., Lopes, S., Reik, W., *et al.* (2004). Active genes dynamically colocalize to shared sites of ongoing transcription. *Nat Genet* 36, 1065.
- Palstra, R.-J., Tolhuis, B., Splinter, E., Nijmeijer, R., Grosveld, F., and de Laat, W. (2003). The beta-globin nuclear compartment in development and erythroid differentiation. *Nat Genet* 35, 190-194.
- Parelho, V., Hadjur, S., Spivakov, M., Leleu, M., Sauer, S., Gregson, H.C., Jarmuz, A., Canzonetta, C., Webster, Z., Nesterova, T., *et al.* (2008). Cohesins Functionally Associate with CTCF on Mammalian Chromosome Arms. *Cell* 132, 422-433.
- Pauli, A., Althoff, F., Oliveira, R.A., Heidmann, S., Schuldiner, O., Lehner, C.F., Dickson, B.J., and Nasmyth, K. (2008). Cell-Type-Specific TEV Protease Cleavage Reveals Cohesin Functions in *Drosophila* Neurons. *Developmental Cell* 14, 239-251.
- Pauli, A., van Bommel, J.G., Oliveira, R.A., Itoh, T., Shirahige, K., van Steensel, B., and Nasmyth, K. (2010). A Direct Role for Cohesin in Gene Regulation and Ecdysone Response in *Drosophila* Salivary Glands. *Current Biology* 20, 1787-1798.
- Peric-Hupkes, D., Meuleman, W., Pagie, L., Bruggeman, S.W.M., Solovei, I., Brugman, W., Gräf, S., Flicek, P., Kerkhoven, R.M., van Lohuizen, M., *et al.* (2010). Molecular Maps of the Reorganization of Genome-Nuclear Lamina Interactions during Differentiation. *Molecular Cell* 38, 603-613.
- Peters, J.-M., Tedeschi, A., and Schmitz, J. (2008). The cohesin complex and its roles in chromosome biology. *Genes & Development* 22, 3089-3114.
- Phillips, J.E., and Corces, V.G. (2009). CTCF: Master Weaver of the Genome. *Cell* 137, 1194-1211.
- Pickersgill, H., Kalverda, B., de Wit, E., Talhout, W., Fornerod, M., and van Steensel, B. (2006). Characterization of the *Drosophila melanogaster* genome at the nuclear lamina. *Nat Genet* 38, 1005.
- Prokocimer, M., Davidovich, M., Nissim-Rafinia, M., Wiesel-Motiuk, N., Bar, D., Barkan, R., Meshorer, E., and Gruenbaum, Y. (2009). Nuclear lamins: key regulators of nuclear structure and activities. *Journal of Cellular and Molecular Medicine* 9999.
- Rajapakse, I., and Groudine, M. (2011). On emerging nuclear order. *The Journal of Cell Biology* 192, 711-721.
- Ram, O., Goren, A., Amit, I., Shores, N., Yosef, N., Ernst, J., Kellis, M., Gymrek, M., Issner, R., Coyne, M., *et al.* (2011). Combinatorial Patterning of Chromatin Regulators Uncovered by Genome-wide Location Analysis in Human Cells. *Cell* 147, 1628-1639.
- Reddy, K.L., Zullo, J.M., Bertolino, E., and Singh, H. (2008). Transcriptional repression mediated by repositioning of genes to the nuclear lamina. *Nature*.
- Ren, B., Robert, F.o., Wyrick, J.J., Aparicio, O., Jennings, E.G., Simon, I., Zeitlinger, J., Schreiber, J.r., Hannett, N., Kanin, E., *et al.* (2000). Genome-Wide Location and Function of DNA Binding Proteins. *Science* 290, 2306-2309.
- Robertson, G., Hirst, M., Bainbridge, M., Bilenky, M., Zhao, Y., Zeng, T., Euskirchen, G., Bernier, B., Varhol, R., Delaney, A., *et al.* (2007). Genome-wide profiles of STAT1 DNA association using chromatin immunoprecipitation and massively parallel sequencing. *Nat Meth* 4, 651-657.
- Rubio, E.D., Reiss, D.J., Welch, P.L., Distech, C.M., Filippova, G.N., Baliga, N.S., Aebersold, R., Ranish, J.A., and Krumm, A. (2008). CTCF physically links cohesin to chromatin. *Proceedings of the National Academy of Sciences* 105, 8309-8314.
- Ruthenburg, Alexander J., Li, H., Milne, Thomas A., Dewell, S., McGinty, Robert K., Yuen, M., Ueberheide, B., Dou, Y., Muir, Tom W., Patel, Dinshaw J., *et al.* (2011a). Recognition of a Mononucleosomal Histone Modification Pattern by BPTF via Multivalent Interactions. *Cell* 145, 692-706.
- Sawarkar, R., and Paro, R. (2010). Interpretation of Developmental Signaling at Chromatin: The Polycomb Perspective. *Developmental Cell* 19, 651-661.
- Schmitges, Frank W., Prusty, Archana B., Faty, M., Stützer, A., Lingaraju, Gondichatnahalli M., Aiwazian, J., Sack, R., Hess, D., Li, L., Zhou, S., *et al.* (2011). Histone Methylation by PRC2 Is Inhibited by Active Chromatin Marks. *Molecular Cell* 42, 330-341.

- Schoenfelder, S., Sexton, T., Chakalova, L., Cope, N.F., Horton, A., Andrews, S., Kurukuti, S., Mitchell, J.A., Umlauf, D., Dimitrova, D.S., *et al.* (2010). Preferential associations between co-regulated genes reveal a transcriptional interactome in erythroid cells. *Nat Genet* 42, 53-61.
- Schuldiner, O., Berdnik, D., Levy, J.M., Wu, J.S., Luginbuhl, D., Gontang, A.C., and Luo, L. (2008). piggyBac-Based Mosaic Screen Identifies a Postmitotic Function for Cohesin in Regulating Developmental Axon Pruning. *Developmental Cell* 14, 227-238.
- Seitan, V.C., Hao, B., Tachibana-Konwalski, K., Lavagnoli, T., Mira-Bontenbal, H., Brown, K.E., Teng, G., Carroll, T., Terry, A., Horan, K., *et al.* (2011). A role for cohesin in T-cell-receptor rearrangement and thymocyte differentiation. *Nature* 476, 467-471.
- Sha, K., Gu, S., Pantalena-Filho, L., Goh, A., Fleenor, J., Blanchard, D., Krishna, C., and Fire, A. (2010). Distributed probing of chromatin structure in vivo reveals pervasive chromatin accessibility for expressed and non-expressed genes during tissue differentiation in *C. elegans*. *BMC Genomics* 11, 465.
- Shevelyov, Y.Y., Lavrov, S.A., Mikhaylova, L.M., Nurminsky, I.D., Kulathinal, R.J., Egorova, K.S., Rozovsky, Y.M., and Nurminsky, D.I. (2009). The B-type lamin is required for somatic repression of testis-specific gene clusters. *Proceedings of the National Academy of Sciences* 106, 3282-3287.
- Shogren-Knaak, M., Ishii, H., Sun, J.-M., Pazin, M.J., Davie, J.R., and Peterson, C.L. (2006). Histone H4-K16 Acetylation Controls Chromatin Structure and Protein Interactions. *Science* 311, 844-847.
- Simonis, M., Klous, P., Splinter, E., Moshkin, Y., Willemsen, R., de Wit, E., van Steensel, B., and de Laat, W. (2006). Nuclear organization of active and inactive chromatin domains uncovered by chromosome conformation capture-on-chip (4C). *Nat Genet* 38, 1348.
- Sims, R.J., Belotserkovskaya, R., and Reinberg, D. (2004). Elongation by RNA polymerase II: the short and long of it. *Genes & Development* 18, 2437-2468.
- Solomon, M.J., Larsen, P.L., and Varshavsky, A. (1988). Mapping protein DNA interactions *in vivo* with formaldehyde: Evidence that histone H4 is retained on a highly transcribed gene. *Cell* 53, 937-947.
- Spilianakis, C.G., Lalioti, M.D., Town, T., Lee, G.R., and Flavell, R.A. (2005). Interchromosomal associations between alternatively expressed loci. *Nature* 435, 637.
- Splinter, E., Heath, H., Kooren, J., Palstra, R.-J., Klous, P., Grosveld, F., Galjart, N., and de Laat, W. (2006). CTCF mediates long-range chromatin looping and local histone modification in the beta-globin locus. *Genes & Development* 20, 2349-2354.
- Strahl, B.D., and Allis, C.D. (2000). The language of covalent histone modifications. *Nature* 403, 41-45.
- Suganuma, T., and Workman, J.L. (2011). Signals and Combinatorial Functions of Histone Modifications. *Annual Review of Biochemistry* 80, 473-499.
- Sun, H.B., Shen, J., and Yokota, H. (2000). Size-Dependent Positioning of Human Chromosomes in Interphase Nuclei. *Biophys J* 79, 184-190.
- Taddei, A., Hediger, F., Neumann, F.R., and Gasser, S.M. (2004). The Function of Nuclear Architecture: A Genetic Approach. *Annual Review of Genetics* 38, 305-345.
- Tan, M., Luo, H., Lee, S., Jin, F., Yang, Jeong S., Montellier, E., Buchou, T., Cheng, Z., Rousseaux, S., Rajagopal, N., *et al.* (2011). Identification of 67 Histone Marks and Histone Lysine Crotonylation as a New Type of Histone Modification. *Cell* 146, 1016-1028.
- The *C. elegans* Sequencing Consortium (1998). Genome Sequence of the Nematode *C. elegans*: A Platform for Investigating Biology. *Science* 282, 2012-2018.
- Tolhuis, B., Palstra, R.-J., Splinter, E., Grosveld, F., and de Laat, W. (2002). Looping and Interaction between Hypersensitive Sites in the Active beta-globin Locus. *Molecular Cell* 10, 1453-1465.
- Towbin, B.D., Meister, P., and Gasser, S.M. (2009). The nuclear envelope -- a scaffold for silencing? *Current Opinion in Genetics & Development* 19, 180-186.
- Towbin, B.D., Meister, P., Pike, B.L., and Gasser, S.M. (2011). Repetitive Transgenes in *C. elegans* Accumulate Heterochromatic Marks and Are Sequestered at the Nuclear Envelope in a Copy-Number- and Lamin-Dependent Manner. *Cold Spring Harbor Symposia on Quantitative Biology*.
- Vakoc, C.R., Letting, D.L., Gheldof, N., Sawado, T., Bender, M.A., Groudine, M., Weiss, M.J., Dekker, J., and Blobel, G.A. (2005a). Proximity among Distant Regulatory Elements at the beta-Globin Locus Requires GATA-1 and FOG-1. *Molecular Cell* 17, 453-462.
- Vakoc, C.R., Mandat, S.A., Olenchok, B.A., and Blobel, G.A. (2005b). Histone H3 Lysine 9 Methylation and HP1gamma Are Associated with Transcription Elongation through Mammalian Chromatin. *Molecular Cell* 19, 381-391.

- van Holde, K.E. (1989). *Chromatin* (Cambridge, MA, Springer).
- van Nimwegen, E. (2003). Scaling laws in the functional content of genomes. *Trends in Genetics* *19*, 479-484.
- van Steensel, B. (2011). Chromatin: constructing the big picture. *Embo J* *30*, 1885-1895.
- Veening, J.-W., Smits, W.K., and Kuipers, O.P. (2008). Bistability, Epigenetics, and Bet-Hedging in Bacteria. *Annual Review of Microbiology* *62*, 193-210.
- Vermeulen, M., Eberl, H.C., Matarese, F., Marks, H., Denissov, S., Butter, F., Lee, K.K., Olsen, J.V., Hyman, A.A., Stunnenberg, H.G., *et al.* (2010). Quantitative Interaction Proteomics and Genome-wide Profiling of Epigenetic Histone Marks and Their Readers. *Cell* *142*, 967-980.
- Vermeulen, M., Mulder, K.W., Denissov, S., Pijnappel, W.W.M.P., van Schaik, F.M.A., Varier, R.A., Baltissen, M.P.A., Stunnenberg, H.G., Mann, M., and Timmers, H.T.M. (2007). Selective Anchoring of TFIID to Nucleosomes by Trimethylation of Histone H3 Lysine 4. *Cell* *131*, 58-69.
- Vernimmen, D., Gobbi, M.D., Sloane-Stanley, J.A., Wood, W.G., and Higgs, D.R. (2007). Long-range chromosomal interactions regulate the timing of the transition between poised and active gene expression. *Embo J* *26*, 2041-2051.
- Waddington, C.H. (1957). *The strategy of the genes; a discussion of some aspects of theoretical biology* (London, Allen & Unwin).
- Wang, Z., and Patel, D.J. (2011). Combinatorial Readout of Dual Histone Modifications by Paired Chromatin-associated Modules. *Journal of Biological Chemistry* *286*, 18363-18368.
- Wang, Z., Zang, C., Rosenfeld, J.A., Schones, D.E., Barski, A., Cuddapah, S., Cui, K., Roh, T.-Y., Peng, W., Zhang, M.Q., *et al.* (2008). Combinatorial patterns of histone acetylations and methylations in the human genome. *Nat Genet* *40*, 897-903.
- Weintraub, H., and Groudine, M. (1976). Chromosomal subunits in active genes have an altered conformation. *Science* *193*, 848-856.
- Wen, B., Wu, H., Shinkai, Y., Irizarry, R.A., and Feinberg, A.P. (2009). Large histone H3 lysine 9 dimethylated chromatin blocks distinguish differentiated from embryonic stem cells. *Nat Genet* *41*, 246-250.
- Wendt, K.S., Yoshida, K., Itoh, T., Bando, M., Koch, B., Schirghuber, E., Tsutsumi, S., Nagae, G., Ishihara, K., Mishiro, T., *et al.* (2008). Cohesin mediates transcriptional insulation by CCCTC-binding factor. *Nature* *451*, 796-801.
- Williams, R.R.E., Azuara, V., Perry, P., Sauer, S., Dvorkina, M., Jorgensen, H., Roix, J., McQueen, P., Misteli, T., Merkenschlager, M., *et al.* (2006). Neural induction promotes large-scale chromatin reorganisation of the *Mash1* locus. *J Cell Sci* *119*, 132-140.
- Yaffe, E., and Tanay, A. (2011). Probabilistic modeling of Hi-C contact maps eliminates systematic biases to characterize global chromosomal architecture. *Nat Genet* *43*, 1059-1065.
- Ye, Q., and Worman, H.J. (1996). Interaction between an Integral Protein of the Nuclear Envelope Inner Membrane and Human Chromodomain Proteins Homologous to *Drosophila* HP1. *Journal of Biological Chemistry* *271*, 14653-14656.
- Yun, M., Wu, J., Workman, J.L., and Li, B. (2011). Readers of histone modifications. *Cell Res* *21*, 564-578.
- Zhao, Z., Tavoosidana, G., Sjolinder, M., Gondor, A., Mariano, P., Wang, S., Kanduri, C., Lezcano, M., Singh Sandhu, K., Singh, U., *et al.* (2006). Circular chromosome conformation capture (4C) uncovers extensive networks of epigenetically regulated intra- and interchromosomal interactions. *Nat Genet* *38*, 1341.
- Zhou, V.W., Goren, A., and Bernstein, B.E. (2011). Charting histone modifications and the functional organization of mammalian genomes. *Nat Rev Genet* *12*, 7-18.

Chapter 2: The nuclear envelope - a scaffold for silencing?

Benjamin D. Towbin, Peter Meister and Susan M. Gasser

Friedrich Miescher Institute for Biomedical Research, Maulbeerstrasse 66, CH-4058 Basel, Switzerland

Current Opinion in Genetics & Development 2009, Volume 19, pg. 180–186

Summary

An increasing number of studies indicate that chromosomes are spatially organized in the interphase nucleus and that certain genes tend to occupy characteristic zones of the nuclear volume. FISH studies in mammalian cells suggest a differential localization of active and inactive loci, with inactive heterochromatin being largely perinuclear. Recent genome-wide mapping techniques confirm that the nuclear lamina, which lies beneath the nuclear envelope, interacts preferentially with silent genes. To address the functional significance of spatial compartmentation, gain-of-function assays in which chromatin is targeted to the nuclear periphery have now been carried out. Such experiments yield coherent models in yeast, however conflicting results in mammalian cells leave many questions unanswered. Nevertheless, the recent discovery that evolutionarily conserved inner nuclear membrane proteins support peripheral anchoring of yeast heterochromatin, suggests that certain principles of nuclear organization may hold true from yeast to human.

author contributions: BT, PM and SG wrote the manuscript. PM designed the figures

The nuclear envelope – a scaffold for silencing?

Benjamin D Towbin, Peter Meister and Susan M Gasser

An increasing number of studies indicate that chromosomes are spatially organized in the interphase nucleus and that some genes tend to occupy characteristic zones of the nuclear volume. FISH studies in mammalian cells suggest a differential localization of active and inactive loci, with inactive heterochromatin being largely perinuclear. Recent genome-wide mapping techniques confirm that the nuclear lamina, which lies beneath the nuclear envelope, interacts preferentially with silent genes. To address the functional significance of spatial compartmentation, gain-of-function assays in which chromatin is targeted to the nuclear periphery have now been carried out. Such experiments yielded coherent models in yeast; however, conflicting results in mammalian cells leave it unclear whether these concepts apply to higher organisms. Nevertheless, the recent discovery that evolutionarily conserved inner nuclear membrane proteins support the peripheral anchoring of yeast heterochromatin suggests that certain principles of nuclear organization may hold true from yeast to man.

Addresses

Friedrich Miescher Institute for Biomedical Research, Maulbeerstrasse 66, CH-4058 Basel, Switzerland

Corresponding author: Gasser, Susan M (susan.gasser@fmi.ch)

Current Opinion in Genetics & Development 2009, **19**:180–186

This review comes from a themed issue on
Chromosomes and expression mechanisms
Edited by Marie-Laure Caparros, Amanda Fisher and Matthias
Merkenschlager

Available online 19th March 2009

0959-437X/\$ – see front matter

© 2009 Elsevier Ltd. All rights reserved.

DOI [10.1016/j.gde.2009.01.006](https://doi.org/10.1016/j.gde.2009.01.006)

Introduction

The cell nucleus contains the essential genetic information of an organism and is responsible for the expression, duplication, and repair of this precious material. Its structure is defined by a double lipid bilayer studded with nuclear pores, which allow macromolecular trafficking in and out of the nuclear compartment. The outer bilayer of the nuclear envelope (NE) closely resembles the endoplasmic reticulum, while the inner nuclear membrane (INM) is specialized to meet the unique nuclear structural and functional needs [1]. In higher eukaryotes, the spherical shape of the nucleus is maintained by a dense network of specialized intermediate filaments, the

nuclear lamins. Lamins extend from pore to pore, providing rigidity and a platform for the binding of a large number of lamin-associated proteins and specific genomic domains. A small fraction of lamins are found at internal sites in the nucleus, where again they are thought to organize genomic function [2]. Plants and lower, single-celled organisms do not have nuclear lamins, although other structural proteins of the INM are conserved both in primary structure and in function. In particular, the nuclear pore complex, an elaborate machine for macromolecular transport, harbors many highly conserved proteins [3].

Given this structural conservation it is to be expected that the functions of the NE are also conserved. Indeed, it has long been recognized that dense-staining, transcriptionally silent heterochromatin tends to lie next to the NE or surround the nucleolus, and is specifically excluded from nuclear pores. This has been demonstrated for the repetitive noncoding sequences of vertebrates, and also for silent telomeric chromatin in yeast [4].

Recently, genome-wide techniques have allowed the exploration of sequences and proteins involved in this organization of heterochromatin in higher eukaryotes [5[•],6[•]] as well as in yeast [7]. A number of important questions have emerged from these studies: Does peripheral localization reflect a passive exclusion of heterochromatin from active zones, or do proteins that bind or nucleate heterochromatin have functional anchorage sites at the nuclear periphery? Do all types of silent chromatin bind the NE? Does positioning contribute actively to either heterochromatin establishment or maintenance? Recent reports showing that highly transcribed genes are actively recruited to nuclear pores [7–11] further complicate the picture. How are active and inactive domains kept apart in the nucleus? Nuclear pore attachment has been implicated in providing a boundary function to limit the spread of heterochromatin [12]. This imposes a further question: is localization essential for boundary function or does pore association occur by default?

Correlative evidence has long been used to argue that subnuclear repositioning of genes influences their transcriptional activity. However, such studies cannot directly prove the functional relevance of nuclear architecture. To demonstrate that functional read-outs stem from structural changes one must both perturb nuclear architecture genetically and evaluate gain-of-function assays, for example by tethering chromatin to the nuclear periphery. Such spatial targeting of chromatin was first applied in budding yeast a decade ago [13] and has recently been adapted to experiments in cultured mammalian cells [14[•],15[•],16[•]]. Here,

we review these recent experiments and discuss them in view of genetic studies of the nuclear periphery in yeast.

Gene organization along the chromosome arm: functional domains

Chromatin is a contiguous fiber of compact structure and limited flexibility [17]. Therefore, the relocation of a locus to a specific nuclear compartment will inevitably influence the subnuclear position of neighboring genes, encompassing several megabases in mammalian cells [15^{••}]. Consequently, if subnuclear position plays a role in gene regulation, there may be evolutionary pressure toward a linear grouping of coregulated genes along the chromosome arm. A classic example is the linear alignment of the mammalian *HOX* genes, which are arranged in the order of their spatio-temporal activation during limb development [18]. Recent genome-wide analyses indicate that highly transcribed genes are frequently found in clusters [19,20] and that tissue-specific genes are also grouped along the chromosome in higher eukaryotes [21–24]. In *Drosophila*, a computational analysis of 30 occupancy maps extended this observation to chromatin-associated proteins and histone modifications. This study showed that at least 50% of all fly genes are organized in chromosomal domains in which genes bear a similar epigenetic status. Interestingly, the enrichment of common functional annotation keywords (Gene Ontology terms) associated with genes organized in this manner further supported the idea that genes with a common function are grouped into chromosomal units [25[•]].

Genome-wide studies on nuclear organization

Datasets obtained from microscopic analysis of gene position will never be sufficiently large to test generally whether the transcriptional activity of chromosomal domains correlates with their subnuclear position. However, genome-wide tagging methods such as DamID [26–28] have been used as an alternative method to determine the molecular association of genes with the nuclear lamina. In brief, lamin is expressed as a fusion to the *E. coli* *dam* methylase, which exclusively methylates adenines. DNA fragments located close to the nuclear lamina are then amplified by a methylation-specific PCR protocol and identified by hybridization to microarrays. This method was recently used to map genomic interactions with B-type lamins in *Drosophila* Kc cells [5^{••}] and human fibroblasts [6^{••}].

In *Drosophila* cells, as well as human fibroblasts, transcriptionally silent genes were found strongly enriched in the lamin-associated fraction. These lamin-bound genes clustered in domains of approximately 500 kb, in agreement with the domain-based model for genome architecture. These domains were depleted for active chromatin marks, were typically flanked by binding sites of the insulator protein CTCF and by CpG islands [6^{••}], and frequently contained coregulated genes [5^{••}].

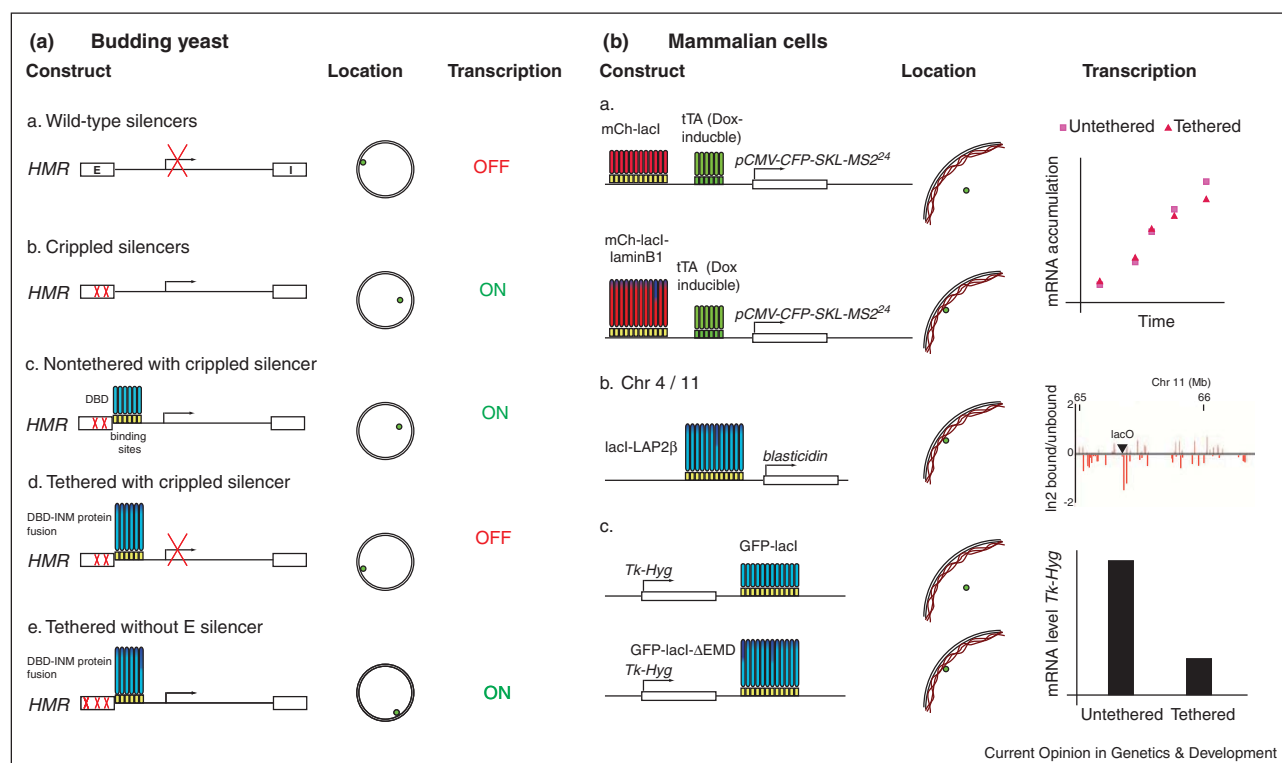
These studies have shown that the association of silent genes with the nuclear periphery is true not only for the handful of genes analyzed by microscopic approaches, but is valid genome-wide. Key questions remaining are what function heterochromatic clustering at the periphery might serve, and which factors determine the peripheral association of silent genes. Studies done with yeast indicate that the structural proteins that form heterochromatin themselves anchor silent loci to the periphery. Indeed, a silenced gene can attach to the periphery even when excised from its genomic context [29]. However, one should not conclude from this that peripheral association is merely a consequence of repression without any functional impact. It is conceivable that the clustering of heterochromatin at the nuclear periphery stabilizes the silent state or helps ensure its epigenetic propagation, for instance by influencing chromatin assembly after replication [30]. The best way to experimentally assess the function of nuclear organization is to modify a gene's subnuclear position. Below, we summarize results obtained using such approaches.

Lessons from genetic manipulation of yeast and flies

Early evidence for a regulatory role of nuclear organization stems from the study of a *Drosophila* translocation mutant allele (*bw^D*), which contains a block of heterochromatic sequence inserted at the *brown* locus. The mutation causes *brown* to associate with centromeric heterochromatin [31,32]. In animals heterozygous for *bw^D*, the wild-type allele also associated *in trans* with centromeric heterochromatin owing to the somatic pairing of homologous *Drosophila* chromosomes. Coincident with this association, the wild-type *brown* locus was silenced in a variegated manner. Similarly, silent mating-type loci (*HML* and *HMR*) associate *in trans* with telomeric repeats in yeast [33].

The influence of gene position on the silent mating-type locus *HMR* was assessed more directly in *S. cerevisiae* about 10 years ago [13]. Repression of this locus can be alleviated by the partial disruption of a *cis*-acting silencer element (Figure 1(a)b). However, silencing is restored when *HMR* is artificially recruited to the NE by the expression of a recombinant protein that specifically binds a sequence motif inserted next to *HMR* (Figure 1(a)d). The proposed mechanism for this facilitated silencing was that the perinuclear tethering positioned *HMR* near telomeric foci that sequester the silencing factors (SIR factors) [34]. In support of this concept, it was recently shown that peripheral tethering is unable to restore silencing in a genetic background in which SIR factors are dispersed from foci [35[•]]. However, placing a gene near SIR foci is not sufficient to cause gene repression, as the *HMR* locus lacking silencer elements is still expressed when recruited to the NE (Figure 1(a)e)

Figure 1



Artificial tethering of chromatin at the nuclear periphery in yeast and mammalian cells. **(a)** Transcription of tethered loci at the nuclear envelope in budding yeast. a. The wild-type silent mating-type locus *HMR*, encoding the mating pheromone is naturally silenced in yeast. The gene is flanked by two silencers, E and I, which target the locus to the nuclear periphery. b. Partial disruption of the E silencer leads to gene expression and delocalization of the locus away from the nuclear envelope. c. Targeting of the locus is achieved by the insertion of binding sites for a DNA binding domain (DBD). Binding of the DBD alone has no effect on gene expression and subnuclear localization. d. Targeting of the DBD (light blue) fused to an inner nuclear membrane protein (dark blue) leads to the relocation of *HMR* to the nuclear envelope. Relocation of a crippled silencer to the nuclear rim can restore silencing. e. This displacement has no effect if the E silencer is entirely removed. This shows the need for *cis*-acting factors for nucleation of silencing. **(b)** Tethering systems used to target chromatin to the nuclear lamina in mammalian cells. a. The system set up by Kumaran and Spector allows one to follow in real time and in live cells inducible transcription and translation of a gene using fluorescent reporters. The locus can be targeted using a fusion between a lac repressor and laminB1. The authors show that the induction rate is similar whether the construct is tethered to the lamina or not. However, tethering decreases the efficiency of induction, since only 70% of the genes can be activated, compared to 90% in the untethered condition. b. A fusion protein between lacI and the lamin associated protein LAP2β is used by Finlan et al. to monitor the effects of peripheral tethering. Expression of a transgenic reporter (blastidicin) is decreased by 20–30%. Transcription of most flanking genes is unaffected, except for three genes which show significantly reduced mRNA levels. c. Reddy et al. use a fusion protein with another lamin binding protein, Emerin. A truncated form of Emerin is used that has no transcriptional modulatory function. Tethering a reporter gene (*Hyg*) at the nuclear lamina decreases the transcription level significantly.

[13]. Thus, anchorage near SIR pools at the nuclear envelope facilitates, but is not sufficient for repression.

The influence of peripheral attachment on gene transcription in mammalian cells

Three laboratories have recently adapted such peri-nuclear targeting experiments to mammalian cell culture systems (Figure 1(b)) [14^{••},15^{••},16^{••}]. All three studies made use of cell lines carrying stable genomic integrations of tandem repeats of lac operator (lacO) sites. Through expression of the lacO-binding lacI protein fused directly to Lamin B1 or to the lamin-associated INM proteins Emerin and Lap2β, the lacO arrays and adjacent genes could be tethered to the NE.

The laboratory of David Spector compared the activation dynamics of a doxycyclin-inducible transgene that encodes a fluorescently marked RNA, in the presence or absence of tethering by a LaminB1–lacI fusion (Figure 1(b)a) [14^{••}]. Careful quantification of fluorescence intensity did not reveal any effect of peripheral location on the kinetics of mRNA accumulation in individual cells. However, the fraction of cells in which the transgene could be activated at all was reduced from 90% to 70%.

Similarly, the Bickmore laboratory observed that peripheral tethering using a lacI–Lap2β fusion led to a reduction in the fraction of cells in which a lacO-tagged transgene showed an RNA-FISH signal, and the corresponding

mRNA levels were decreased by 20–30% (Figure 1(b)b) [15^{••}]. More importantly, the expression of most endogenous genes in the neighborhood of the lacO array remained unchanged upon tethering, with the exception of three genes located within 5 Mb of the lacO array whose mRNA levels dropped between 35% and 50%.

The Singh laboratory found that two genes located next to lacO repeats had reduced expression levels when the locus was recruited to the periphery by an Emerin–lacI fusion (Figure 1(b)c) [16^{••}]. Again, the majority of the neighboring genes were unaffected. In contrast to the two other studies, however, the expression of a transgenic reporter located next to the lacO array was robustly reduced by 75%.

In summary, all three studies show that, as in yeast [13,36,37], attachment to the nuclear periphery does not generally preclude transcriptional activity. Nonetheless, the expression of at least some genes is influenced by peripheral tethering. It is likely that the fraction of affected genes is underestimated because of experimental noise that can obscure small expression changes of tethered genes. Moreover, in all cases in which endogenous gene activity was measured, only one of the two homologs was lacO-tagged. Consequently, even complete silencing of a tethered locus would generate only a 50% reduction in expression. Furthermore, the changes in activity may be masked by upregulation of the non-targeted allele through regulatory feedback loops.

It remains to be explored why only a subset of the reporter genes is affected by peripheral attachment. We note that a different peripheral anchor was used in each study, and it is possible that the anchor itself contributes to silencing [14^{••},15^{••},16^{••}]. Different anchoring proteins or pathways may function to create distinct microdomains with various levels of transcriptional repression (Figure 2(b)).

Inherent promoter strength could also account for the differential effects of peripheral attachment. For instance, it is well established in yeast that strong promoters block the spread of heterochromatin [38,39]. Similarly, in human cells, active promoters were often found at the edge of lamin-associated chromosomal domains [6^{••}], and in flies it was shown that not all genes respond equally to association with heterochromatic domains [40]. Thus, there is likely to be a complex relationship between gene promoter strength and the effects of tissue-specific factors that influence whether a gene's spatial position affects its expression.

What mechanism confers repression on tethered genes? A simple explanation would be that silencing is not induced by subnuclear relocation, but by the recruitment of transcriptional repressors that are known to bind the INM proteins used for tethering [41]. However, this model was

ruled out for Emerin, since the targeting of an Emerin–lacI construct lacking its transmembrane domain failed to induce gene silencing [16^{••}]. Alternatively, gene repression may be stabilized at the nuclear lamina by interaction with other heterochromatic domains *in trans*. In such a model, the NE could serve as a platform for efficient chromatin packing, and its silencing properties would depend on heterochromatin itself.

Finally, a combination of these two models is possible: Lap2 β has been shown to directly interact with a histone deacetylase (HDAC) [42], and inhibition of HDAC activity by Trichostatin A (TSA) was able to relieve Lap2 β tethering-induced repression [15^{••}]. In this experiment the tethered locus remained attached at the periphery, whereas in *Drosophila* Kc cells naturally occurring heterochromatic domains were released from the nuclear periphery by the treatment with TSA [5^{••}]. Together these studies suggest a model in which peripheral localization facilitates silencing owing to a peripherally sequestered HDAC activity. At the same time, deacetylated histones themselves may serve as a signal to anchor chromatin at the NE.

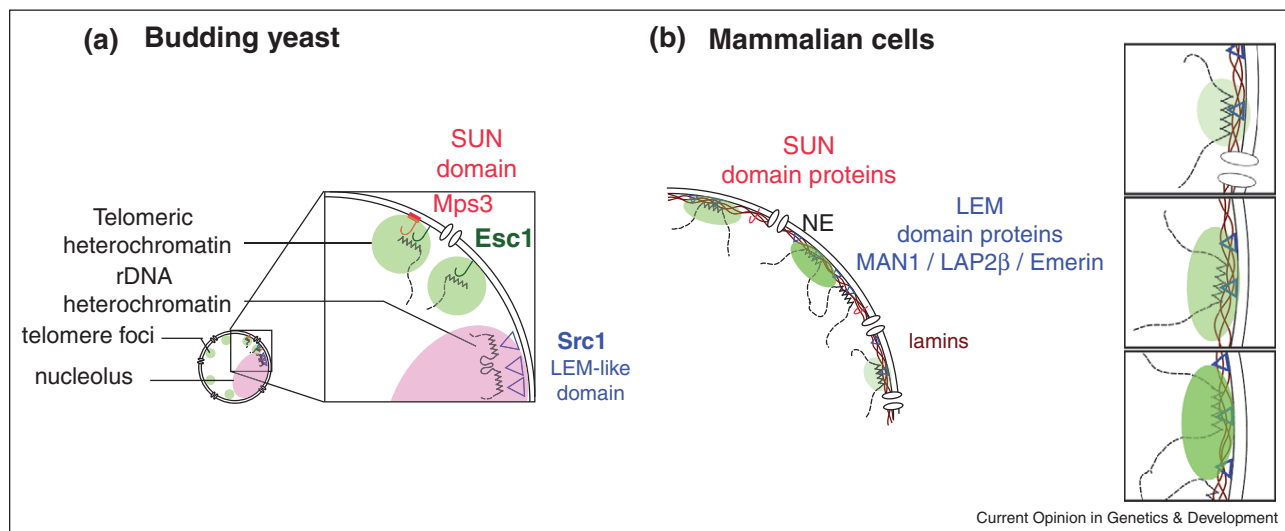
This model is reminiscent of the mechanism suggested for telomere silencing in yeast. In brief, yeast telomeres are maintained at the nuclear periphery by two partially redundant pathways that depend on the DNA-end binding heterodimer Ku70/Ku80, and a structural component of yeast silent chromatin — the silent information regulator Sir4 [43]. In the so-called ‘Circe Effect’, the nuclear periphery facilitates gene repression by clustering telomeric repeats, which in turn sequester and accumulate the factors required for silencing, including the histone deacetylase Sir2 [30]. Silencing and tethering are thus interdependent: repression promotes attachment, and attachment favors repression as long as telomeric tethers are in place [35[•],44].

The yeast nuclear envelope: conserved functions in the absence of lamins

Although an understanding of silencing at the nuclear periphery in yeast is conceptually informative, the mechanistic relevance for mammalian systems has been debated since yeast lack nuclear lamins. Challenging this view, members of evolutionary conserved SUN-domain and LEM-domain INM-protein families have recently been described to play a role in heterochromatin localization and genome stability in budding yeast (Figure 2(a)) [45[•],46[•],47^{••}].

Members of the SUN-domain family are transmembrane proteins that span the INM and which are anchored in place by binding lamins or other factors. The C-terminal SUN domain of these proteins interacts with Nesprins in the intermembrane space, which forms a link to the cytoplasm through the outer nuclear membrane

Figure 2



SUN and LEM domain proteins organize chromatin at the nuclear periphery in both yeast and mammalian cell nuclei. **(a)** In budding yeast nuclei, where nuclear lamins are absent, telomeres are clustered together at the nuclear periphery (green domains). This depends on Esc1 and the INM SUN-domain protein, Mps3. The nucleolus (red domain) is maintained close to the nuclear envelope by Src1, a LEM-domain family protein. For both proteins, however, no direct interaction with chromatin has been shown to date. **(b)** In mammalian cell nuclei, LEM-domain and SUN-domain containing proteins interact with nuclear lamins and probably indirectly with chromatin (for review, see [50]). LEM-domain proteins may create microdomains at the nuclear periphery. These microdomains may vary in their silencing efficiency which would explain the differences between the three tethering experiments presented in the text. More experiments will have to be carried out using different targeting constructs for tethering of the same reporter to resolve whether anchor specificity or reporter dependent characteristics, such as promoter strength, lead to the variable results.

(ONM), while the N-terminus reaches into the nucleoplasm [48]. Bupp and coworkers have recently shown that even in yeast, where no lamin is present, the SUN-domain protein Mps3 is involved in silent telomere anchoring. The N-terminal domain of Mps3 interacts with Sir4 by pull-down and yeast-two-hybrid experiments, although it is unclear whether this interaction is direct. Via an adjacent domain, called the PAD domain, Sir4 also interacts with the NE protein Esc1 [34]. Nonetheless, in an *mps3* mutant lacking the N-terminal domain, telomeres are partially detached from the periphery, weakly compromising telomeric repression [45[•]].

Similarly, a role in gene regulation has been shown for a yeast LEM-domain protein by Grund and coworkers. The three types of LEM-domain proteins present in mammalian cells are sequestered at the INM by nuclear lamins. Two of these, Lap2β and Emerin, have an effect on gene expression when tethered to a locus (see above). The yeast protein Src1 (also called Heh1 [47^{••}]) shares homology with the third mammalian LEM protein Man1. Src1 is found at subtelomeric regions, the silent mating-type loci, and the heterochromatin-like rDNA. Gene deletion of *src1* does not affect telomere localization or silencing, although a group of subtelomeric genes is misregulated. This again suggests a role for NE association in gene regulation [46[•]]. Derepression of subtelomeric

genes was also shown to result from telomere delocalization [35[•]].

Independently, the group of Danesh Moazed reported a function of Src1 at the tandemly repeated yeast rDNA locus [47^{••}]. The deletion of *src1* causes decondensation of the rDNA and partial release of the nucleolus from the nuclear periphery. This release does not affect the silencing of a PolIII-transcribed reporter within the rDNA array, which is maintained by the Sir2 HDAC. Instead, the rDNA showed increased recombination rates and changes in array size [47^{••}]. This finding supports another model whereby the sequestration at the nuclear periphery plays a role in the regulation of DNA repair and genomic stability [49[•]], rather than gene repression. It is not clear whether these two phenomena are linked.

Conclusions

Recent advances have shown that clusters of silent genes associate with the nuclear lamina in mammalian cells [6^{••}]. It is likely that the peripheral localization of heterochromatin is both a cause and a consequence of its repressed state. Careful analysis in mammalian cells using identical reporter systems with a range of peripheral anchors is needed to resolve the conflicts among current results. Nonetheless, these important studies show that, as demonstrated in budding yeast, the positioning of

chromatin at the nuclear periphery can affect gene expression. On the other hand, new studies in yeast reveal another type of perinuclear anchoring that helps to stabilize the genome, rather than conferring transcriptional repression. Whether this also parallels events in higher eukaryotic cells remains to be seen.

Acknowledgements

We apologize to the many workers in the field whose work we could not cover owing to space constraints. We thank Vincent Dion, Stephanie Kueng, Shigeki Nagai, and Brietta Pike for carefully reading the manuscript and for helpful comments. The Gasser laboratory is supported by the EU FP6 Epigenome and the Novartis Research Foundation.

References and recommended reading

Papers of particular interest, published within the period of review, have been highlighted as:

- of special interest
- of outstanding interest

1. Schirmer EC, Florens L, Guan T, Yates JR III, Gerace L: **Nuclear membrane proteins with potential disease links found by subtractive proteomics.** *Science* 2003, **301**:1380-1382.
2. Dechat T, Pfliegerhaer K, Sengupta K, Shimi T, Shumaker DK, Solimando L, Goldman RD: **Nuclear lamins, major factors in the structural organization and function of the nucleus and chromatin.** *Genes Dev* 2008, **22**:832-853.
3. D'Angelo MA, Hetzer MW: **Structure, dynamics and function of nuclear pore complexes.** *Trends Cell Biol* 2008, **18**:456-466.
4. Palladino F, Laroche T, Gilson E, Axelrod A, Pillus L, Gasser SM: **SIR3 and SIR4 proteins are required for the positioning and integrity of yeast telomeres.** *Cell* 1993, **75**:543.
5. Pickersgill H, Kalverda B, de Wit E, Talhout W, Fornerod M, van Steensel B: **Characterization of the *Drosophila melanogaster* genome at the nuclear lamina.** *Nat Genet* 2006, **38**:1005.
This is the first study demonstrating genome-wide that silent genes have an increased chance to interact with the nuclear lamina in *Drosophila* Kc cells. Lamin-associated genes were released upon treatment with an HDAC inhibitor and upon differentiation-induced activation.
6. Guelen L, Pagie L, Brasset E, Meuleman W, Faza MB, Talhout W, Eussen BH, de Klein A, Wessels L, de Laat W *et al.*: **Domain organization of human chromosomes revealed by mapping of nuclear lamina interactions.** *Nature* 2008, **453**:948-951.
The authors applied genome-wide DamID to map lamin interacting genes in human fibroblasts, as well as the characteristics of the borders of lamin-associated domains. Lamin-associated genes clustered in domains of 500 kb in size that were enriched in transcriptionally silent genes.
7. Casolari JM, Brown CR, Komili S, West J, Hieronymus H, Silver PA: **Genome-wide localization of the nuclear transport machinery couples transcriptional status and nuclear organization.** *Cell* 2004, **117**:427.
8. Taddei A, Van Houwe G, Hediger F, Kalck V, Cubizolles F, Schober H, Gasser SM: **Nuclear pore association confers optimal expression levels for an inducible yeast gene.** *Nature* 2006, **441**:774.
9. Brickner JH, Walter P: **Gene recruitment of the activated INO1 locus to the nuclear membrane.** *PLoS Biol* 2004, **2**:e342.
10. Cabal GG, Genovesio A, Rodriguez-Navarro S, Zimmer C, Gadal O, Lesne A, Buc H, Feuerbach-Fournier F, Olivo-Marin J-C, Hurt EC *et al.*: **SAGA interacting factors confine sub-diffusion of transcribed genes to the nuclear envelope.** *Nature* 2006, **441**:770.
11. Dieppl G, Iglesias N, Stutz F: **Cotranscriptional recruitment to the mRNA export receptor Mex67p contributes to nuclear pore anchoring of activated genes.** *Mol Cell Biol* 2006, **26**:7858-7870.
12. Ishii K, Arib G, Lin C, Van Houwe G, Laemmli UK: **Chromatin boundaries in budding yeast: the nuclear pore connection.** *Cell* 2002, **109**:551.
13. Andrusis ED, Neiman AM, Zappulla DC, Sternglanz R: **Perinuclear localization of chromatin facilitates transcriptional silencing.** *Nature* 1998, **394**:592.
14. Kumaran RI, Spector DL: **A genetic locus targeted to the nuclear periphery in living cells maintains its transcriptional competence.** *J Cell Biol* 2008, **180**:51-65.
The authors show using a system where they can track the RNA production that a viral promoter-driven transgene has similar activation dynamics when artificially tethered to the nuclear lamina. However, the proportion of cells where the locus can be activated is reduced when tethered.
15. Finlan LE, Sproul D, Thomson I, Boyle S, Kerr E, Perry P, Ylstra B, Chubb JR, Bickmore WA: **Recruitment to the nuclear periphery can alter expression of genes in human cells.** *PLoS Genet* 2008, **4**:e1000039.
This study uses a Lap2 β -LacI fusion to artificially tether a lacO-tagged locus to the nuclear periphery. As a consequence, the transcription of a fraction of genes near the tethered locus shows reduced expression levels, in an HDAC-dependent manner.
16. Reddy KL, Zullo JM, Bertolino E, Singh H: **Transcriptional repression mediated by repositioning of genes to the nuclear lamina.** *Nature* 2008, **452**:243-247.
An Emerin-lacI fusion is used to relocate a lacO-tagged transgene to the nuclear periphery. A linked reporter gene sees its expression reduced by 75%.
17. Langowski J, Heermann DW: **Computational modeling of the chromatin fiber.** *Semin Cell Dev Biol* 2007, **18**:659-667.
18. Duboule D: **The rise and fall of Hox gene clusters.** *Development* 2007, **134**:2549-2560.
19. Caron H, Schaik Bv, Mee Mvd, Baas F, Riggins G, Sluis Pv, Hermus M-C, Asperen Rv, Boon K, Voute PA *et al.*: **The human transcriptome map: clustering of highly expressed genes in chromosomal domains.** *Science* 2001, **291**:1289-1292.
20. Versteeg R, van Schaik BDC, van Batenburg MF, Roos M, Monajemi R, Caron H, Bussemaker HJ, van Kampen AHC: **The human transcriptome map reveals extremes in gene density, intron length, GC content, and repeat pattern for domains of highly and weakly expressed genes.** *Genome Res* 2003, **13**:1998-2004.
21. Roy PJ, Stuart JM, Lund J, Kim SK: **Chromosomal clustering of muscle-expressed genes in *Caenorhabditis elegans*.** *Nature* 2002, **418**:975-979.
22. Kosak ST, Scalzo D, Alworth SV, Li F, Palmer S, Enver T, Lee JSJ, Groudine M: **Coordinate gene regulation during hematopoiesis is related to genomic organization.** *PLoS Biol* 2007, **5**:e309.
23. Spellman P, Rubin G: **Evidence for large domains of similarly expressed genes in the *Drosophila* genome.** *J Biol* 2002, **1**:5.
24. Boutanaev AM, Kalmykova AI, Shevelov YY, Nurmsky DI: **Large clusters of co-expressed genes in the *Drosophila* genome.** *Nature* 2002, **420**:666-669.
25. de Wit E, Braunschweig U, Greil F, Bussemaker HJ, van Steensel B: **Global chromatin domain organization of the *Drosophila* genome.** *PLoS Genet* 2008, **4**:e1000045.
Computational cross analysis of 30 occupancy maps of chromatin-associated proteins is used to define domain architecture of the genome in *Drosophila* Kc cells. Gene function analysis shows enrichment for similar functions in one domain.
26. Gottschling DE: **Telomere-proximal DNA in *Saccharomyces cerevisiae* is refractory to methyltransferase activity in vivo.** *Proc Natl Acad Sci U S A* 1992, **89**:4062-4065.
27. van Steensel B, Delrow J, Henikoff S: **Chromatin profiling using targeted DNA adenine methyltransferase.** *Nat Genet* 2001, **27**:304-308.
28. Steensel Bv, Henikoff S: **Identification of in vivo DNA targets of chromatin proteins using tethered Dam methyltransferase.** *Nat Biotechnol* 2000, **18**:424-428.

29. Gartenberg MR, Neumann FR, Laroche T, Blaszczyk M, Gasser SM: **Sir-mediated repression can occur independently of chromosomal and subnuclear contexts.** *Cell* 2004, **119**:955.
30. Gasser SM, Hediger F, Taddei A, Neumann FR, Gartenberg MR: **The function of telomere clustering in yeast: the Circe Effect.** *Cold Spring Harb Symp Quant Biol* 2004, **69**:327-338.
31. Csink AK, Henikoff S: **Genetic modification of heterochromatic association and nuclear organization in Drosophila.** *Nature* 1996, **381**:529.
32. Dernburg AF, Broman KW, Fung JC, Marshall WF, Philips J, Agard DA, Sedat JW: **Perturbation of nuclear architecture by long-distance chromosome interactions.** *Cell* 1996, **85**:745.
33. Gotta M, Laroche T, Formenton A, Maillet L, Scherthan H, Gasser SM: **The clustering of telomeres and colocalization with Rap1, Sir3, and Sir4 proteins in wild-type Saccharomyces cerevisiae.** *J Cell Biol* 1996, **134**:1349-1363.
34. Taddei A, Gasser SM: **Multiple pathways for telomere tethering: functional implications of subnuclear position for heterochromatin formation.** *Biochim Biophys Acta — Gene Struct Expr* 2004, **1677**:120.
35. Taddei A, Van Houwe G, Nagai S, Erb I, Van Nimwegen E, Gasser SM: **The functional importance of telomere clustering: global changes in gene expression result from SIR factor dispersion.** *Genome Res* 2009, Epub Jan 29. doi:10.1101/gr.083881.108.
Perinuclear tethering assays for silencing in yeast, pioneered by Sternglanz and coworkers [13] are examined here in more detail. It is shown that the sequestration of SIR factors by clustered telomeres is essential for favoring repression at the nuclear envelope. Dispersed SIR factors lead to misregulation genome-wide.
36. Tham W-H, Wytthe JSB, Ferrigno PK, Silver PA, Zakian VA: **Localization of yeast telomeres to the nuclear periphery is separable from transcriptional repression and telomere stability functions.** *Mol Cell* 2001, **8**:189.
37. Mondoux MA, Scaife JG, Zakian VA: **Differential nuclear localization does not determine the silencing status of Saccharomyces cerevisiae telomeres.** *Genetics* 2007, **177**:2019-2029.
38. Aparicio OM, Gottschling DE: **Overcoming telomeric silencing: a trans-activator competes to establish gene expression in a cell cycle-dependent way.** *Genes Dev* 1994, **8**:1133-1146.
39. Lee S, Gross DS: **Conditional silencing: the HMRE mating-type silencer exerts a rapidly reversible position effect on the yeast HSP82 heat shock gene.** *Mol Cell Biol* 1993, **13**:727-738.
40. Sage BT, Wu MD, Csink AK: **Interplay of developmentally regulated gene expression and heterochromatic silencing in trans in Drosophila.** *Genetics* 2008, **178**:749-759.
41. Verstraeten VL, Broers JL, Ramaekers FC, van Steensel MA: **The nuclear envelope, a key structure in cellular integrity and gene expression.** *Curr Med Chem* 2007, **14**:1231.
42. Somech R, Shaklai S, Geller O, Amariglio N, Simon AJ, Rechavi G, Gal-Yam EN: **The nuclear-envelope protein and transcriptional repressor LAP2[beta] interacts with HDAC3 at the nuclear periphery, and induces histone H4 deacetylation.** *J Cell Sci* 2005, **118**:4017-4025.
43. Hediger F, Neumann FR, Van Houwe G, Dubrana K, Gasser SM: **Live imaging of telomeres: yKu and Sir proteins define redundant telomere-anchoring pathways in yeast.** *Curr Biol* 2002, **12**:2076.
44. Taddei A, Hediger F, Neumann FR, Bauer C, Gasser SM: **Separation of silencing from perinuclear anchoring functions in yeast Ku80, Sir4 and Esc1 proteins.** *EMBO J* 2004, **23**:1301-1312.
45. Bupp JM, Martin AE, Stensrud ES, Jaspersen SL: **Telomere anchoring at the nuclear periphery requires the budding yeast Sad1-UNC-84 domain protein Mps3.** *J Cell Biol* 2007, **179**:845-854.
This study identifies the conserved SUN-domain containing protein Mps3 as a peripheral anchor protein for yeast telomeres. This is of particular interest, as molecular conservation of chromatin anchoring mechanisms between mammals and yeast has previously been unclear.
46. Grund SE, Fischer T, Cabal GG, Antunez O, Perez-Ortin JE, Hurt E: **The inner nuclear membrane protein Src1 associates with subtelomeric genes and alters their regulated gene expression.** *J Cell Biol* 2008, **182**:897-910.
The authors identify the gene *SRC1* as a yeast homolog of the mammalian lamin-associated protein Man1. Interestingly, even though yeast does not have lamins, its function to interact with heterochromatin at the nuclear envelope seems to be conserved.
47. Mekhail K, Seebacher J, Gygi SP, Moazed D: **Role for perinuclear chromosome tethering in maintenance of genome stability.** *Nature* 2008, **456**:667-670.
The study reports a function of the LEM-domain-containing protein Src1 (see Ref. [46]) in the maintenance of structural integrity and peripheral attachment of the nucleolus in *S. cerevisiae*. This peripheral attachment plays a role in suppressing recombination at the repetitive rDNA locus.
48. Tzur YB, Wilson KL, Gruenbaum Y: **SUN-domain proteins: 'Velcro' that links the nucleoskeleton to the cytoskeleton.** *Nat Rev Mol Cell Biol* 2006, **7**:782-788.
49. Nagai S, Dubrana K, Tsai-Pflugfelder M, Davidson MB, Roberts TM, Brown GW, Varela E, Hediger F, Gasser SM, Krogan NJ: **Functional targeting of DNA damage to a nuclear pore-associated SUMO-dependent ubiquitin ligase.** *Science* 2008, **322**:597-602.
This study demonstrates that an association of DNA damage with the nuclear pore Nup84 complex and its associated SUMO-dependent ubiquitin ligase, both of which are conserved from yeast to human. These factors promote repair of breaks associated with replication forks.
50. Taddei A, Hediger F, Neumann FR, Gasser SM: **The function of nuclear architecture: a genetic approach.** *Annu Rev Genet* 2004, **38**:305-345.

Chapter 3: Repetitive transgenes in *C. elegans* accumulate heterochromatic marks and are sequestered at the nuclear envelope in a copy-number and lamin-dependent manner

Benjamin D. Towbin, Peter Meister, Brietta L. Pike and Susan M. Gasser

Friedrich Miescher Institute for Biomedical Research, Maulbeerstrasse 66, CH-4058 Basel, Switzerland

Cold Spring Harbor Symposia on Quantitative Biology, Volume 75, pg. 555-565

Summary

Chromatin is non-randomly distributed in nuclear space, yet the functional significance of this remains unclear. Here, we made use of transgenes carrying developmentally regulated promoters to study subnuclear gene positioning during development of *C. elegans*. We found that small transgenes (copy number ≤ 50) are randomly distributed in early embryonic nuclei, independent of promoter activity. However, in differentiated tissues, these same transgenes occupied specific subnuclear positions: when promoters are repressed, transgenes are found at the nuclear periphery, whereas active, developmentally regulated promoters are enriched in the nuclear core. The absence of specific transgene positioning in embryonic nuclei does not reflect an absence of proteins that mediate perinuclear sequestration: embryonic nuclei are able to sequester much larger transgene arrays (copy number 300-500) at the periphery. This size-dependent peripheral positioning of gene arrays in early embryos correlates with the accumulation of heterochromatic marks (H3K9me3 and H3K27me3) on large arrays. Interestingly, depletion of nuclear lamina components caused release of arrays from the nuclear envelope, and interfered with their efficient silencing. Our results suggest that developmentally silenced chromatin binds the nuclear lamina in a manner correlated with the deposition of heterochromatic marks. Peripheral sequestration of chromatin may in turn support the maintenance of silencing.

author contributions: BT did the experiments of figures 1-5. BP did the experiments in Figure 6. PM significantly contributed to the design of the experiments. BT, PM and SG wrote the manuscript.

Repetitive Transgenes in *C. elegans* Accumulate Heterochromatic Marks and Are Sequestered at the Nuclear Envelope in a Copy-Number- and Lamin-Dependent Manner

B.D. TOWBIN, P. MEISTER, B.L. PIKE, AND S.M. GASSER

Friedrich Miescher Institute for Biomedical Research, CH-4058 Basel, Switzerland

Correspondence: susan.gasser@fmi.ch

Chromatin is nonrandomly distributed in nuclear space, yet the functional significance of this remains unclear. Here, we make use of transgenes carrying developmentally regulated promoters to study subnuclear gene positioning during the development of *Caenorhabditis elegans*. We found that small transgenes (copy number ≤ 50) are randomly distributed in early embryonic nuclei, independent of promoter activity. However, in differentiated tissues, these same transgenes occupied specific subnuclear positions: When promoters are repressed, transgenes are found at the nuclear periphery, whereas active, developmentally regulated promoters are enriched in the nuclear core. The absence of specific transgene positioning in embryonic nuclei does not reflect an absence of proteins that mediate perinuclear sequestration: Embryonic nuclei are able to sequester much larger transgene arrays (copy number 300–500) at the periphery. This size-dependent peripheral positioning of gene arrays in early embryos correlates with the accumulation of heterochromatic marks (H3K9me3 and H3K27me3) on large arrays. Interestingly, depletion of nuclear lamina components caused release of arrays from the nuclear envelope and interfered with their efficient silencing. Our results suggest that developmentally silenced chromatin binds the nuclear lamina in a manner correlated with the deposition of heterochromatic marks. Peripheral sequestration of chromatin may, in turn, support the maintenance of silencing.

Differentiation of a pluripotent stem cell into specified cell types is a tightly regulated process that requires multiple layers of control. Cell identity is first set by the activation of tissue-specific gene programs. The expression status of a gene can subsequently be maintained by a local modification of chromatin structure through posttranslational modification of the histone octamer and binding of additional chromatin-associated factors (Boyer et al. 2006; Mohn and Schübeler 2009). Local modulation of chromatin structure may change a gene's accessibility to DNA-binding factors and to the transcriptional machinery and hence regulate its activity.

It has been postulated that the higher-order structure of chromatin, and its spatial organization within the nucleus, may also contribute to gene regulation, possibly independent of local chromatin structure and accessibility (Wilson and Berk 2010). In particular, the spatial separation of inactive loci from active genes in nuclear subdomains is thought to support their efficient repression by locally increasing the concentration of silencing factors (Gasser et al. 2004). Conversely, spatial separation may prevent promiscuous silencing that would occur by silencing factors bound to normally active genes (Taddei et al. 2009). Although specific genes have been found to interact with the nuclear pore and subnuclear bodies, the best evidence for a functional role of subnuclear organization in gene regulation concerns the association of facultative heterochromatin to the perinuclear lamina.

The nuclear lamina consists of a dense meshwork of intermediate filament proteins (lamins) that mechanically

maintain the spherical shape of the nucleus (Dechat et al. 2008). In addition to this morphological function, the nuclear lamina serves as a binding platform for various factors involved in transcriptional regulation and chromatin metabolism, supporting the idea of a regulatory role of perinuclear gene localization (Taddei et al. 2004). Moreover, scientific interest in the association of chromatin with the nuclear lamina has been fostered by the discovery of a large number of genetic diseases (laminopathies) that are caused by mutations in lamin itself or other structural components of the nuclear envelope (Verstraeten et al. 2007).

Historically, one addressed the functional implications of chromatin association to the nuclear lamina by describing the nature of lamina-bound chromatin. The earliest of these studies used electron microscopy to show that electron-dense material is in close proximity to the nuclear lamina (Busch 1966). Subsequently, a number of specific loci have been shown by fluorescent in situ hybridization (FISH) to specifically associate with the nuclear periphery when inactive (Spector 2003; Deniaud and Bickmore 2009). Most recently, a method termed DamID was applied to characterize the nature of DNA bound to the nuclear lamina on a genome-wide level in *Drosophila* embryos (Pickersgill et al. 2006) as well as human cell culture systems (Guelen et al. 2008; Peric-Hupkes et al. 2010). Together, these studies demonstrated that chromatin bound to the nuclear lamina is generally inactive and carries post-translational histone modifications characteristic of silent loci.

Complementing this correlative approach, several laboratories have artificially targeted specific loci to the nuclear periphery (Andrulis et al. 1998; Finlan et al. 2008; Kumaran and Spector 2008; Reddy et al. 2008). In all cases, at least a mild reduction in transcriptional activity was observed for some promoters, although the magnitude of repression varied from study to study and seemed to depend on the nature of the targeted promoter (for discussion, see Towbin et al. 2009). Tethering of chromosome segments to the nuclear envelope could identify a function of the nuclear lamina in repressing genes that are artificially recruited to it. However, these experiments did not address how genes are recruited to the nuclear envelope without an artificial anchor and whether positioning might be used during development to control cell-type-specific expression.

Here, we tracked the subnuclear position of transgenes that contain developmentally regulated promoters during development of the nematode *Caenorhabditis elegans*. We find that subnuclear localization of low-copy transgenes carrying developmentally regulated promoters depends on a cell's differentiation state: In early embryos, transgenes were randomly distributed through nuclear space, independent of promoter activity. In contrast, following differentiation, active and inactive promoters were spatially separated. Transgenes with inactive promoters were peripherally enriched, whereas transgenes with active developmentally regulated promoters were located in the nuclear interior. In contrast to low-copy transgenes, large repetitive gene arrays accumulated heterochromatic marks (H3K9me3 and H3K27me3) and were peripherally anchored in embryonic cells, correlating peripheral attachment with a heterochromatic state. Finally, we show that an intact nuclear envelope is required for efficient gene silencing because promoters located on transgene arrays are strongly up-regulated in animals depleted for the *C. elegans* lamin homolog LMN-1 or associated proteins.

GENERATION OF *LAC*O-TAGGED LOW-COPY TRANSGENES TO MONITOR SUBNUCLEAR GENE POSITION DURING *C. ELEGANS* DEVELOPMENT

We have recently established the nematode *C. elegans* as a genetically tractable model system to investigate the function and mechanism of subnuclear chromatin organization (Meister et al. 2010a). We made use of this system to identify *cis*-acting elements that drive peripheral gene attachment. Using microparticle bombardment, we generated transgenes of developmentally regulated promoters driving a fluorescent reporter (*mCherry* or *his-24::mCherry*) in specified tissues that are flanked by arrays of *lacO* sites. The subnuclear position of these transgenes can therefore be tracked by expression of GFP (green fluorescent protein)-LacI, which accumulates at *lacO* arrays to form a fluorescent focus (Straight et al. 1996). Furthermore, the transgenes contain the neuronal gene *unc-119*, which was used as a selection marker (Fig. 1).

Microparticle bombardment results in chromosomally integrated transgenes with a copy number between 1 and 50 copies (Praitis et al. 2001; Meister et al. 2010a). The

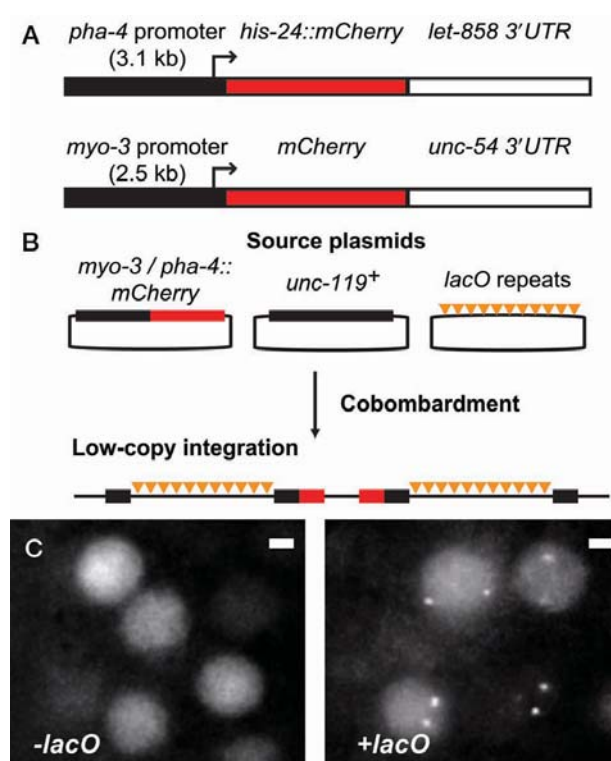


Figure 1. Visualization of *lacO*-tagged transgenes by GFP-LacI. (A) Developmental promoters used for generation of *lacO*-tagged transgenes. (B) Outline of transgenesis: Reporter transgenes of *pha-4* or *myo-3* promoter were cobombarded with the *unc-119* rescuing construct and repeats of 256 *lacO* sites. (C) *C. elegans* embryo expressing GFP-LacI only (left) or carrying in addition a *lacO*-tagged transgene insert (right). Bar, 1 μ m. (Adapted from Meister et al. 2010a.)

site of integration is random. This allows us to separate the localization potential of an individual promoter from the influence of surrounding genomic regions by analysis of several independent integration sites. Using this method, we generated multiple transgenes that harbor the muscle-specific promoter of the *myo-3* gene (2.5 kb upstream of ATG) or a fragment of the *pha-4* promoter that drives expression exclusively in the intestine (3.1 kb upstream of ATG). As a control, we included a strain that carries a *lacO*-tagged transgene with only the selection marker *unc-119*. We quantified the subnuclear distribution of these transgenes in embryonic cells as well as in three different differentiated tissues: muscle, intestine, and hypodermal and seam cells of ectodermal origin. Here, we focus our discussion on one of the *pha-4::his-24::mCherry* transgenes but emphasize that all of the transgenes that we generated behaved very similarly (Meister et al. 2010a).

LOW-COPY TRANSGENES RANDOMLY DISTRIBUTED IN EARLY EMBRYOS

To determine the subnuclear position of the bombardment-derived *pha-4* transgene during early developmental stages, we labeled transgenic *C. elegans* embryos with antibodies directed against the nuclear lamina (LMN-1) to mark the nuclear periphery and with GFP to visualize the

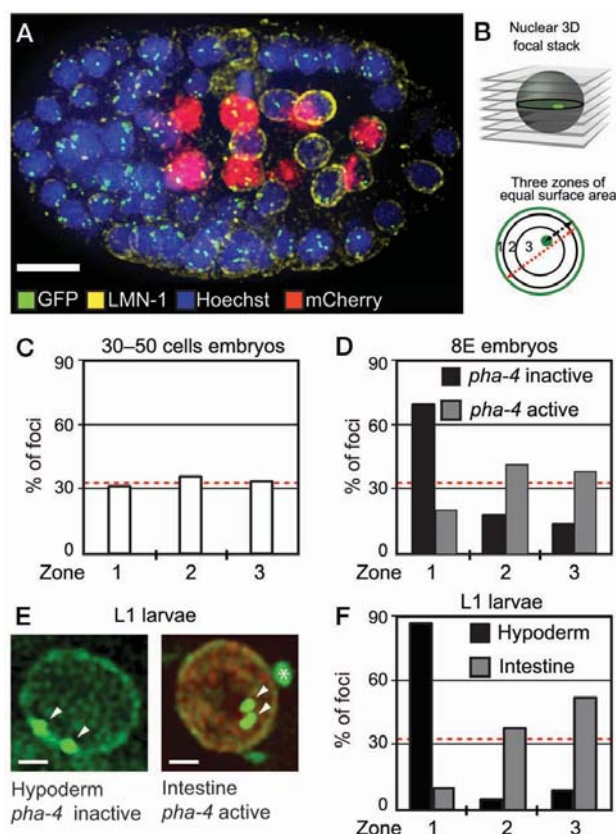


Figure 2. Differentiation-associated spatial separation of active and silent loci. (A) Maximum intensity projection of an 8E-stage *C. elegans* embryo carrying an integrated *lacO*-containing *pha-4::his-24-mCherry* transgene. The embryo is stained for LMN-1 (yellow), mCherry (red), GFP-LacI (green), and DNA (Hoechst blue). Bar, 5 μ m. (B) Quantification of radial spot position. Nuclear cross section at the focal plane with highest spot intensity is divided into three concentric zones of equal surface, with zone 1 being the outermost. Spots are then binned into these three zones, and a randomly localized spot is equally distributed among the three zones. (C,D,F) Quantification of radial distribution of *pha-4* transgene at indicated developmental stages and cell types, using the method described in B. (Red line) Expected random distribution. (E) Hypodermal and intestinal nuclei of L1 larva carrying the same transgene as in A, crossed to a strain expressing GFP-LMN-1. Bar, 1 μ m. (Arrowheads) GFP-LacI foci, (asterisk) autofluorescent gut granule. (Adapted from Meister et al. 2010a.)

position of the transgene. Intestinal precursor cells (E cells), where the *pha-4* promoter is active, could be identified by the presence of the mCherry signal (Fig. 2A). We subsequently acquired z stacks of embryos and for each GFP focus, we identified the focal plane with maximal signal. To quantify the radial distribution of transgene position, we divided the nuclear cross section at this focal plane into three concentric zones of equal surface and determined the relative occupancy of these three zones by the transgene (Fig. 2B). When repeated for many nuclei, the distribution of a randomly positioned locus yields equal occupancy of all three zones (33% of the foci in each zone). In contrast, a peripheral or a centrally located focus will be enriched in zone 1 or 3, respectively (Meister et al. 2010b).

We first quantified the subnuclear distribution of the *pha-4* transgene in very early embryos of 30–50 cells. At

this developmental stage, most embryonic cells are still uncommitted to cell fate such that they can be differentiated into all classes of tissues by ectopic expression of the corresponding transcription factor (Sulston et al. 1983; Zhu et al. 1998; Yuzyuk et al. 2009). Analysis by three-zone scoring revealed that the *pha-4* transgene was randomly distributed throughout the nuclear space (Fig. 2C). This was true for independent transgene integrations of the *pha-4* promoter as well as for small arrays of the inactive tissue-specific *myo-3* promoter and the control strain carrying only the *unc-119⁺* selection marker (Meister et al. 2010a). Note that at this developmental stage, none of the transgene-borne promoters are active, and no mCherry signal was detected.

Previous work has shown inactive loci at the nuclear periphery in tissue culture cells and *Drosophila* embryos (Pickersgill et al. 2006; Guelen et al. 2008; Peric-Hupkes et al. 2010). Our results on the other hand suggest that transcriptional inactivity alone is insufficient for a perinuclear localization, at least in early *C. elegans* embryos.

LOW-COPY TRANSGENES OCCUPY DEFINED POSITIONS IN DIFFERENTIATED TISSUES

C. elegans embryos undergo cell-type commitment at a developmental stage where eight intestinal precursor cells are present (8E stage) (Zhu et al. 1998). This restriction in cell-fate potential coincides with a global compaction of chromatin (Yuzyuk et al. 2009).

In our system, the 8E stage can be easily identified by the presence of eight cells expressing *HIS-24::mCherry* (Fig. 2A, red). To investigate the effect of cell-type commitment and promoter activity on gene position, we next quantified the *pha-4* transgene position at the 8E stage in cells, where it is active in the eight intestinal precursors but silent in the rest of the embryo. In contrast to the situation in nuclei in the 30–50 cell embryos, the *pha-4* transgene was now enriched at the nuclear periphery in cells where the promoter was silent (Fig. 2D, black bars). On the other hand, in cells in which *his-24::mCherry* was expressed, the random distribution shifted slightly toward the nuclear center (Fig. 2D, gray bars).

Finally, we analyzed transgene distribution in fully differentiated cells of the first larval stage. Because immunofluorescence staining under conditions where nuclear structure is preserved is technically challenging in *C. elegans* larvae, we used a strain expressing GFP-tagged lamin (GFP-LMN-1) to mark the nuclear envelope, and we imaged live larvae. Three larval cell types were analyzed: ectodermal hypoderm and seam cells, which do not express *pha-4*, and intestine, where *pha-4* is active (Fig. 2E). Similar to the subnuclear distribution at the 8E stage, the transgene was enriched at the periphery in the hypodermis and seam cells, with nearly 90% of the foci located in zone 1. In contrast, in intestinal nuclei, the transgenes were depleted from the nuclear periphery and most often located in the nuclear center (Fig. 2F).

We performed equivalent experiments with a small transgene array (called *gwls28*) carrying the muscle-spe-

cific *myo-3* promoter driving *mCherry*. Similar to the *pha-4* promoter, this transgene was randomly distributed in early embryonic nuclei. In contrast, the *myo-3* promoter-containing transgenes were enriched at the periphery in differentiated intestine and hypodermal nuclei. This is consistent with the promoter inactivity in these tissues. Importantly, we observed that the *myo-3* promoter transgene relocated to the nuclear center in muscle cells of L1 larvae, where this promoter is active (Meister et al. 2010a).

To summarize, these results indicate that in undifferentiated and uncommitted cells, developmentally regulated promoters have no specific subnuclear position. When cells undergo differentiation, genes are spatially separated based on their activity: Silent loci are relocated to the nuclear envelope, whereas active loci become enriched in the nuclear center. Similar to our findings, in a mouse embryonic stem cell (ESC) differentiation system, stronger lamin-DamID signals were found in differentiated astrocytes (ACs) than in pluripotent ESCs (Peric-Hupkes et al. 2010). However, in this case, it is unclear whether measurement of increased lamin interaction is due to technical differences in the analysis of ACs and ESCs or truly reflects a change in gene position. Moreover, it is unclear as to what degree pluripotent ESCs mimic early embryonic states.

COPY-NUMBER-DEPENDENT PERIPHERAL ATTACHMENT OF REPETITIVE TRANSGENES IN EMBRYONIC CELLS

Given that peripheral attachment of developmentally regulated promoters only occurs in differentiated tissues, we next asked what distinguishes embryonic nuclei from differentiated cells in their ability to recruit the same locus to the nuclear envelope. In principle, at least three explanations are possible: (1) Anchoring may be mediated by a binding factor recognizing the *pha-4/myo-3* promoter that is only expressed after differentiation in the cells where these are inactive. (2) The nuclear envelope in embryonic cells may be unable to bind silent chromatin and only gain this function by incorporation of additional factors during development. (3) Finally, perinuclear anchoring may be mediated by chromatin modifications that are deposited on developmentally regulated promoters after differentiation.

To test whether the nuclear envelope contains the proteins needed to bind heterochromatin in early embryonic cells, we next investigated a chromosomally integrated, *lacO*-containing [*pha-4::lacZ*] transgene that was generated by gonadal microinjection (Azzaria et al. 1996; Meister et al. 2010a). In contrast to transgenes generated by microparticle bombardment, gonadal injection results in large repetitive arrays of 300–500 copies of the injected DNA. Quantitative polymerase chain reaction (qPCR) revealed that the copy number of the [*pha-4::lacZ*] array used in this study was approximately 300 (Fig. 3A).

As a consequence of their repetitiveness, promoters on large arrays are often at least partially repressed and in a heterochromatic state (Hsieh and Fire 2000; Bessler et al. 2010). Therefore, visualization of the large [*pha-4::lacZ*] array by GFP-LacI allowed us to test whether a large het-

erochromatic domain was able to bind the nuclear envelope in early embryos. Indeed, these arrays were strongly enriched at the nuclear periphery with >80% of the foci found in the outermost zone (Fig. 3A,C). We similarly generated another chromosomally integrated, large array (called *gwl4*) by microinjection and X-ray irradiation. This array contains a GFP-LacI expression plasmid, a plasmid with a *myo-3* promoter driving *rfp*, as well as *lacO* sites and can be visualized microscopically by GFP-LacI that is transcribed from the array itself. By qPCR, we estimate the plasmid copy number of *gwl4* to be ~500 copies (Meister et al. 2010a). Quantification of the radial distribution of the *gwl4* array revealed that, similar to the [*pha-4::lacZ*] array, this large array was strongly enriched at the nuclear envelope (Fig. 3E). Thus, the embryonic nuclear envelope is able to recruit large gene arrays.

To confirm that peripheral sequestration is size dependent and not reflective of the site of transgene integration, we isolated a strain in which the large [*pha-4::lacZ*] array had spontaneously reduced its copy number. qPCR confirmed that the array was about sixfold smaller than in the parental strain (Fig. 3B). Remarkably, this smaller array was no longer found almost exclusively at the nuclear envelope (Fig. 3D). Similarly, a bombardment-derived *myo-3::mCherry* transgene (*gwl28*) with 10-fold fewer copies than the large *gwl4[myo-3::rfp]* array was randomly distributed in early embryos (Fig. 3F) (Meister et al. 2010a).

We note that the low- and high-copy version of the [*pha-4::lacZ*] array are integrated at the same position on the chromosome because the low-copy array was generated from the high-copy array through a spontaneous recombination event. From this, we can therefore exclude that the differential subnuclear localization of these arrays is due to differences in their genomic integration site or method of transgenesis. We conclude that the high copy number of a transgene can direct it to the nuclear envelope. Furthermore, our findings argue against a sequence-specific DNA-binding factor initiating perinuclear gene attachment because the large and small [*pha-4::lacZ*] array share the same sequence composition but are differently localized in the nucleus. However, we cannot rule out that in later development, a tissue-specific factor also contributes to the anchoring event.

HIGH-COPY BUT NOT LOW-COPY TRANSGENES ACCUMULATE HETEROCHROMATIC MARKS

What could distinguish high- from low-copy transgenes in their nuclear localization? Given that promoters on large arrays have previously been shown to be subject to transcriptional silencing (Hsieh and Fire 2000) and to accumulate heterochromatic marks (Bessler et al. 2010), we tested whether small and large arrays differ in their histone modifications. Indeed, when we stained embryos that contain the large array *gwl4[myo-3::rfp]* for the heterochromatic mark H3K9me3, we saw a spotty pattern with two bright spots in every nucleus. These bright foci colocalized precisely with the GFP signal marking the array position (Fig.

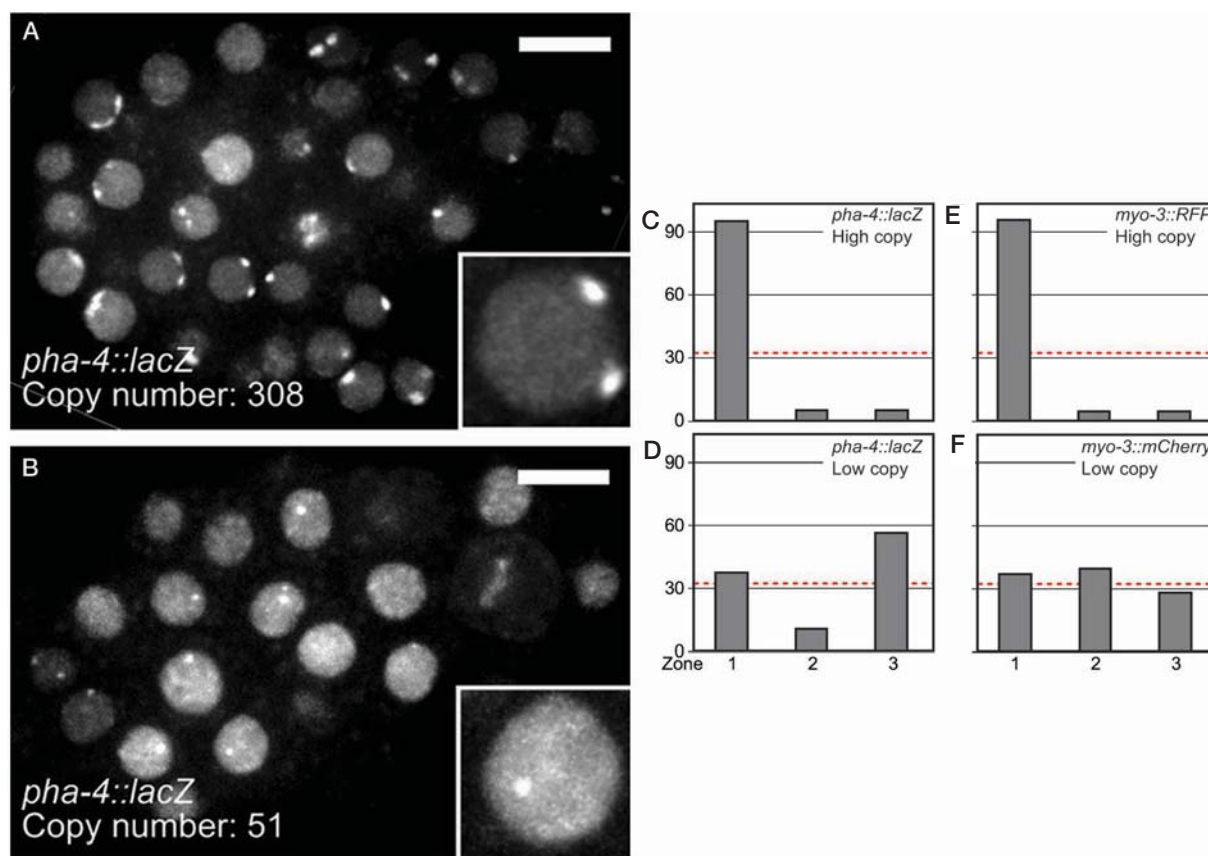


Figure 3. Peripheral anchoring of transgenes depends on their copy number. (A) Projection of six focal planes spanning 1.2 μm of an embryo carrying a large [*pha-4::lacZ*] array with 300 copies, visualized with GFP-LacI. Bar, 5 μm. (B) As in A, but the same transgene with spontaneously reduced size (51 copies). (C–F) Quantification of radial transgene positioning using three-zone scoring as described in Fig. 2B. (Red line) Random distribution. (C) Large [*pha-4::LacZ*] array shown in A. (D) Array with reduced size shown in B. (E) Large *gwlIs4*[*myo-3::rfp*] array. (F) Bombardment-derived *gwlIs28*[*myo-3::mCherry*] transgene with low copy number. (Adapted from Meister et al. 2010a.)

4A). Similarly, the *gwlIs4* array was enriched for the Polycomb-associated mark H3K27me3 (Fig. 4B). In agreement with its repressed state, we found no H3K4me3, which marks active promoters, enriched on the array (Fig. 4C). This exclusion of H3K4me3 was not due to potential technical problems in the staining procedure because this modification was enriched on the *gwlIs4* array in muscle cells of late-stage embryos when the *myo-3* promoter on the array is activated (Fig. 4D).

To compare the level of histone modifications on large and small arrays, we created a strain carrying both the large *gwlIs4*[*myo-3::rfp*] array and the low-copy *gwlIs28*[*myo-3::mCherry*] transgene. Hence, four GFP foci in every nucleus were detected. Two of these foci had an extended shape and correspond to the large array *gwlIs4*, whereas the other two GFP signals had a spot-like appearance, with a size close to the diffraction limit, reflecting the smaller size of the low-copy transgene *gwlIs28* (Fig. 3E,F; GFP). When we stained these embryos with antibodies against H3K9me3 and H3K27me3, only the two large GFP foci showed colocalization with either of the methylated histones (Fig. 3E,F). We therefore conclude that low-copy transgenes accumulate far less histone modifications typical for heterochromatic marks than large arrays.

The observation that copy-number-dependent perinu-

clear anchoring of repetitive transgenes correlated with their acquisition of H3K9me3 and H3K27me3 marks indicates that the heterochromatic state itself could serve as a signal for gene repositioning to the nuclear envelope. Genetic mutation of the histone methyltransferases that deposit these methyl marks will allow us to test this model.

C. *ELEGANS* LAMIN HOMOLOG LMN-1 REQUIRED FOR PERINUCLEAR ATTACHMENT OF GENE ARRAYS

To determine what might provide peripheral chromatin anchoring *in trans*, we tested whether an intact nuclear lamina was important for peripheral binding of gene arrays. *C. elegans* encodes a single lamin protein (LMN-1) that shares characteristics of both A- and B-type lamins. As previously described, down-regulation of *lmn-1* by RNA interference (RNAi) reduced LMN-1 levels in *C. elegans* embryos to <10% of wild-type levels (Fig. 5A) and caused arrest at early embryonic stages (Liu et al. 2000).

To test whether a functional nuclear lamina is required to maintain gene arrays at the nuclear envelope, L4 larvae carrying the large transgene array *gwlIs4* were subjected to *lmn-1* RNAi for 24 h. Array position was determined in the 50-cell-stage embryonic progeny of these animals.

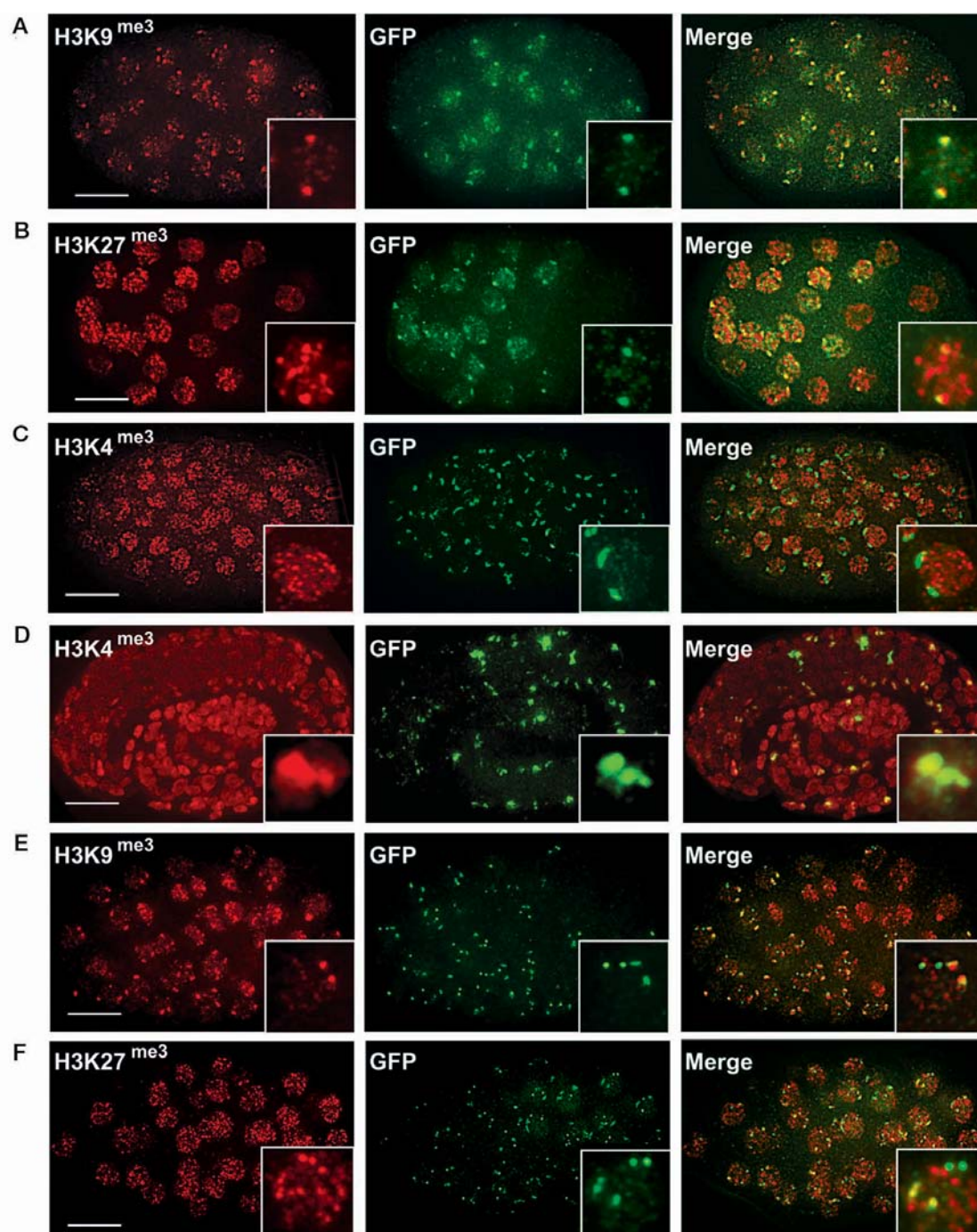


Figure 4. Large arrays but not small transgenes accumulate heterochromatic chromatin modifications. (A–F) Maximum intensity projections of *C. elegans* embryos carrying large *myo-3::rfp* array (A–D) or both large *myo-3::rfp* array and low-copy *myo-3::mCherry* transgene. (E,F) Embryos were stained with antibodies directed against indicated specific histone methylation marks and for GFP-LacI. Bars, 5 μ m. (A–C,E,F) Early-stage embryos in which *myo-3* promoter is not active. (D) Late-stage embryo just before hatching. (D, inset) Muscle cell, where the *myo-3* promoter is active. (Adapted from Meister et al. 2010a.)

In 20% of the embryonic nuclei, at least one, and sometimes two, arrays shifted away from the nuclear envelope (Fig. 5B, *lmn-1[RNAi]*). In contrast, only 5% of the nuclei had at least one internal focus in embryos treated with a control RNAi vector (Fig. 5B,C; *mock[RNAi]*). An intact nuclear lamina is therefore necessary to retain arrays at the nuclear periphery. It remains unclear, however, whether there is a direct interaction between LMN-1 and the array or whether this involves lamin-associated chromatin-binding factors.

DEPLETION OF LMN-1 CAUSES STOCHASTIC DEREPRESSION OF ARRAY-BORNE PROMOTERS

The *gwIs4* array used in this study serves a dual purpose: The position of the GFP focus reflects the position of the transgene in the nucleus, and total GFP levels reflect the activity of the array-borne *baf-1* promoter that controls GFP-LacI expression. By monitoring GFP levels in animals carrying the genetic null allele *lmn-1(tm1502)*, we

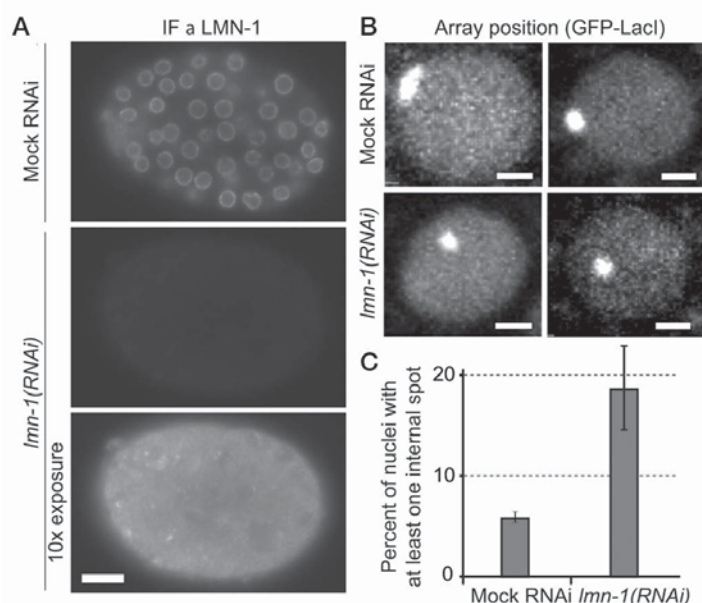


Figure 5. High levels of LMN-1 are required for efficient perinuclear array anchoring. (A) L4 larvae were subjected to *lmn-1* RNAi or mock RNAi, and embryonic progeny were immunostained for LMN-1 after 24 hours. Control and *lmn-1*(RNAi) embryos shown at same exposure and at 10-fold longer exposure for *lmn-1*(RNAi). Note that LMN-1 is reduced to at least 10% of wild-type level but is still detectable. Bar, 5 μ m. (B) GFP-LacI signal of nuclei of mock and *lmn-1*(RNAi)-treated embryos carrying large *myo-3::rfp* array. Shown is single focal plane of a stack. Bar, 1 μ m. (C) Quantification of array detachment in 50-cell-stage embryos. Shown is fraction of nuclei that show at least one internal focus. Data reflect mean of two biologically independent replicas. Error bars indicate maxima and minima of data series.

could therefore test whether loss of array anchoring correlated with a reduced ability to maintain its partially repressed state.

In contrast to the high penetrance of embryonic death observed after RNAi against *lmn-1*, most animals homozygous for the genetic null allele *tm1502* complete embryogenesis and form sterile adults (Haithcock et al. 2005). This weaker phenotype of the *lmn-1* null allele is most likely due to rescue by the maternal load of *lmn-1* transcripts. Using the *tm1502* null allele, we examined

whether the nuclear lamina had a role in array repression in differentiated tissues.

Whereas GFP-LacI was hardly detectable in adult wild-type animals (Fig. 6A), 67% of the *lmn-1(tm1502)* homozygous mutants had a few cells with very high GFP signal stemming from a derepressed *gwl54* array (Fig. 6B). Array derepression seemed to occur stochastically in most tissues of the worm but always only in a subset of cells per animal. The reason for this low penetrance is unclear but may reflect either a stochastic loss of maternally con-

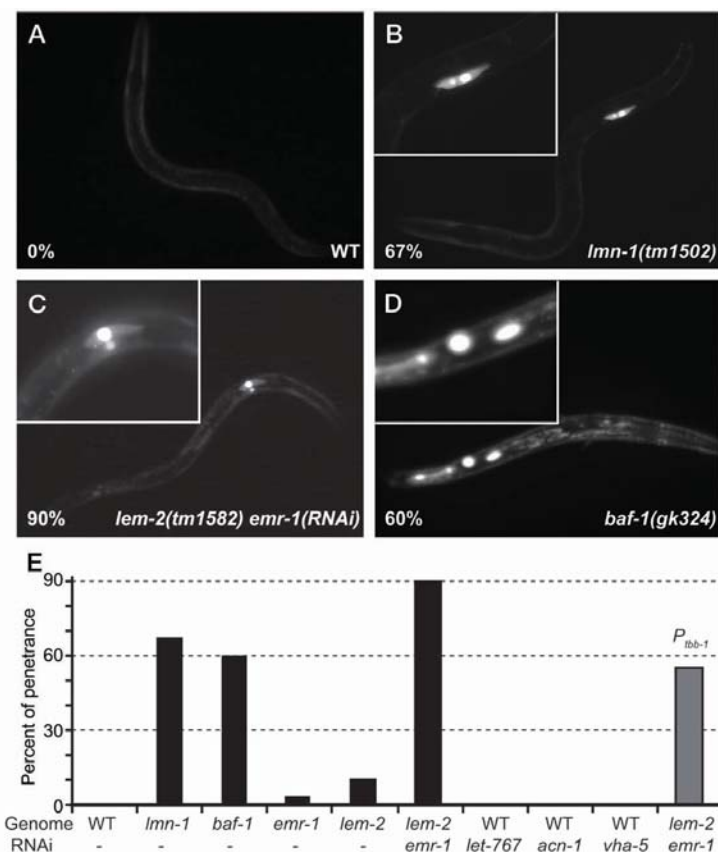


Figure 6. Intact nuclear envelope is required for efficient array repression. (A–D) GFP images of strains carrying the large integrated *gwl54[baf-1:gfp-lacI; myo-3::rfp]* array in indicated backgrounds. GFP-LacI is barely detectable in wild type (WT) (A), but is found at high levels in *lmn-1(tm1502)* (B), *lem-2(tm1582)emr-1(RNAi)* (C), and *baf-1(gk324)* (D) mutants. Frequency of worms with at least one bright green nucleus indicated at bottom left of each image. (E) Quantification of the frequency of *gwl54[baf-1:gfp-lacI; myo-3::rfp]* or *[tbb-1::mCherry-lacI]* (P_{tbb-1}) array derepression in indicated backgrounds and treated with indicated RNAi. Shown is fraction of worms with at least one bright nucleus.

tributed lamin during cell divisions or the stochastic nature of heterochromatin control over transcription. Nevertheless, this result suggests that the nuclear lamina is necessary to stably maintain transcriptional repression of arrays.

MUTATION OF LAMIN-INTERACTING FACTORS *BAF-1*, *EMR-1*, AND *LEM-2* PHENOCOPY ARRAY DEREPRESSION IN LMN-1-DEPLETED WORMS

LMN-1 interacts with the two transmembrane proteins, EMR-1 (homolog of human Emerin) and LEM-2 (hMAN1), that span the inner nuclear membrane (Liu et al. 2003). At their nucleoplasmic amino terminus, both proteins contain a LEM (LAP2, Emerin, and MAN1) domain that binds the small DNA cross-linking protein BAF-1 (Margalit et al. 2005).

Mutation of *baf-1*, or concurrent depletion of the lamin-associated LEM domain containing transmembrane proteins EMR-1 and LEM-2, causes phenotypes very similar to *lmn-1* mutation (Liu et al. 2000, 2003; Margalit et al. 2005), including chromosome segregation defects and promiscuous chromatin condensation. Therefore, we tested whether BAF-1 and EMR-1/LEM-2 were also required for array silencing. Indeed, we observed array derepression at high penetrance in animals homozygous for the *baf-1* null allele *gk324* (60%; Fig. 6D, *baf-1*). Single mutants of *emr-1* and *lem-2* had only minor defects in array silencing, in agreement with their previously described redundant functions (Fig. 6E, *emr-1* and *lem-2*) (Liu et al. 2003). By down-regulation of *emr-1* with RNAi in a *lem-2* null-mutant background, we depleted both proteins concurrently. This caused high-penetrance embryonic lethality (>98%; data not shown), as previously described for double RNAi against these two factors (Liu et al. 2003). The rare escapers arrested at the L2 or L3 larval stage, and 90% of these showed strong up-regulation of GFP-LacI in at least one cell (Fig. 6C, *lem-2*, *emr-1*[RNAi]).

Derepression cannot be explained exclusively by the larval arrest phenotype of *emr-1 lem-2*(RNAi) double-depleted animals because unrelated RNAi clones causing larval arrest (*let-767*[RNAi], *acn-1*[RNAi], and *vha-5*[RNAi]) did not cause array derepression (Fig. 6E). Finally, the observed increased levels of GFP-LacI are not due to a promoter-specific activation, because an *mCherry-LacI* transgene driven by the unrelated *tbb-1* promoter (β -tubulin) shows a similar derepression as the *baf-1* promoter (Fig. 6E, P_{tbb-1}). In conclusion, perturbation of the nuclear lamina by depletion of LMN-1, or its interacting partners BAF-1, EMR-1, and LEM-2, results in strong up-regulation of a usually silent transgene.

CONCLUSIONS

Our studies on nuclear organization in *C. elegans* have revealed that active and inactive developmentally regulated promoters are spatially separated in the nuclei of differentiated tissues of the first larval stage: Tissue-specific promoters are in the nuclear lumen when active and close to the nuclear periphery when silent. This is in agreement

with studies in other experimental systems, where inactive genes were often found close to the nuclear lamina (Pickersgill et al. 2006; Guelen et al. 2008; Peric-Hupkes et al. 2010). In contrast to previous studies, we exogenously inserted fragments of developmentally regulated promoters (3.1 kb and 2.5 kb for *pha-4* and *myo-3*, respectively) at random sites in the genome. We analyzed multiple insertions of these two different promoters in a range of tissues (intestine, muscle, hypodermal cells, and seam cells). In all cases, the developmentally regulated promoters assumed a position within the nucleus that reflected their activity state, i.e., inactive promoters were perinuclear and active promoters internal. Our results therefore strongly suggest that the tissue-specific promoter fragments that we inserted are sufficient to control subnuclear position.

Although low-copy transgenes were randomly distributed in early embryonic cells, the nuclear envelope is capable of recruiting chromatin even at this early developmental stage. Much larger arrays of transgenes (repetitive copy number 250–500) were strongly enriched at the nuclear periphery in embryos as well as larval cells. This peripheral sequestration correlated with an accumulation of heterochromatic marks and is unlikely to be dictated by the site of integration or by sequence-specific binding factors. Promoters of identical sequence inserted at the same locus, in reduced copy number, were not peripherally enriched. It is therefore tempting to speculate that the formation of heterochromatin itself drives nuclear organization. According to such a model, the relocation of inactive low-copy transgenes to the nuclear envelope during development may be a consequence of a change in chromatin state of the promoters upon cell commitment and differentiation. The exact nature of the molecular players involved in this process remains to be identified.

Although our findings suggest that deposition of heterochromatic marks itself contributes to peripheral chromatin anchoring, we find that a functional nuclear envelope is required, for both chromatin sequestration and efficient silencing. Arrays are delocalized upon RNAi against *lmn-1*, whereas depletion of the nuclear envelope components LMN-1 and BAF-1 or codepletion of EMR-1 and LEM-2 caused a stochastic derepression of heterochromatic transgene arrays. This result is reminiscent of a recent study showing up-regulation of a normally silent testis-specific gene cluster in flies deficient for the *Drosophila* lamin homolog lamDm0 (Shevelyov et al. 2009).

To summarize, our data suggest that the peripheral sequestration of heterochromatin reinforces its silent state (Fig. 7). This may occur through local abundance of histone methyltransferases and methylhistone-binding factors or through indirect effects such as late replication or local depletion of active RNA polymerase. The value of RNAi screens in resolving this is an obvious advantage of the *C. elegans* system described here.

MATERIALS AND METHODS

Molecular Biology and Transgenic Strains

Table 1 lists the strains used in this study; most strains and plasmids are described elsewhere (Meister et al. 2010a).

POSITIONING OF CHROMATIN DURING *C. ELEGANS* DEVELOPMENT

9

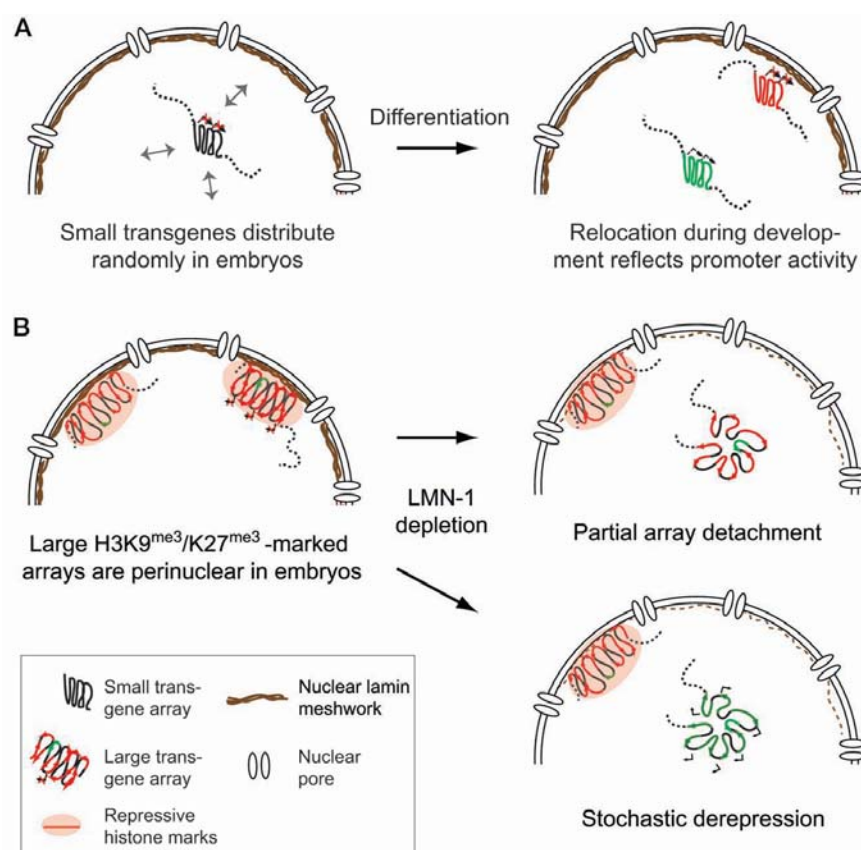


Figure 7. Model for function of perinuclear gene attachment in gene silencing. (A) Low-copy transgenes are randomly distributed in undifferentiated embryonic cells, independent of promoter activity. During differentiation, inactive promoters relocate to nuclear envelope, and active promoters become enriched in nuclear center. (B) Large heterochromatic transgene arrays are bound to nuclear lamina in wild-type embryos, and promoters on the transgene are transcriptionally repressed. Depletion of LMN-1 by RNAi or its mutation causes release of large arrays from the nuclear lamina. Not all arrays detach from the nuclear periphery; some LMN-1 remains due to incomplete RNAi or because of remaining maternally contributed LMN1 protein. Detachment of arrays impairs their efficient silencing, such that a fraction of the arrays gets derepressed stochastically.

Table 1. Strains used in this study

Strain name	Genotype	References
N2	Wild-type Bristol isolate	
GW76	<i>gwIs4[myo-3::rfp baf-1::gfp-lacI let-858 3'UTR]</i>	Meister et al. (2010a)
GW115	<i>gwIs4; lmn-1(tm1502)/hT2[bli-4(e937) let-?(q782) qIs48]</i>	This study
GW164	<i>gwIs4; emr-1(gk119)</i>	This study
GW201	<i>gwIs4; lem-2(tm1582)</i>	This study
GW205	<i>gwIs4; baf-1(gk324)/hT2[bli-4(e937) let(q782) qIs48]</i>	This study
GW318	<i>gwIs4; gwIs28[myo-3::mCherry; 256xlacO; unc-119⁺]; unc-119(ed3)</i>	Meister et al. (2010a)
GW395	<i>gwIs39[baf-1::gfp-lacI::let-858 3'UTR; vit-5::gfp]; unc-119(ed3)</i>	Meister et al. (2010a)
GW397	<i>gwIs39; gwIs28; unc-119(ed3)</i>	Meister et al. (2010a)
GW429	<i>gwIs39; gwIs59[pha-4::mCherry::his-24; 256xlacO; unc-119⁺]; unc-119(ed3)</i>	Meister et al. (2010a)
GW430	<i>gwIs25[tbb-1::wmCherry-LacI::tbb-2 unc-119⁺]; unc-119(ed3); lem-2(tm1582)</i>	This study
GW431	<i>gwIs39; gwIs59; ygIs[lmn-1::lmn-1::gfp::lmn-1 3'UTR, unc-119⁺]</i>	Meister et al. (2010a)
GW457	<i>gwIs4; gwIs39</i>	This study
GW470	<i>gwIs39; cals*[pha-4::lacZ; rol-6(su1006)]; unc-119(ed3)</i>	This study
GW471	<i>gwIs39; cals[pha-4::lacZ; rol-6(su1006)]; unc-119(ed3)</i>	Meister et al. (2010a)

*Transgene with reduced copy number.

Strains were made by back-crossing deletion alleles obtained from the *C. elegans* knockout consortium to wild-type N2 animals and subsequently to GW76. GW76 is an 8x outcrossed strain that carries a large integrated array expressing GFP-LacI under control of a *baf-1* promoter (*gwIs4*) but is otherwise wild type. The following alleles were used: *lmn-1(tm1502)*, *emr-1(gk119)*, *lem-2(tm1582)*, and *baf-1(gk324)*. For *lmn-1* RNAi experiments, GW76 was supplemented with a transgene (*gwIs39*) expressing GFP-LacI under the *baf-1* promoter to enhance the GFP signal for microscopy. *gwIs39* does not contain *lacO* sites and is therefore not visible as a fluorescent focus.

RNAi and Microscopy

RNAi was performed by feeding according to standard methods (Timmons et al. 2001). RNAi clones were obtained from the Vidal library (Rual et al. 2004) (*lmn-1*) or Ahringer library (Kamath et al. 2003) (all others). The empty vector L4440 was modified by removal of an EcoRV fragment containing a 25-bp stretch of perfect identity to linker DNA in the *gfp-lacI* construct and was used as control RNAi. For *lmn-1* RNAi, L4 larvae were subjected to RNAi, and embryonic progeny were analyzed after 24 h. To this end, embryos were mounted on 2% agarose pads, and 3D focal stacks were acquired on a spinning-disk confocal microscope as described by Meister et al. (2010a). Stacks of images were quantified manually using ImageJ. For derepression assays, L1 larvae were subjected to RNAi, and progeny was imaged with a wide-field Axioplan microscope using a 20x objective (Zeiss). Immunofluorescence and quantification of radial spot position were performed as in Meister et al. (2010a). A Gaussian filter was applied to the mCherry channel in Fig. 2A (0.3- μ m radius) and to the GFP signal in Fig. 3A,B (0.05- μ m radius).

Copy-Number Quantification

Genomic DNA was isolated according to standard methods. Copy number was determined by qPCR from the ratio of amplicons from the ampicillin-resistance marker on the plasmid backbone and the single-copy locus *lmn-1* as described in Meister et al. (2010a).

ACKNOWLEDGMENTS

We thank Y. Gruenbaum for strains and helpful discussions, J.D. McGhee and the *Caenorhabditis* Genetics Center for strains, T. Jenuwein for antibodies, R. Waterston for plasmids, and M. Thomas for excellent technical assistance. This work was supported by the European Union Network of Excellence "Epigenome," the Swiss National Science Foundation National Center of Competence in Research "Frontiers in Genetics," the Novartis Research Foundation, and a fellowship from the Human Frontiers Science Program to B.L.P.

REFERENCES

- Andrulis ED, Neiman AM, Zappulla DC, Sternglanz R. 1998. Perinuclear localization of chromatin facilitates transcriptional silencing. *Nature* **394**: 592–595.
- Azzaria M, Goszczynski B, Chung MA, Kalb JM, McGhee JD. 1996. A fork head/HNF-3 homolog expressed in the pharynx and intestine of the *Caenorhabditis elegans* embryo. *Dev Biol* **178**: 289–303.
- Bessler JB, Andersen EC, Villeneuve AM. 2010. Differential localization and independent acquisition of the H3K9me2 and H3K9me3 chromatin modifications in the *Caenorhabditis elegans* adult germ line. *PLoS Genet* **6**: e1000830.
- Boyer LA, Mathur D, Jaenisch R. 2006. Molecular control of pluripotency. *Curr Opin Genet Dev* **16**: 455–462.
- Busch H. 1966. The cell nucleus. *Nature* **211**: 1347–1348.
- Dechat T, Pflieger K, Sengupta K, Shimi T, Shumaker DK, Solimando L, Goldman RD. 2008. Nuclear lamins: Major factors in the structural organization and function of the nucleus and chromatin. *Genes Dev* **22**: 832–853.
- Deniaud E, Bickmore WA. 2009. Transcription and the nuclear periphery: Edge of darkness? *Curr Opin Genet Dev* **19**: 187–191.
- Finlan LE, Sproul D, Thomson I, Boyle S, Kerr E, Perry P, Ylstra B, Chubb JR, Bickmore WA. 2008. Recruitment to the nuclear periphery can alter expression of genes in human cells. *PLoS Genet* **4**: e1000039.
- Gasser SM, Hediger F, Taddei A, Neumann FR, Gartenberg MR. 2004. The function of telomere clustering in yeast: The circe effect. *Cold Spring Harb Symp Quant Biol* **69**: 327–337.
- Guelen L, Pagie L, Brasset E, Meuleman W, Faza MB, Talhout W, Eussen BH, de Klein A, Wessels L, de Laat W, et al. 2008. Domain organization of human chromosomes revealed by mapping of nuclear lamina interactions. *Nature* **453**: 948–951.
- Haithcock E, Dayani Y, Neufeld E, Zahand AJ, Feinstein N, Matout A, Gruenbaum Y, Liu J. 2005. From the cover: Age-related changes of nuclear architecture in *Caenorhabditis elegans*. *Proc Natl Acad Sci* **102**: 16690–16695.
- Hsieh J, Fire A. 2000. Recognition and silencing of repeated DNA. *Annu Rev Genet* **34**: 187–204.
- Kamath RS, Fraser AG, Dong Y, Poulin G, Durbin R, Gotta M, Kanapin A, Le Bot N, Moreno S, Sohrmann M, et al. 2003. Systematic functional analysis of the *Caenorhabditis elegans* genome using RNAi. *Nature* **421**: 231–237.
- Kumaran RI, Spector DL. 2008. A genetic locus targeted to the nuclear periphery in living cells maintains its transcriptional competence. *J Cell Biol* **180**: 51–65.
- Liu J, Ben-Shahar TR, Riemer D, Treinin M, Spann P, Weber K, Fire A, Gruenbaum Y. 2000. Essential roles for *Caenorhabditis elegans* lamin gene in nuclear organization, cell cycle progression, and spatial organization of nuclear pore complexes. *Mol Biol Cell* **11**: 3937–3947.
- Liu J, Lee KK, Segura-Totten M, Neufeld E, Wilson KL, Gruenbaum Y. 2003. MAN1 and emerlin have overlapping function(s) essential for chromosome segregation and cell division in *Caenorhabditis elegans*. *Proc Natl Acad Sci* **100**: 4598–4603.
- Margalit A, Segura-Totten M, Gruenbaum Y, Wilson KL. 2005. Barrier-to-autointegration factor is required to segregate and enclose chromosomes within the nuclear envelope and assemble the nuclear lamina. *Proc Natl Acad Sci* **102**: 3290–3295.
- Meister P, Towbin BD, Pike BL, Ponti A, Gasser SM. 2010a. The spatial dynamics of tissue-specific promoters during *C. elegans* development. *Genes Dev* **24**: 766–782.
- Meister P, Gehlen LR, Varela E, Kalck V, Gasser SM, Jonathan W, Christine G, Gerald RF. 2010b. Visualizing yeast chromosomes and nuclear architecture. *Methods Enzymol* **470**: 535–567.
- Mohn F, Schübeler D. 2009. Genetics and epigenetics: Stability and plasticity during cellular differentiation. *Trends Genet* **25**: 129–136.
- Peric-Hupkes D, Meuleman W, Pagie L, Bruggeman SW, Solovei I, Brugman W, Gräf S, Flicek P, Kerkhoven RM, van Lohuizen M, et al. 2010. Molecular maps of the reorganization of genome-nuclear lamina interactions during differentiation. *Mol Cell* **38**: 603–613.

- Pickersgill H, Kalverda B, de Wit E, Talhout W, Fornerod M, van Steensel B. 2006. Characterization of the *Drosophila melanogaster* genome at the nuclear lamina. *Nat Genet* **38**: 1005–1014.
- Praitis V, Casey E, Collar D, Austin J. 2001. Creation of low-copy integrated transgenic lines in *Caenorhabditis elegans*. *Genetics* **157**: 1217–1226.
- Reddy KL, Zullo JM, Bertolino E, Singh H. 2008. Transcriptional repression mediated by repositioning of genes to the nuclear lamina. *Nature* **452**: 243–247.
- Rual JF, Ceron J, Koreth J, Hao T, Nicot A-S, Hirozane-Kishikawa T, Vandenhaute J, Orkin SH, Hill DE, van den Heuvel S, et al. 2004. Toward improving *Caenorhabditis elegans* phenome mapping with an orfeome-based RNAi library. *Genome Res* **14**: 2162–2168.
- Shevelyov YY, Lavrov SA, Mikhaylova LM, Nurminsky ID, Kulathinal RJ, Egorova KS, Rozovsky YM, Nurminsky DI. 2009. The B-type lamin is required for somatic repression of testis-specific gene clusters. *Proc Natl Acad Sci* **106**: 3282–3287.
- Spector DL. 2003. The dynamics of chromosome organization and gene regulation. *Annu Rev Biochem* **106**: 573–608.
- Straight AF, Belmont AS, Robinett CC, Murray AW. 1996. GFP tagging of budding yeast chromosomes reveals that protein-protein interactions can mediate sister chromatid cohesion. *Curr Biol* **16**: 1599–1608.
- Sulston JE, Schierenberg E, White JG, Thomson JN. 1983. The embryonic cell lineage of the nematode *Caenorhabditis elegans*. *Dev Biol* **100**: 64–119.
- Taddei A, Hediger F, Neumann FR, Gasser SM. 2004. The function of nuclear architecture: A genetic approach. *Annu Rev Genet* **38**: 305–345.
- Taddei A, Van Houwe G, Nagai S, Erb I, van Nimwegen E, Gasser SM. 2009. The functional importance of telomere clustering: Global changes in gene expression result from Sir factor dispersion. *Genome Res* **19**: 611–625.
- Timmons L, Court DL, Fire A. 2001. Ingestion of bacterially expressed dsRNAs can produce specific and potent genetic interference in *Caenorhabditis elegans*. *Gene* **263**: 103–112.
- Towbin BD, Meister P, Gasser SM. 2009. The nuclear envelope: A scaffold for silencing? *Curr Opin Genet Dev* **19**: 180–186.
- Verstraeten VL, Broers JL, Ramaekers FC, van Steensel MA. 2007. The nuclear envelope, a key structure in cellular integrity and gene expression. *Curr Med Chem* **14**: 1231–1248.
- Wilson KL, Berk JM. 2010. The nuclear envelope at a glance. *J Cell Sci* **123**: 1973–1978.
- Yuzyuk T, Fakhouri THI, Kiefer J, Mango SE. 2009. The polycomb complex protein *mes-2/E(z)* promotes the transition from developmental plasticity to differentiation in *C. elegans* embryos. *Dev Cell* **16**: 699–710.
- Zhu J, Fukushige T, McGhee JD, Rothman JH. 1998. Reprogramming of early embryonic blastomeres into endodermal progenitors by a *Caenorhabditis elegans* GATA factor. *Genes Dev* **12**: 3809–3814.

Chapter 4: Step-wise methylation of histone H3K9 positions heterochromatin at the nuclear periphery

Benjamin D. Towbin^{1,3}, Cristina Gonzalez², Ragna Sack¹, Dimos Gaidatzis¹, Véronique Kalck¹, Peter Meister^{1,4}, Peter Askjaer², and Susan M. Gasser^{1,3}

¹⁾ Friedrich Miescher Institute for Biomedical Research, Maulbeerstrasse 66, CH-4058 Basel, Switzerland

²⁾ Centro Andaluz de Biología del Desarrollo (CABD), Consejo Superior de Investigaciones Científicas, Universidad Pablo de Olavide, Seville 41013, Spain

³⁾ Faculty of Sciences, University of Basel, 4056 Basel, Switzerland

⁴⁾ current address: University of Bern, Institute of Cell Biology, Baltzerstrasse 4, CH-3012 Bern, Switzerland

Cell 2012, Volume 150 (5), pg. 934-947

Summary

The factors that sequester transcriptionally repressed heterochromatin at the nuclear periphery are currently unknown. In a genome-wide RNAi screen, we found that depletion of S-adenosylmethionine (SAM) synthetase reduces histone methylation globally and causes derepression and release of heterochromatin from the nuclear periphery in *Caenorhabditis elegans* embryos. Analysis of histone methyltransferases (HMTs) showed that elimination of two HMTs, MET-2 and SET-25, mimics the loss of SAM synthetase, abrogating the perinuclear attachment of heterochromatic transgenes and of native chromosomal arms rich in histone H3 lysine 9 methylation. The two HMTs target H3K9 in a consecutive fashion: MET-2, a SETDB1 homolog, mediates mono- and dimethylation, and SET-25, a previously uncharacterized HMT, deposits H3K9me3. SET-25 colocalizes with its own product in perinuclear foci, in a manner dependent on H3K9me3, but not on its catalytic domain. This colocalization suggests an autonomous, self-reinforcing mechanism for the establishment and propagation of repeat-rich heterochromatin.

author contributions: BT designed and performed the experiments in all figures except figure 5D-F, figure S5 and S3. CG did the experiments in Figure 5D-F and Figure S5. RS did the mass-spectrometry for experiments in Figure 3D and S3, DG did the computational analysis in Figure 5D-F and Figure S5, VK created strains in Figure 6, PM designed the experiments and did the experiments in Figure S2F. SG designed the experiments and wrote the manuscript together with BT.

Step-Wise Methylation of Histone H3K9 Positions Heterochromatin at the Nuclear Periphery

Benjamin D. Towbin,^{1,2} Cristina González-Aguilera,³ Ragna Sack,¹ Dimos Gaidatzis,¹ Véronique Kalck,¹ Peter Meister,^{1,4} Peter Askjaer,³ and Susan M. Gasser^{1,2,*}

¹Friedrich Miescher Institute for Biomedical Research, Maulbeerstrasse 66, 4058 Basel, Switzerland

²Faculty of Sciences, University of Basel, 4056 Basel, Switzerland

³Centro Andaluz de Biología del Desarrollo (CABD), Consejo Superior de Investigaciones Científicas, Universidad Pablo de Olavide, Seville 41013, Spain

⁴Present address: University of Bern, Institute of Cell Biology, Baltzerstrasse 4, 3012 Bern, Switzerland

*Correspondence: susan.gasser@fmi.ch

<http://dx.doi.org/10.1016/j.cell.2012.06.051>

SUMMARY

The factors that sequester transcriptionally repressed heterochromatin at the nuclear periphery are currently unknown. In a genome-wide RNAi screen, we found that depletion of S-adenosylmethionine (SAM) synthetase reduces histone methylation globally and causes derepression and release of heterochromatin from the nuclear periphery in *Caenorhabditis elegans* embryos. Analysis of histone methyltransferases (HMTs) showed that elimination of two HMTs, MET-2 and SET-25, mimics the loss of SAM synthetase, abrogating the perinuclear attachment of heterochromatic transgenes and of native chromosomal arms rich in histone H3 lysine 9 methylation. The two HMTs target H3K9 in a consecutive fashion: MET-2, a SETDB1 homolog, mediates mono- and dimethylation, and SET-25, a previously uncharacterized HMT, deposits H3K9me3. SET-25 colocalizes with its own product in perinuclear foci, in a manner dependent on H3K9me3, but not on its catalytic domain. This colocalization suggests an autonomous, self-reinforcing mechanism for the establishment and propagation of repeat-rich heterochromatin.

INTRODUCTION

Transcriptional control of the eukaryotic genome involves the differential organization of chromatin into euchromatic and heterochromatic domains (Kind and van Steensel, 2010). These two active and silent compartments differ in characteristic posttranslational modifications of the core histones, as well as in the incorporation of specific histone variants, linker histones, and nonhistone proteins. Trimethylation of lysine 9 on histone H3 (H3K9me3) or H3K27me3 is associated with silent domains,

whereas euchromatin is enriched for acetylated histones and H3K4me3 (Black and Whetstone, 2011).

From yeast to man, euchromatin and heterochromatin are spatially segregated within the nucleus. In metazoans, repeat-containing centromeric heterochromatin is typically clustered into foci that are enriched for H3K9me3 and Heterochromatin protein 1 (HP1) (Maison and Almouzni, 2004). Similarly, the Polycomb repressor complex is found in nuclear foci that bear H3K27me3 (Luo et al., 2009). A distinct type of heterochromatin enriched for both H3K9 and H3K27 methylation binds the nuclear lamina (Kind and van Steensel, 2010), a meshwork of intermediate filament proteins and several lamin-associated factors that underpin the inner nuclear membrane (INM) (Goldman et al., 2002). Genome-wide analysis has shown that lamin-bound heterochromatin comprises up to 40% of the mammalian genome and occurs in lamin-associated domains (LADs) that often span several megabases in *cis* (Guelen et al., 2008; Peric-Hupkes et al., 2010). Similarly, in the nematode *Caenorhabditis elegans*, LADs cover large regions of the repeat-rich distal third of all chromosome arms (Ikegami et al., 2010).

Downregulation of *C. elegans* lamin, or of the lamin-associated proteins EMR-1 and LEM-2, leads to the derepression of promoters on perinuclear heterochromatic arrays (Mattout et al., 2011). In flies as well, lamin is required to repress testis-specific genes in somatic tissues (Shevelyov et al., 2009), suggesting that the attachment of a locus to the nuclear lamina can affect its expression. In support of this, artificial relocation of genes to the nuclear lamina contributes to their transcriptional repression in mammals and flies, although in a promoter-specific manner (reviewed in Kind and van Steensel, 2010). How this is achieved is unclear.

To understand the functional implications of chromatin attachment to the INM one must identify and interfere with the factors involved. Only a few lamin ligands with chromatin binding capacity have been described. One example, BAF (barrier to autointegration factor), binds both histones and DNA and associates with the lamin-interacting INM proteins LAP2, MAN1, and Emerin (Margalit et al., 2007). A second example is HP-1, which binds the INM-associated Lamin B receptor (Ye and Worman,

1996). The relevance of these interactions in vivo and how they might selectively recruit genes to the nuclear periphery remain unclear.

Repetitive gene arrays have been useful tools to study the mechanism and dynamics of perinuclear heterochromatin anchoring (Meister et al., 2010; Yuzyuk et al., 2009). In worms, as well as in mammals, transgene arrays are frequently subject to transcriptional repression (Hsieh and Fire, 2000; Martin and Whitelaw, 1996) and accumulate repressive histone marks, namely histone H3K9me3 and H3K27me3 (Bessler et al., 2010; Meister et al., 2010). Most important for this study, repetitive arrays integrated into the worm genome recapitulate the perinuclear sequestration of endogenous heterochromatin on chromosome arms.

Here, we used such gene arrays in a genome-wide RNAi screen to identify conserved factors required for the anchoring of heterochromatin. This screen yielded a single RNAi target whose loss impaired both repression and anchoring in *C. elegans* embryos. The target encodes S-adenosyl methionine synthetase, which generates S-adenosylmethionine (SAM), the universal donor for methylation reactions in eukaryotic cells. Given that interference with SAM synthesis caused a drop in histone methylation, we systematically monitored the roles of histone methyl transferases (HMTs) and found that the peripheral anchoring of arrays depends on two HMTs, MET-2 and SET-25, both of which target H3K9. Consistently, endogenous domains of H3K9 methylation on chromosome arms were released from the nuclear lamina in the *met-2 set-25* double mutant.

We show that MET-2, a SETDB1 homolog, deposits mono- and dimethyl groups at H3K9, whereas SET-25, a previously uncharacterized HMT, trimethylates the same residue. SET-25 colocalizes with peripheral heterochromatin in an H3K9me3-dependent fashion, thus becoming sequestered at the nuclear periphery by the product of its own methylation reaction. The increased concentration of SET-25 in perinuclear heterochromatin is compatible with a self-reinforcing mechanism, whereby this enzyme acts to establish and stabilize heterochromatic repression at the nuclear periphery.

RESULTS

A Genome-Wide RNAi Screen Identifies Regulators of Gene Array Silencing in *C. elegans* Embryos

To identify factors required for perinuclear sequestration of heterochromatin, we designed a genetic screen, in which we monitored the derepression and relocalization of two genomically integrated gene arrays in *C. elegans* embryos at the 50- to 100-cell stage. Both arrays encode green fluorescent protein (GFP) under the control of a ubiquitously expressed promoter (either the *let-858* or the *baf-1* promoter). Each reporter was integrated in approximately 300 copies at a single site in the genome, generating a transcriptionally repressed locus bearing the heterochromatic histone modifications H3K9me3 and H3K27me3 (Bessler et al., 2010; Meister et al., 2010).

In a strain that is homozygous for an integrated *let-858::GFP* gene array, we downregulated 80% of all *C. elegans* genes by RNAi and selected clones that could derepress the ubiquitously active *let-858::GFP* reporter in embryos (Figure 1A). Specifically,

synchronized L1 worms carrying the array were exposed to RNAi for 4 days (Kamath et al., 2003). As the larvae developed to gravid adults, we visually inspected the embryonic progeny in utero for increased GFP expression (Figure 1A). We retained only hits that caused array upregulation throughout embryonic cell types. Similarly, we discarded clones targeting essential genes (based on Kamath et al., 2003) because embryonic lethality often led to an unspecific deregulation of the *let-858::GFP* transgene in a small number of cells per embryo (unpublished observation). Viable hits were retested in triplicate next to negative controls on the same plate. We identified 29 RNAi clones that reproducibly caused array derepression in at least two out of three replicates without inducing embryonic death (Table S1; Figure 1C). These 29 hits were enriched for chromatin factors (Figure 1C; $p = 9.7 \times 10^{-4}$, DAVID gene ontology term enrichment, Dennis et al., 2003), including two histone methyl transferases (*mes-4* and *set-25*), three histone binding proteins (*mrg-1*, *lin-61*, *hpl-2*), and the Polycomb repressor complex 2 (PRC2) components *mes-3* and *mes-6*. The catalytic subunit of PRC2, *mes-2*, was among the 20% of genes that were not covered by the RNAi library used for this screen, but an analysis of mutant alleles confirmed derepression upon loss of *mes-2* as well (see below; Figure S2B available online).

Depletion of Two Related S-Adenosylmethionine Synthetases Causes Array Detachment

We subsequently used confocal microscopy to test which of the factors involved in array repression were also required to position arrays at the nuclear periphery (Figure 1B). To this end, we used a second array (termed *gwls4*), which contains 300 copies of the ubiquitously active *baf-1* promoter driving the expression of GFP fused to the bacterial repressor LacI (Meister et al., 2010). Each plasmid copy within the *gwls4* array contained a *lacO* site, allowing the GFP-LacI protein to bind the transgene array from which it is expressed, generating a focus visible by fluorescence microscopy (Meister et al., 2010; Figure 1B). This array thus serves a dual purpose: total GFP levels monitor the expression level of the *baf-1* promoter, whereas the position of the GFP-LacI focus marks the position of the array relative to the nuclear periphery.

Visual inspection by confocal microscopy revealed that arrays were displaced from the nuclear periphery in only two of the 29 primary hits. Both positive clones targeted the SAM synthetases *sams-3* and *sams-4* (Figures 2A–2D). Because the two genes share extensive homology with each other (100% identity over 665 nucleotides of coding sequence, Figure S1A), including the sequences targeted by the RNAi, it was clear that each RNAi clone alone downregulated both genes. Therefore, for all subsequent experiments a single RNAi clone (*sams-3*) was used.

To quantify the degree of array detachment upon *sams-3/4* downregulation, we acquired focal stacks of RNAi-treated embryos. We determined the radial distribution of GFP-foci by binning the spots into three concentric zones of equal surface area in the focal plane with the highest GFP-spot intensity (Figure 2E). For spherical nuclei, this method yields an equal distribution among the three zones for a randomly positioned focus (Meister et al., 2010). Whereas the *gwls4* array was strongly

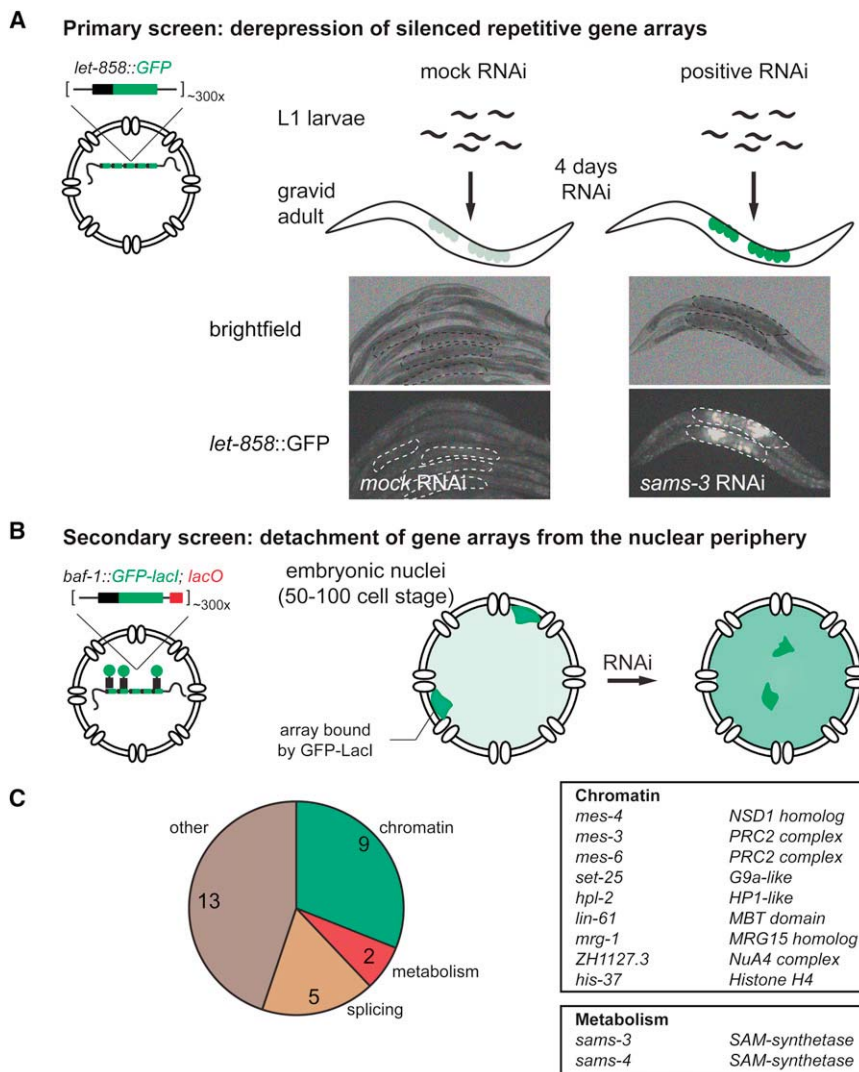


Figure 1. Design of a High-Throughput Two-Step RNAi Screen to Identify Factors Involved in Perinuclear Chromatin Anchoring

(A) Primary screen for derepression of array-borne promoters. L1 larvae of strain NL2507 carrying the repetitive transgene *pkIs1582[let-858::GFP; rol-6(su1006)]* were subjected to all clones of a genome-wide RNAi library. After 4 days, the embryonic progeny within their uterus was screened for increased levels of GFP, exemplified by *sams-3* RNAi.

(B) Secondary screen for gene array detachment. Strain GW566 carrying the *gwIs4[baf-1::GFP-lacI; myo-3::RFP]* transgene was subjected for 4 days to RNAi against all hits of the primary screen described in (A). The *gwIs4* transgene contains *lacO* sites, which are bound by GFP-LacI, such that the transgene position can be determined microscopically.

(C) Summary and classification of the hits of the primary screen. Selected hits are shown, and the complete list is in Table S1.

array was efficiently delocalized in all cells, we conclude that array detachment from the INM arising from the down-regulation of SAMS-3/4 synthetases can occur independently of transcriptional activation.

We did not observe array detachment for any of the other 27 primary screen hits that showed derepression of the array-borne GFP reporter. This argues against the simple explanation that transcriptional activation drives array delocalization. To ensure that the persistence of derepressed arrays at the INM was not due to inefficient RNAi, we generated strains carrying the *gwIs4* array and a

genetic null allele of a subset of the screen hits. Using genetic null mutants, we observed a 20% drop in array attachment in the *set-25* mutant (70% bound, Figure 3B; see below). For all other mutants, including the H3K27 and H3K36 HMTs *mes-2* and *mes-4*, arrays remained firmly anchored at the nuclear periphery (Figures 3B and S2B and S2C). We conclude that transgene array derepression is neither sufficient nor necessary for detachment. This does not exclude, of course, roles for other factors that are either redundant or insufficiently sensitive to RNAi, in array anchoring.

High Levels of SAM Synthetase Are Required for Normal Histone Methylation

The enzymes SAMS-3/4 generate SAM, the unique cellular methyl-group donor. Although there are other, more divergent SAM synthetases in the *C. elegans* genome, the downregulation of *sams-3/4* is expected to reduce cellular methylation, including that on histones. Because specific histone H3 methylation sites are robustly associated with heterochromatic

enriched in the most peripheral zone in embryos treated with control RNAi (>90% in zone 1; Figure 2F, left, gray bars), the array consistently shifted toward the nuclear center after *sams-3/4* RNAi (<25% in zone 1, $p < 2.45 \times 10^{-11}$, Fisher's exact test; Figure 2F, left, black bars).

To see whether array detachment upon *sams-3/4* RNAi required activation of an array-borne promoter, we repeated the *sams-3/4* RNAi experiment with an array that carried two tissue-specific promoters, namely a truncated *pha-4* promoter driving LacZ and the *rol-6* gene, instead of the *baf-1* promoter. Both of these tissue-specific promoters are silent in most early embryonic cells (Azzaria et al., 1996; Sassi et al., 2005). To visualize the array, we expressed GFP-LacI in *trans* from an independent transgene that lacked *lacO* sites. As observed for the *gwIs4* array, depletion of SAMS-3/4 abrogated the association of the [*pha-4::lacZ; rol-6*] array with the INM (Figure 2F, right), yet *pha-4::lacZ* remained silent in all cells except the four to eight intestinal precursor cells that expressed the factors necessary for *pha-4* promoter induction (Figure S1B). Because the

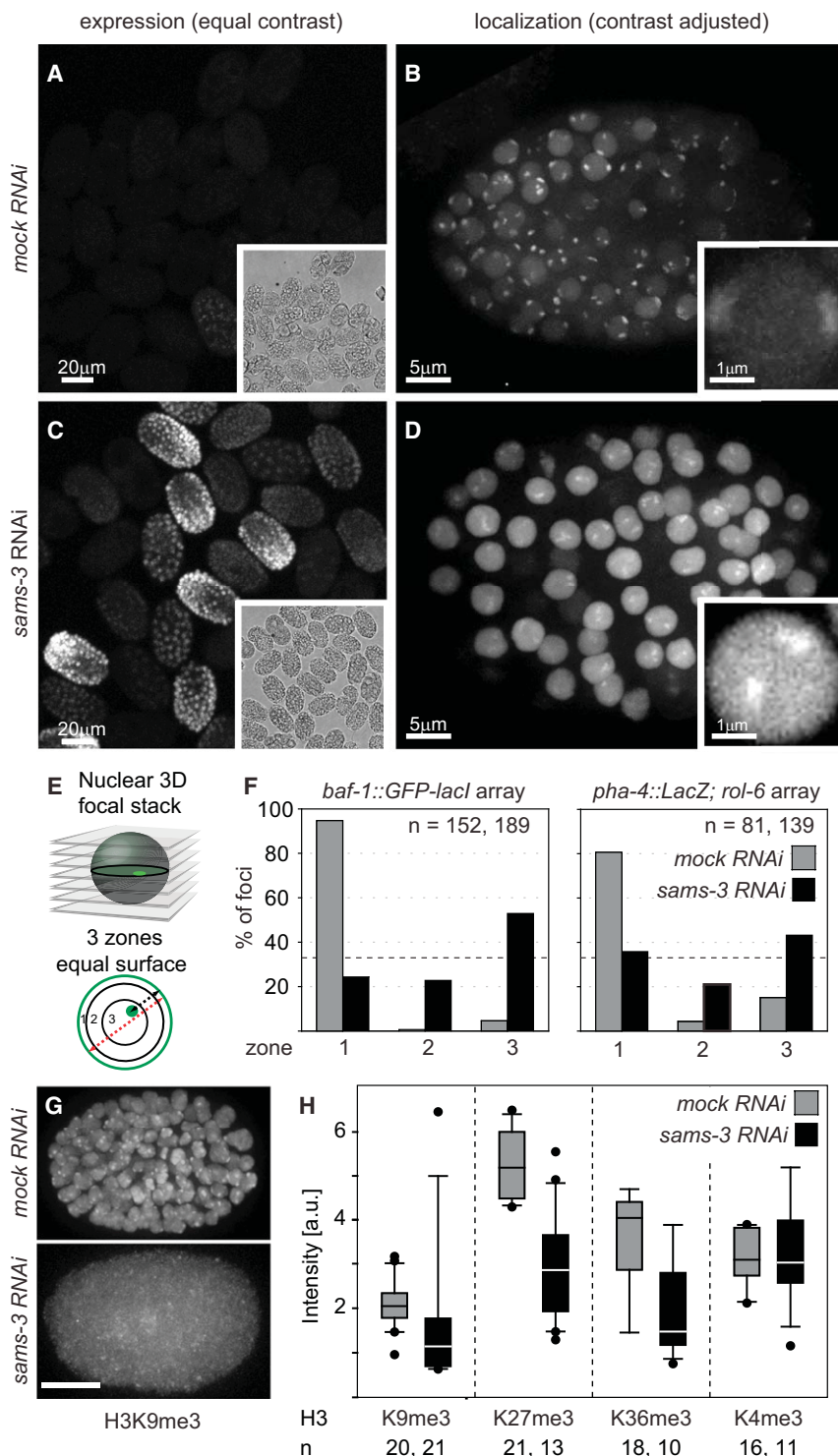


Figure 2. Depletion of SAM Synthetases Globally Reduces Histone Methylation Coincident with Array Derepression and Detachment

(A and C) The *gwl4*[*baf-1::GFP-LacI*] transgene is strongly derepressed upon *sams-3* RNAi. Shown are the GFP and brightfield (inset) signal of many embryos. Control and *sams-3* RNAi were imaged at the same illumination settings and are displayed with the same contrast.

(B and D) z-projection of representative embryos carrying the *gwl4* array after *sams-3* and control RNAi. Significant array detachment is observed for *sams-3* but not for control RNAi. Insets show a single focal plane of one nucleus.

(E) Array distribution is scored in a three-zone assay using the focal plane in which the spot has the highest intensity. Each cross-section was divided into three concentric zones of equal surface. Foci from many nuclei were binned into the three zones. A random distribution gives 33% per zone.

(F) Quantification of array distribution as in (E). Significant array detachment upon *sams-3* RNAi is observed for the *baf-1::GFP-lacI* array (left) and for the *pha-4::LacZ; rol-6* array (right), which lacks active housekeeping promoters ($p < 2.45 \times 10^{-11}$, Fisher's exact test). n, foci scored per condition; dotted line, expected random distribution.

(G) Embryos treated with *sams-3* and control RNAi stained for H3K9me3. Scale bar, 5 μ m

(H) Quantification of fluorescence intensities from the indicated number of embryos (n), stained for the indicated histone methyl marks. H3K9, H3K27, and H3K36 me3 is significantly reduced upon RNAi ($p \leq 0.004$, rank sum test). H3K4me3 did not change significantly ($p = 0.846$). Whiskers: 10th and 90th percentile; black dots: outliers; horizontal line: median.

See also Figure S1.

arrays (Bessler et al., 2010; Meister et al., 2010), we probed RNAi-treated embryos with antibodies specific for a range of methylated histones, namely trimethylated K4, K9, K27, and K36 on histone H3. The fluorescent immunostaining of methylated histone H3K9, K27, and K36 was strongly reduced, often

to a point below the background signal (Figures 2G, 2H, and S1C). Interestingly, we did not detect a strong reduction in trimethylation of H3K4 (Figures 2H and S1C), although we cannot exclude that the high residual signal after *sams-3/4* RNAi stems from off-target antibody binding. Alternatively, the H3K4 methyltransferase may be less sensitive to reduced SAM levels than are other HMTs.

Remarkably, the severe reduction in methylation of H3K9, K27, and K36 provoked by *sams-3/4* RNAi was compatible with embryonic development. We did not observe an increase in embryonic

lethality after *sams-3/4* depletion for up to three generations, although we did detect a significant reduction in brood size (Figure S1D). This is consistent with results showing that HMT mutations affecting H3K9, K27, and K36 methylation have relatively mild somatic defects but much stronger phenotypes in

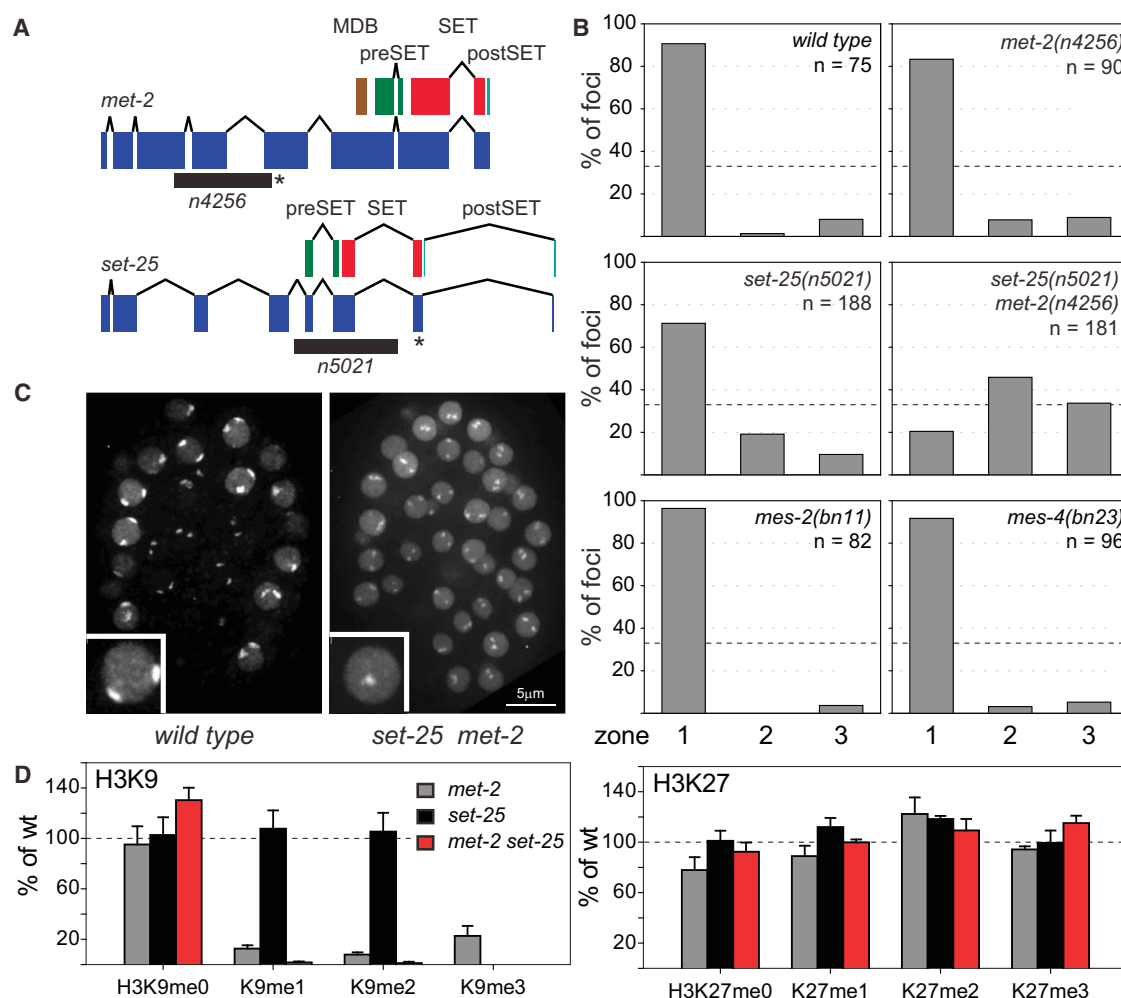


Figure 3. H3K9 Methyltransferases MET-2 and SET-25 Are Required for Gene Array Anchoring

(A) Scheme of *met-2* and *set-25* exon and domain structure, and deletion alleles used. * STOP codon caused by frame shift.

(B) Quantification of array distribution in 50–100 cell embryos as described in Figure 2E. Significant array detachment occurs in *set-25* and *set-25 met-2* but not in *mes-2* and *mes-4* mutants ($p \leq 8 \times 10^{-4}$ for comparisons: *set-25* versus wild-type, *set-25 met-2* versus wild-type, and *set-25* versus *set-25 met-2*; $p \geq 0.16$ for comparisons wild-type versus *met-2*, wild-type versus *mes-2*, and wild-type versus *mes-4*, Fisher's exact test). Dotted line, expected random distribution.

(C) Partial z-projection of GFP signal of wild-type and *set-25(n5021) met-2(n4256)* double-mutant embryos carrying the *gwis4[baf-1::GFP-LacI]* array.

(D) Quantification of H3K9 and H3K27 methylation levels in *met-2* and *set-25* single- and double-mutant early embryos by quantitative mass spectrometry. Data are shown relative to wild-type (dotted line, 100%). Error bars indicate the SEM in positive direction from three biological replica. See also Figures S2 and S3 and Tables S2 and S4.

the germline (Andersen and Horvitz, 2007; Bender et al., 2004; Bender et al., 2006).

In addition to *sams-3* and *sams-4*, the *C. elegans* genome encodes two more divergent SAM synthetases (*sams-1* and *sams-5*). RNAi of *sams-3/4* in a *sams-1/5* double mutant was not compatible with somatic growth, causing larval arrest at high penetrance (Figure S1E). Hence, despite the presence of multiple, partially redundant enzymes in *C. elegans*, downregulation of the enzymes SAMS-3 and SAMS-4 reduced SAM sufficiently to have a pronounced effect on histone methylation and transgene array localization while supporting embryonic development.

The Methyltransferases MET-2 and SET-25 Act Redundantly to Position Chromatin at the Nuclear Periphery

To test whether histone methylation itself is required for perinuclear chromatin anchoring, we next focused specifically on HMT mutants. We retrieved loss-of-function alleles for all HMTs identified in our primary screen, as well as for those predicted to target the same histone residues. Using this genetic resource, we scored for defects in heterochromatic array attachment at the INM in 11 different strains carrying mutations for individual or multiple SET domain proteins (Table S2). The tested single and double mutants included all known HMTs that target

H3K9, K27, K36, or combinations of multiple of these, all of which yielded viable embryos. For mutations in *mes-2* and *mes-4*, which cause maternal effect sterility (Capowski et al., 1991), we scored embryos of the second homozygous generation, which lack both maternal and zygotic MES proteins.

Ten out of the 11 single and double mutants tested were defective in array silencing, albeit not all to the same degree (Figure S2B; Table S2). However, arrays remained peripheral in all but two strains (Figure 3B; Table S2). The only single mutant with even partial array detachment was a *set-25* deletion (Figure 3B). Although the effect of *set-25* mutation on array position was significant ($p < 8 \times 10^{-4}$), 70% of the arrays nonetheless remained at the nuclear periphery in this mutant (Figure 3B). Complete release of arrays was only seen when we additionally deleted *met-2*, another HMT. Notably, the mutation of *met-2* alone did not cause significant array detachment and only mildly derepressed it (Figures 3B and S2A and S2B).

We confirmed that the observed array detachment in the double *set-25 met-2* mutant did not stem from allele-specific effects, or an unrelated background mutation, by scoring transgene position in another deletion allele of *met-2* combined with a *set-25* mutation and in a *met-2* mutant treated with *set-25* RNAi (Figure S2E). All three deletion alleles either span the SET domain or introduce a premature stop codon upstream of it (Figure S2D). These results allow us to conclude that *met-2* and *set-25* function redundantly to promote perinuclear localization and gene array silencing in *C. elegans* embryos. Loss of both recapitulates the loss of heterochromatin anchoring phenotype associated with *sams-3/-4* RNAi.

***met-2* and *set-25* Are Required for Mono-, Di- and Trimethylation of H3K9**

The SET domain of SET-25 is homologous to the mammalian enzymes EHMT1/G9a (28.8% identity, 44.6% similarity) and Suv39h1/2 (27.9% identity, 45.7% similarity), which both target histone H3K9 (Rea et al., 2000; Tachibana et al., 2002). SET-25, however, lacks both the Chromodomain and the Ankyrin repeats present in Suv39h1/2 or G9a (Figure 3A). Similarly, MET-2 is homologous to the mammalian H3K9 HMT SETDB1 (Andersen and Horvitz, 2007; Bessler et al., 2010). This suggests that MET-2 and SET-25 target H3K9, although additional nonhistone targets may exist.

To test whether the deletion of *met-2* and *set-25* indeed altered specific histone methylation states, we measured global histone methylation in early *C. elegans* embryos carrying mutations in either *met-2*, *set-25*, or in both genes by relative quantification using LC-MRM mass spectrometry. We found no systematic differences in the methylation levels of H3K23, K27, or K36 in either single or double mutants, but we found striking changes in the methylation of H3K9 (Figures 3D and S3). In agreement with previous reports (Andersen and Horvitz, 2007; Bessler et al., 2010), mono-, di-, and trimethylation of H3K9 were all reduced in the *met-2* single mutant, although each could be detected at 10% to 30% of wild-type levels (Figure 3D). In the *set-25* single mutant, on the other hand, H3K9me1 and me2 were at wild-type levels, whereas no H3K9me3 could be scored. Importantly, in the *met-2 set-25* double mutant, we could detect no mono-, di- or trimethylation of H3K9 whatsoever

(Figure 3D). This shows that there are no other histone H3K9 methyltransferase activities in the worm embryo and allows us to conclude that in the absence of SET-25, MET-2 catalyzes only H3K9 mono- and dimethylation. Moreover, whereas SET-25 alone can generate all three methylation states, its efficiency for H3K9 trimethylation is strongly increased when H3K9me1/2 is provided by MET-2. Together these data suggest that the two enzymes act in a step-wise manner. First, MET-2 mono- and dimethylates H3K9. Subsequently, SET-25 uses H3K9me1/2 as a substrate for trimethylation.

Heterochromatin anchoring was only partially compromised in the absence of SET-25 but was completely lost in the double mutant (Figure 3B). This suggests that H3K9me1/2 is sufficient to anchor ~70% of the arrays at the INM in the *C. elegans* embryo (versus 90% in wild-type). Even though the arrays remained peripheral in the absence of H3K9me3 arrays, they were strongly derepressed (Figure 3B and S2A and S2B). Trimethylation of H3K9 on peripheral arrays by SET-25 is therefore crucial for efficient array repression but anchoring can be mediated by either H3K9me1/2 or H3K9me3.

Mass spectrometry of histones from L1 larvae also showed strongly reduced levels of H3K9 methylation in the *set-25 met-2* double mutant, yet peripheral anchoring in these differentiated cells was affected to a much smaller degree (Figures S2F and S3). This suggests that additional anchoring mechanisms exist in differentiated tissues that may not rely exclusively on H3K9 methylation.

H3K9me1 and me2 Are Enriched at the Nuclear Periphery, Independently of H3K9me3

We next asked whether endogenous genomic domains carrying H3K9 methylation are similarly enriched at the INM. To test this, we localized H3K9me1, me2, and me3, and total histone H3 by indirect immunofluorescence with specific antibodies (Figure S4A) in the nuclei of wild-type and *set-25* mutant embryos lacking a transgene array. We counterstained the INM with antibodies for either *C. elegans* lamin (LMN-1) or nuclear pores (Figure 4A).

We measured ~150 H3K9 methylation profiles across the nuclear diameter of the equatorial focal plane of embryonic nuclei. As expected, the distribution of total histone H3 was identical to that of the DNA signal. In contrast, all three methylated forms of H3K9 showed enrichment at the nuclear periphery (Figure 4B, left). Repeating the same analysis in the *set-25* mutant, in which we detected no H3K9me3, revealed persistent perinuclear enrichment of H3K9me1 and H3K9me2 (Figure 4B, right). This is consistent with the INM attachment observed for gene arrays in the absence of H3K9me3 and suggests that endogenous domains carrying H3K9me1/2 bind the nuclear envelope independently of H3K9me3.

Mutation of *met-2* and *set-25* Globally Reduces Lamin Interaction of Chromosome Arms

We next asked whether the positioning of endogenous domains bearing H3K9 methylation is similarly sensitive to the loss of SET-25 and MET-2. In the worm, H3K9 methylation is enriched in the distal third of each chromosome arm (Liu et al., 2011; Figure 5C). In agreement with our proposal that H3K9me

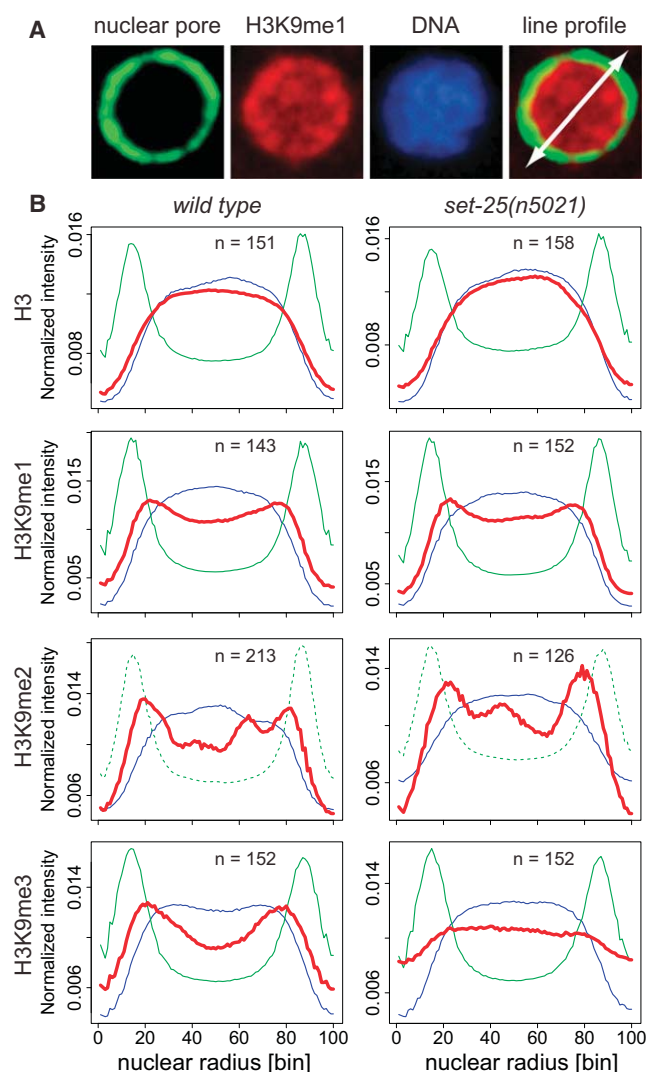


Figure 4. H3K9me1, me2, and me3 Are Enriched at the INM Independent of *set-25*

(A) Representative nuclear central focal plane of a wild-type embryo stained for H3K9me1 and the nuclear pore.

(B) Quantification of radial intensity of staining in wild-type and *set-25(n5021)* mutant embryos as described in [Experimental Procedures](#). Embryos were stained for the indicated histone modification (red), DNA (blue), and LMN-1 (green dotted) or the nuclear pore (green). For each panel, the indicated number (n) of radial line profiles was scaled and pooled into 100 bins, normalized, and averaged. The nearly flat curve for H3K9me3 in the right panel reflects the absence of this mark in the *set-25* mutant. See also [Figure S4](#).

serves as a trigger for perinuclear chromatin anchoring, H3K9me-rich chromosome arms were found to coimmunoprecipitate with LEM-2, a lamin-associated component of the INM ([Ikegami et al., 2010](#)). To see whether H3K9me contributes to the peripheral localization of these endogenous domains, we applied lamin-DamID ([Pickersgill et al., 2006](#)) to probe their subnuclear position in wild-type and *set-25 met-2* mutant worm embryos.

Specifically, we expressed a fusion protein between *C. elegans* lamin (LMN-1) and the *E. coli* adenine DNA methyltransferase (Dam) at low levels in *C. elegans* embryos. The LMN-1-Dam fusion was incorporated into the endogenous lamin meshwork at the nuclear periphery (data not shown) where it preferentially methylated DNA in close proximity. We amplified adenine methylated DNA by PCR from three biological replicates of each genotype and hybridized it to genomic tiling arrays by using DNA extracted from strains expressing a freely diffusible Dam-GFP fusion as competitor. This neutralizes the impact of sequence context on Dam activity.

Consistent with published chromatin immunoprecipitation (ChIP) results for the lamin interacting factor LEM-2 ([Ikegami et al., 2010](#)), we found that the LMN-1-DamID signal was strongly enriched on the arms of all autosomes and on the left arm of the X chromosome in wild-type embryos ([Figure 5A](#), black line). In contrast, the enrichment of the LMN-1-DamID signal on chromosome arms as compared to central domains was significantly reduced in the *set-25 met-2* double mutant ([Figure 5A](#), red line). This argues that the methylation deposited by SET-25 and MET-2 plays a role in the peripheral positioning of endogenous heterochromatin.

Intriguingly, the magnitude of reduction in LMN-1 DamID upon mutation of *met-2* and *set-25* was correlated with levels of H3K9 methylation in wild-type cells ([Figure 5D](#) and [S5A](#)). The more enriched for H3K9 methylation, the stronger the effect of the double mutant. This suggests that regions on chromosome arms with low H3K9me (e.g., ChrIV-R) use an alternative anchoring mechanism that is independent of this mark that accounts for the residual enrichment of LMN-1 on the distal chromosome arms in the *set-25 met-2* double mutant. Interestingly, positioning of the X chromosome was completely insensitive to loss of H3K9 methylation ([Figure 5A](#)).

To verify that domains with either high or low H3K9 methylation levels behave differentially in response to the double mutant, we measured the subnuclear position of two loci on the right arm of chromosome V (ChrV-R) by fluorescence in situ hybridization (FISH) and microscopy. We first scored a 30 kb domain next to the C18D4.6 locus that lies in a region of very high H3K9me3 and showed strongly reduced LMN-1 interaction in the *set-25 met-2* mutant ([Figures 5A](#) and [5C](#)). Indeed, 3D FISH confirmed that this locus shifted from a peripherally enriched to a near random distribution upon loss of H3K9 methylation ([Figures 5E](#) and [5F](#)). On the other hand, for the *pha-4* locus, which is 170 kb away from the telomere of ChrV-R and has comparatively low levels of H3K9 methylation, we did not score a significant shift away from the nuclear lamina in the double mutant, either by DamID or by microscopy ([Figures S5B](#) and [S5C](#)). This suggests that the *pha-4* locus may be positioned at the INM by an H3K9me-independent mechanism.

Taken together, by lamin-DamID and by microscopy we confirm an important role of SET-25 and MET-2 HMTs and the mono-, di- and trimethylation of histone H3K9 in the anchoring of native chromosome arms. At the same time, we identify a residual anchoring pathway that confers H3K9-independent positioning.

We next compared gene expression of wild-type and *set-25 met-2* mutant embryos by using genome-wide expression

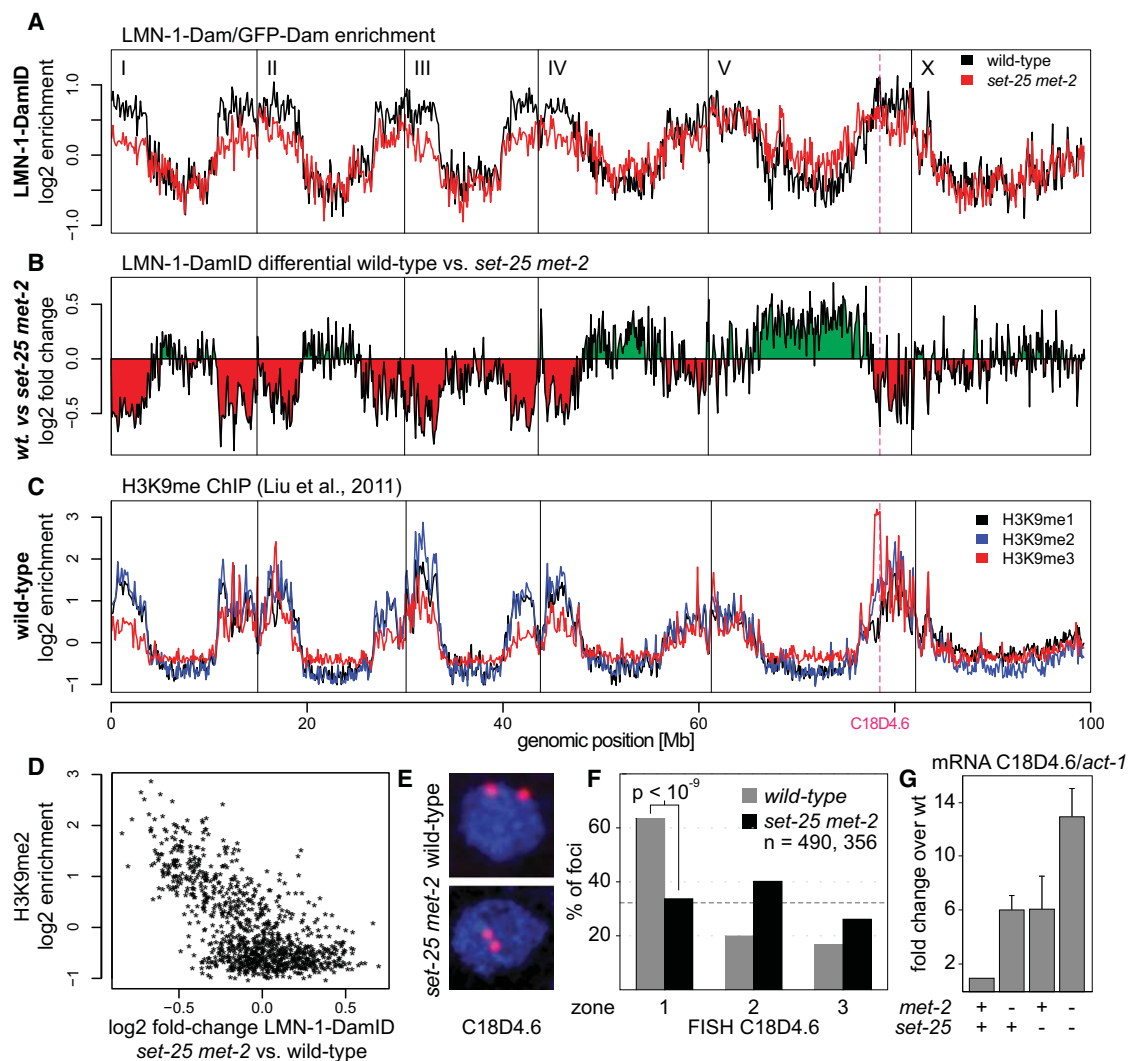


Figure 5. SET-25 and MET-2 Contribute to the Positioning of Chromosome Arms at the Nuclear Lamina

(A) LMN-1-Dam signal in wild-type (black) and *set-25 met-2* (red) embryos (averaged from three biological replicates). Tracks for all six chromosomes are shown. The pink dashed line indicates the position of the FISH probe used in (E and F). Each point reflects mean signal averaged from 2,000 array probes spanning 150 kb. (B) Differential of LMN-1-Dam signal from wild-type and *set-25 met-2* embryos. (C) H3K9me1, me2, and me3 enrichment in early embryos (data from Liu et al., 2011). (D) Changes in LMN-1-Dam methylation between wild-type and *set-25 met-2* mutant correlate with high levels of H3K9 methylation. (E) Single focal plane of *set-25 met-2* and wild-type nuclei probed by FISH for the C18D4.6 locus (red) and counterstained for DNA (blue). (F) Quantification of FISH signal shown in (E) by three-zone scoring. n, number of scored foci. (G) Quantification of expression levels of the C18D4.6 gene in indicated mutants by quantitative PCR. Data are shown normalized to *act-1* and relative to expression in wild-type. Error bars indicate the SEM from three biological replicates. See also Figure S5.

arrays. Consistent with our conclusion that transcriptional activity and position are not obligately linked, we did not find a strong genome-wide correlation of gene detachment and upregulation (data not shown). Nevertheless, among the genes upregulated in the double mutant, the C18D4.6 locus had strongly increased expression (12-fold) in the *set-25 met-2* mutant (Figure 5G). This indicates that subnuclear position mediated by H3K9me correlates with the silencing of some, but not all, genes.

MET-2 Is Enriched in the Cytoplasm

To examine the direct function of SET-25 and MET-2 in chromatin anchoring and silencing, we next studied the subcellular localization of the enzymes themselves. This was performed by expressing each enzyme as a fusion to mCherry (mCh). Both fusions were functional, as their expression in the *set-25* and *met-2* mutants restored H3K9 methylation (Figure S4B). Intriguingly, mCh-MET-2 was primarily cytoplasmic, whereas mCh-SET-25 was strongly enriched in the nucleus (Figure 6A).

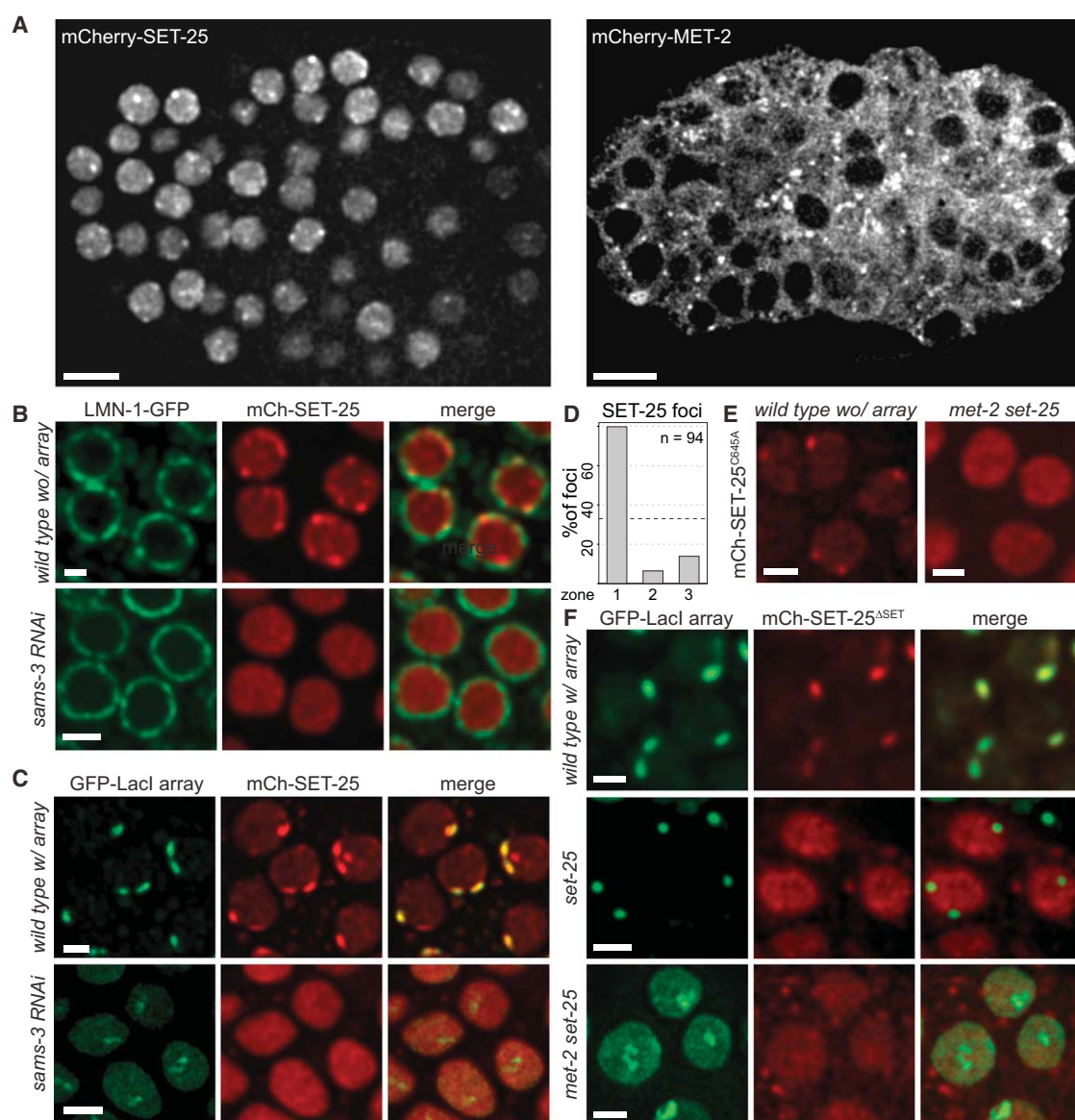


Figure 6. SET-25 Localizes to Perinuclear Foci in an H3K9 Methylation-Dependent Manner

(A) SET-25 and MET-2 were tagged N terminally with mCherry (mCh) and expressed in *C. elegans* embryos under control of the ubiquitously active *his-72* promoter. Scale bar, 5 μ m.

(B and C) Representative nuclei of embryos expressing mCh-SET-25 as described in (A) under control and *sams-3* RNAi conditions. mCh-SET-25 forms perinuclear foci in the absence (B) and presence (C) of the *gw/ls4* array. Strong SET-25 foci in C colocalize with the GFP-LacI signal that marks the *gw/ls4* transgene. Peripheral SET-25 foci and array-associated SET-25 are dispersed upon *sams-3* RNAi.

(D) Quantification of the radial distribution of mCh-SET-25 foci as shown in B (top) by three-zone scoring (Figure 2E). SET-25 foci are significantly enriched at the nuclear envelope over a random distribution (dotted line, $p < 10^{-15}$, Fisher's exact test).

(E) Localization of mCh-SET-25-C645A mutant in wild-type and *met-2(n4256)* *set-25(n5021)* embryos.

(F) As in (C, bottom), but for mCh-SET-25^{ΔSET} and in wild-type, *set-25(n5021)* and *met-2(n4256)* *set-25(n5021)* embryo. (B, C, E and F). Scale bar, 2 μ m.

See also Figure S6.

We scored an identical localization for MET-2 with either a C-terminal or an N-terminal tag (Figure S4C). It is therefore unlikely that the cytoplasmic localization of mCh-MET-2 is due to a disruption of normal protein function by mCherry. In the cytoplasm, MET-2 would methylate nonnucleosomal histones,

similar to the role proposed for the cytoplasmic fraction of the mammalian MET-2 homolog SETDB1 (Loyola et al., 2006; Loyola et al., 2009). The cytoplasmic localization of MET-2 also agrees with the step-wise deposition of H3K9 methylation, as suggested by our mass spectrometry data (Figure 3D).

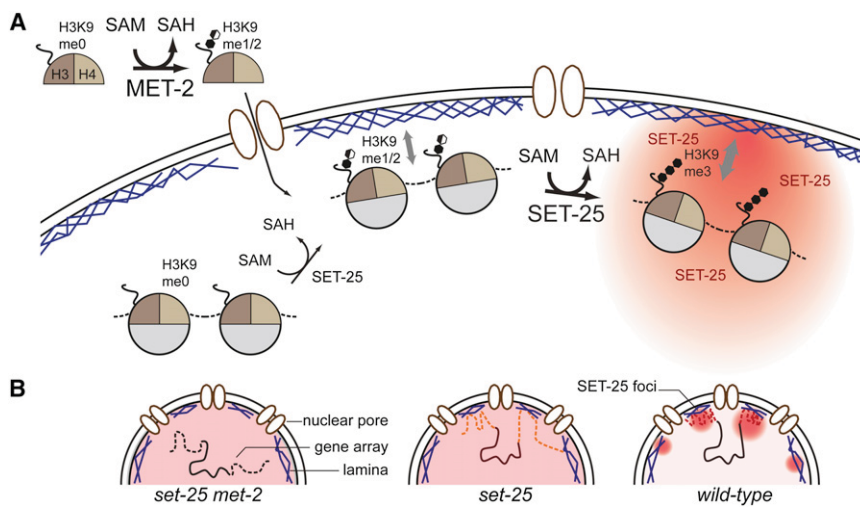


Figure 7. A Self-Reinforcing Mechanism for Perinuclear Anchoring and Heterochromatin Silencing

(A) The step-wise establishment of H3K9me3 involves deposition of H3K9me1/2 by cytoplasmic MET-2 prior to nucleosome assembly, and trimethylation by nuclear foci-associated SET-25. H3K9me1/2 initiates perinuclear chromatin targeting, and H3K9me3 is needed for complete array silencing and enhanced attachment. SET-25 requires its own reaction product, H3K9me3, to accumulate in perinuclear foci.

(B) The implications of (A) for the positioning of chromosome arms (dashed line) and generation of heterochromatic foci are shown. See Discussion for details.

SET-25 Localizes to Heterochromatic Perinuclear Foci

Careful inspection of mCh-SET-25 localization revealed that it was enriched in subnuclear foci that were often located at the nuclear periphery (80% in zone 1, Figures 6B and 6D) and which colocalized with both H3K9me3 and the worm HP1 homolog HPL-1 (Figure S6A). We did not see overlap of mCh-SET-25 and HPL-2 foci (Figure S6A), confirming that HPL-1 and HPL-2 occupy distinct subnuclear domains and have nonredundant functions (Schott et al., 2006).

Although mRNA levels of transgenic mCh-SET-25 were significantly higher than endogenous SET-25 (data not shown), the appearance of mCh-SET-25 foci is not simply a result of its expression level. Notably, we find that SET-25 foci are completely dispersed in embryos depleted for *sams-3* but have equal or even higher levels of mCh-SET-25 expression (see below). More importantly, the overexpressed mCh-SET-25 protein is functional because it rescued the loss of H3K9me3 in the *met-2 set-25* mutant (Figure S4B). To see whether the SET-25 foci correspond to heterochromatic domains, we next expressed mCh-SET-25 in embryos carrying the repetitive *gws4* array. In this strain, over the weaker perinuclear signal stemming from endogenous SET-25 foci, mCh-SET-25 formed two very bright foci that precisely colocalized with the GFP-LacI signal in every cell (Figure 6C).

SET-25 Localization Depends on H3K9 Methylation, but Is Independent of Its SET Domain

The colocalization of SET-25 with H3K9me3 and its enrichment on repetitive transgene arrays prompted us to test whether SET-25 localization was dependent on H3K9 methylation. Indeed, upon depletion of *sams-3/4* mCh-SET-25 distribution became diffuse, and it no longer accumulated in subnuclear foci (Figures 6B and 6C). To test whether SET-25 foci depend specifically on H3K9 methylation, we created a point mutation in the catalytic site of SET-25 (C645A), which corresponds to a catalytic null mutation in the homologous SET domain of human Suv39h (Rea et al., 2000). Like the wild-type mCh-SET-25, the C645A mutant still formed perinuclear foci, yet mCh-SET-25-C645A was completely dispersed in the *met-2 set-25*

mutant, which specifically loses H3K9 methylation (Figure 6E). We conclude that SET-25 enrichment at the INM and focus formation are dependent on methylated H3K9 yet do not require that the bound SET-25 itself is catalytically active.

Given that SET-25 has no obvious methyl-binding domain, we tested whether its recruitment to peripheral foci would depend on its SET domain. To this end, we expressed an mCh-SET-25 fusion that was truncated upstream of the SET domain (SET-25^{ΔSET}) in a strain carrying the repetitive gene array *gws4*. Like full-length SET-25, SET-25^{ΔSET} was strongly enriched on the *gws4* array (Figure 6F) and was dispersed in both a *met-2 set-25* double mutant and the *set-25* single mutant that lose H3K9me3 (Figure 6F and S6C). We conclude that the localization of SET-25 to perinuclear foci involves molecular interactions outside its catalytic domain and requires H3K9me3.

We can exclude that SET-25 is recruited to H3K9me3 by the Chromodomain-containing HP1 homologs HPL-1 and HPL-2. Although SET-25 colocalizes with HPL-1, it remained enriched on the *gws4* array in endogenous perinuclear foci in the *hpl-1 hpl-2* double-deletion strain (Figure S6B). Because we have not seen a specific direct interaction of SET-25^{ΔSET} with H3K9me3 in peptide binding assays (data not shown), we propose that SET-25 acts in a complex with other factors.

In summary, our results show H3K9me-dependent recruitment of gene arrays and chromosome arms to the nuclear envelope. SET-25, which deposits trimethylation, becomes enriched in H3K9me3 foci at the nuclear periphery, in a manner dependent on its own reaction product. This circularity could generate a self-sustaining subnuclear compartment that is enriched for H3K9 HMT activity, which in turn stabilizes silencing by efficiently trimethylating H3K9me1 and me2 (Figure 7).

DISCUSSION

Methylation of H3K9 Provides a Molecular Signal for Perinuclear Chromatin Localization

The eukaryotic nucleus shows remarkable spatial organization, with heterochromatin often associated with the nuclear envelope (NE) (Akhtar and Gasser, 2007; Kind and van Steensel, 2010).

Here, we report the first systematic screen for factors required for the perinuclear sequestration of heterochromatin within a multicellular organism. Using a repetitive GFP-expressing transgene as a model for heterochromatin, we performed a genome-wide RNAi screen for both derepression and detachment. The only targets that compromised both encoded S-adenosylmethionine synthetases (Figure 2). This prompted us to carry out a systematic survey of putative HMTs, from which we identified two enzymes, MET-2 and SET-25, that mediate anchoring by methylation of histone H3K9 (Figure 3). In mutants lacking only one of the two HMTs, repetitive gene arrays remained perinuclear (Figure 3), whereas loss of both removed all H3K9me and eliminated array anchoring.

The only histone residue for which we scored reduced methylation in *met-2* and *set-25* mutants is H3K9. However, we do not exclude that it has other nonhistone substrates. The loss of HMTs that modify residues other than H3K9 did not affect array anchoring. We tested conditions that eliminated H3K27me3 (Figure S2C, *mes-2*; Bender et al., 2004), as well as H3K36me2/3 (Table S2, *mes-4 met-1*; Furuhashi et al., 2010), yet arrays remained anchored. Thus, we conclude that H3K9 methylation is a molecular signal for chromatin positioning at the NE and rule out a requirement for other histone H3 methyl marks in this process.

Despite strong correlations between peripheral localization and transcriptional inactivity, the two are not strictly linked in worms or in mammals (Meister et al., 2010; Peric-Hupkes et al., 2010). Indeed, we show that expression from the *baf-1* promoter on the GFP-LacI array is not sufficient for detachment. In the *set-25* single mutant, arrays were devoid of H3K9me3 and strongly derepressed, but due to the MET-2 deposited H3K9me1 and H3K9me2 modifications they remained enriched at the NE (Figures 3B and S2A and S2B). Similarly, *mes-4* and *hpl-2* mutations, and loss of several other chromatin factors, provoked strong derepression without altering array position (Figures S2B and S2C; Table S2). We can therefore exclude that the release of chromatin from the nuclear periphery in the *set-25 met-2* double mutant is explained by changes in promoter activity.

H3K9 Methylation Correlates with Lamin-Associated Domains from Worms to Man

The role of SET-25 and MET-2 in tethering chromatin to the NE is not limited to transgene arrays. We have shown that the same is true for endogenous loci in the repeat-rich arms of *C. elegans* chromosomes. Thus, our study provides the first causal evidence for a role of H3K9 methylation in perinuclear chromatin anchoring. DamID studies showed that 80% of non-centromeric H3K9me2 domains overlap with LADs in mammals (Peric-Hupkes et al., 2010; Wen et al., 2009). The anchoring of mammalian LADs has not previously been shown to be H3K9 dependent, but this striking correlation makes it likely that the function of H3K9me1/2 in perinuclear chromatin anchoring is conserved beyond worms.

We show that H3K9me provides a signal to position chromatin at the NE. But what recognizes the H3K9me mark? Using genetic null alleles, we show that none of the H3K9me binding factors previously characterized in *C. elegans* are involved:

array anchoring was unaltered upon loss of the HP1 homologs HPL-1 or HPL-2, alone or together, even in cells lacking the MBT domain protein LIN-61 (Figure S2C). This indicates that a novel class of yet uncharacterized factors mediates the molecular link between the nuclear periphery and H3K9me. Given that we identify a two-step anchoring process in which either H3K9me1/2 or H3K9me3 can signal peripheral localization, we also expect redundancy among these H3K9me readers, requiring combinatorial RNAi and/or screens in sensitized backgrounds to allow their identification.

Additional Pathways Position Chromatin in an H3K9me-Independent Manner

Diminished H3K9 methylation levels or loss of *met-2* causes a reduction in brood-size, low-penetrance embryonic lethality, a high incidence of males, and the formation of ectopic vulvae in sensitized backgrounds (Andersen and Horvitz, 2007; Koester-Eiserfunke and Fischle, 2011 and data not shown). Nevertheless, most *set-25 met-2* double-mutant animals are viable and fertile even though they lack detectable H3K9 methylation. Given the strict conservation of perinuclear chromatin anchoring from yeast to man (Kind and van Steensel, 2010), it is perhaps surprising that loss of anchoring is compatible with worm development. We note, however, that although the amplitude of LMN-1-DamID on chromosome arms was strongly reduced in the *met-2 set-25* mutant, chromosome arms retained slightly higher LMN-1-DamID signals than did chromosome centers (Figure 5). We also found that arrays become peripheral even in the absence of H3K9me upon cell differentiation (Figures S2F and S3). Thus, although we demonstrate a clear role for H3K9 methylation in perinuclear anchoring of chromatin in *C. elegans* embryos, partially redundant pathways of chromatin anchoring may ensure normal worm development even in the absence of H3K9 methylation.

A Conserved Two-Step Model for Generating H3K9me3-Containing Heterochromatic Foci

The establishment of H3K9me3 at mammalian centromeres has been proposed to occur in a step-wise manner by at least two enzymes (Loyola et al., 2006; Loyola et al., 2009; Peters et al., 2001). The methylation specificities of MET-2 and SET-25 argue for a similar step-wise methylation of H3K9 on perinuclear heterochromatin. Moreover, a step-wise mechanism is supported by the distinct subcellular localizations of the two enzymes. H3K9me1/2 is deposited by MET-2, which largely resides in the cytoplasm (Figure 6A). Similarly, SETDB1, the mammalian homolog of MET-2 (Loyola et al., 2006), and the two redundant mouse enzymes PRDM3 and PRDM16 (Pinheiro, et al., 2012, this issue of Cell) are abundant in the cytoplasm and mediate H3K9me1. Indeed, one-third of nonnucleosomal H3 carries K9me1 in mammals (Loyola et al., 2006).

We propose that after its nuclear import and incorporation into nucleosomes, H3K9me1/2 serves as a substrate for trimethylation by SET-25 (Figures 6B and 7). Given the enrichment of SET-25 in perinuclear foci, this latter step may occur preferentially at the nuclear periphery. The ability of H3K9me1/2 to mediate association with the nuclear envelope thus would promote trimethylation and repression. In mammalian cells

lacking both Suv39h isozymes, centromeres are devoid of H3K9me3, yet they remain clustered. A proposed explanation was that H3K9me1, which accumulates on centromeres in *suv39h1/2* double mutants (Peters et al., 2001), compensates for me3. Here, we show that this model holds for peripheral heterochromatin in *C. elegans*: arrays remained peripherally enriched in the absence of H3K9me3, but were entirely released in the *set-25 met-2* double mutant, which lacks all H3K9 methylation.

It has so far not been possible to deplete H3K9me1 completely from mammalian centromeres. However, recent evidence suggests that this can be achieved by simultaneous downregulation of the two H3K9-specific monomethyltransferases, PRDM3 and PRDM16 (Pinheiro et al., 2012, this issue of Cell). Analogous to our data implicating H3K9me1/2 in chromatin positioning, loss of H3K9me1 in mice provokes dispersion of centromeric foci and transcription of major satellite (Pinheiro et al., 2012, this issue of Cell).

A Self-Reinforcing Mechanism to Sequester Silent Chromatin at the Nuclear Periphery

Several HMTs are recruited to chromatin by the marks they deposit. It is generally assumed that this triggers the modification of neighboring nucleosomes and results in spreading of the chromatin mark (Bannister et al., 2001; Lachner et al., 2001). Evidence for such a mechanism exists for the propagation of H3K27me3 by PRC2 (Hansen et al., 2008), for the spreading of H3K9me3 in fission yeast by Clr4 (Zhang et al., 2008), and for the maintenance of H3K9me3 at centromeric repeats in mammals by Suv39 (Bannister et al., 2001; Lachner et al., 2001). In this sense, SET-25 fits the paradigm because it becomes enriched in foci that colocalize with H3K9me3. However, in contrast to Suv39h1/2, which are recruited to methylated H3K9 via HP1 (Bannister et al., 2001; Lachner et al., 2001), localization of SET-25 to perinuclear foci is independent of the two worm HP1 homologs (Figure S6). Moreover, SET-25 has little or no sequence homology to Suv39h outside its SET domain and lacks an identifiable Chromodomain. Future work will determine whether SET-25 binds directly to H3K9me3 or whether it is recruited by another nonhistone protein.

If H3K9 methylation is the trigger for perinuclear anchoring, the formation of heterochromatin itself should be able to drive its spatial separation from active chromatin domains. Because SET-25 associates with H3K9me3, the spatial separation of euchromatin and heterochromatin generates an unequal subnuclear distribution of the HMT that deposits the repressive H3K9me3 mark. Its perinuclear sequestration, in turn, has the potential to render the nuclear periphery a favorable zone for H3K9 trimethylation. This could act as a self-reinforcing silencing mechanism that ensures a robust spatial separation of active and inactive chromatin domains (Figure 7).

In conclusion, the histone modification and deposition pathway documented here suggests a means for the autonomous assembly of a subnuclear compartment that supports efficient heterochromatin formation. The many analogies to mammalian silencing suggest that the principles identified here have cross-species relevance.

EXPERIMENTAL PROCEDURES

Molecular Biology and Transgenic Strains

All plasmids, except plasmids for DamID constructs, were generated by MultiSite Gateway cloning (Invitrogen). The C645A mutation in *set-25* was introduced by site-directed mutagenesis. Strains used in this study are listed in Table S3. DamID strains were backcrossed twice, the *set-25(n5021)* and *met-2(n4256)* alleles five times to wild-type strains. Worms were grown at 22.5°C, except for the zoning assays in *lin-61 hpl-2* mutants (25°C) and for DamID (20°C).

RNAi

For individual assays, RNAi was performed by feeding on plates (Timmons et al., 2001). The RNAi screen was done in liquid cultures (adapted from Lehner et al., 2006, see Extended Experimental Procedures). An *EcoRV* fragment containing 25 bp identical to GFP-LacI was removed from vector L4440 (Fire vector library) and used as mock RNAi control. A strain supplemented with an additional copy of a *lacO* free *baf-1::GFP-lacI* transgene was used to enhance the GFP signal for *gwls4* visualization.

Immunofluorescence and Fluorescence In Situ Hybridization

Immunofluorescence (IF) was carried out as previously described by freeze-cracking and brief fixation in 1% paraformaldehyde followed by short post-fixation in methanol (Meister et al., 2010). For quantitative histone IF and antibodies used see Extended Experimental Procedures.

Fluorescent probes were made by nick-translation using fluorescent dUTP-Atto647N (Jena Bioscience) and fosmid WRM0637cA03 as a template. For FISH, embryos were fixed in methanol (−20°C, 2') followed by 4% paraformaldehyde (4°C, 10') after freeze-cracking. Embryos were permeabilized in PBS-Triton X-100 (0.5%) and treated briefly with 0.1M HCl and RNase. FISH probe and sample were denatured at 72°C and hybridized in 50% formamide/2X SSC for 3 days at 37°C, followed by three low- and two high-stringency washes (2X SSC, 37°C / 0.2X SSC, 55°C).

Microscopy

Microscopy was carried out on a spinning disc confocal microscope (Visitron, Puchheim), as previously described (Meister et al., 2010). Deconvolution (Huygens Pro) was applied to Figures 5, 6, S5, and S6. 3D reconstructions were generated by using Imaris (Bitplane). Quantitation of array distribution on focal stacks of images using the ImageJ plugin PointPicker (<http://bigwww.epfl.ch/thevenaz/pointpicker/>) was performed as previously described (Meister et al., 2010). For radial quantitation of H3K9me, 200 nm spaced image stacks were acquired and processed by deconvolution. Using >120 independent manually selected line profiles (5 pixels wide) at the central nuclear plane, lines were extended laterally by 12.5% of the nuclear diameter, and signal intensities were extracted and pooled into 100 bins. Individual profiles were normalized, averaged, and plotted by using R.

Isolation of Histones and Mass Spectrometry

Early embryos were obtained by bleaching from synchronized young adults grown for 53 to 58 hr after L1 stage at 22.5°C. H3 was isolated for mass spectrometry as described in Extended Experimental Procedures. Free and monomethylated amino groups were chemically modified with propionic anhydride prior trypsin digestion (Peters et al., 2003). After elution from gel the differently methylated peptides were quantified by LC-MRM on an AB SCIEX 4000 QTRAP, and peak area ratios were normalized to wild-type and histone H3.

LMN-1-DamID

All DamID constructs were integrated as a single-copy on Chromosome II by MosSCI (Frøkjær-Jensen et al., 2008). Details on strains, plasmids, DNA isolation, and computational analysis are in Extended Experimental Procedures.

ACCESSION NUMBERS

The GEO accession number for the DamID microarray raw data is GSE37226.

SUPPLEMENTAL INFORMATION

Supplemental Information includes Extended Experimental Procedures, six figures, and four tables and can be found with this article online at <http://dx.doi.org/10.1016/j.cell.2012.06.051>.

ACKNOWLEDGMENTS

We thank Y. Gruenbaum and T. Jenuwein for antibodies; M. Thomas, R. Arpagaus, R. Son, and T. Sakuragi for excellent technical assistance; I. Katic for help with injections; the *Caenorhabditis* Genetics Center; R. Horvitz, M. Tijsterman and F. Palladino for strains; D. Schübeler, A. Peters, and H. Ferreira for critical reading of the manuscript; and L. Hoerner for help with array hybridization. This work was supported by the European Union Network of Excellence “Epigenome”, the Novartis Research Foundation, the “Fondation Suisse de recherche sur les maladies musculaires”, the Spanish Ministry of Science and Innovation (BFU2010-15478 to P.A.), and EMBO (ASTF 478-2011 to C.G.A.).

Received: June 12, 2011

Revised: April 5, 2012

Accepted: June 26, 2012

Published: August 30, 2012

REFERENCES

- Akhhtar, A., and Gasser, S.M. (2007). The nuclear envelope and transcriptional control. *Nat. Rev. Genet.* 8, 507–517.
- Andersen, E.C., and Horvitz, H.R. (2007). Two *C. elegans* histone methyltransferases repress *lin-3* EGF transcription to inhibit vulval development. *Development* 134, 2991–2999.
- Azzaria, M., Goszczynski, B., Chung, M.A., Kalb, J.M., and McGhee, J.D. (1996). A fork head/HNF-3 homolog expressed in the pharynx and intestine of the *Caenorhabditis elegans* embryo. *Dev. Biol.* 178, 289–303.
- Bannister, A.J., Zegerman, P., Partridge, J.F., Miska, E.A., Thomas, J.O., Allshire, R.C., and Kouzarides, T. (2001). Selective recognition of methylated lysine 9 on histone H3 by the HP1 chromo domain. *Nature* 410, 120–124.
- Bender, L.B., Cao, R., Zhang, Y., and Strome, S. (2004). The MES-2/MES-3/MES-6 complex and regulation of histone H3 methylation in *C. elegans*. *Curr. Biol.* 14, 1639–1643.
- Bender, L.B., Suh, J., Carroll, C.R., Fong, Y., Fingerman, I.M., Briggs, S.D., Cao, R., Zhang, Y., Reinke, V., and Strome, S. (2006). MES-4: an autosome-associated histone methyltransferase that participates in silencing the X chromosomes in the *C. elegans* germ line. *Development* 133, 3907–3917.
- Bessler, J.B., Andersen, E.C., and Villeneuve, A.M. (2010). Differential localization and independent acquisition of the H3K9me2 and H3K9me3 chromatin modifications in the *Caenorhabditis elegans* adult germ line. *PLoS Genet.* 6, e1000830.
- Black, J.C., and Whetstone, J.R. (2011). Chromatin landscape: methylation beyond transcription. *Epigenetics* 6, 9–15.
- Capowski, E.E., Martin, P., Garvin, C., and Strome, S. (1991). Identification of grandchildless loci whose products are required for normal germ-line development in the nematode *Caenorhabditis elegans*. *Genetics* 129, 1061–1072.
- Dennis, G., Jr., Sherman, B.T., Hosack, D.A., Yang, J., Gao, W., Lane, H.C., and Lempicki, R.A. (2003). DAVID: Database for Annotation, Visualization, and Integrated Discovery. *Genome Biol.* 4, 3.
- Frøkjær-Jensen, C., Davis, M.W., Hopkins, C.E., Newman, B.J., Thummel, J.M., Olesen, S.-P., Grunnet, M., and Jorgensen, E.M. (2008). Single-copy insertion of transgenes in *Caenorhabditis elegans*. *Nat. Genet.* 40, 1375–1383.
- Furuhashi, H., Takasaki, T., Rechtsteiner, A., Li, T., Kimura, H., Checchi, P.M., Strome, S., and Kelly, W.G. (2010). Trans-generational epigenetic regulation of *C. elegans* primordial germ cells. *Epigenetics Chromatin* 3, 15.
- Goldman, R.D., Gruenbaum, Y., Moir, R.D., Shumaker, D.K., and Spann, T.P. (2002). Nuclear lamins: building blocks of nuclear architecture. *Genes Dev.* 16, 533–547.
- Guelen, L., Pagie, L., Brasset, E., Meuleman, W., Faza, M.B., Talhout, W., Eussen, B.H., de Klein, A., Wessels, L., de Laat, W., and van Steensel, B. (2008). Domain organization of human chromosomes revealed by mapping of nuclear lamina interactions. *Nature* 453, 948–951.
- Hansen, K.H., Bracken, A.P., Pasini, D., Dietrich, N., Gehani, S.S., Monrad, A., Rappsilber, J., Lerdrup, M., and Helin, K. (2008). A model for transmission of the H3K27me3 epigenetic mark. *Nat. Cell Biol.* 10, 1291–1300.
- Hsieh, J., and Fire, A. (2000). Recognition and silencing of repeated DNA. *Annu. Rev. Genet.* 34, 187–204.
- Ikegami, K., Egelhofer, T.A., Strome, S., and Lieb, J.D. (2010). *Caenorhabditis elegans* chromosome arms are anchored to the nuclear membrane via discontinuous association with LEM-2. *Genome Biol.* 11, R120.
- Kamath, R.S., Fraser, A.G., Dong, Y., Poulin, G., Durbin, R., Gotta, M., Kanapin, A., Le Bot, N., Moreno, S., Sohrmann, M., et al. (2003). Systematic functional analysis of the *Caenorhabditis elegans* genome using RNAi. *Nature* 421, 231–237.
- Kind, J., and van Steensel, B. (2010). Genome-nuclear lamina interactions and gene regulation. *Curr. Opin. Cell Biol.* 22, 320–325.
- Koester-Eiserfunke, N., and Fischle, W. (2011). H3K9me2/3 binding of the MBT domain protein LIN-61 is essential for *Caenorhabditis elegans* vulva development. *PLoS Genet.* 7, e1002017.
- Lachner, M., O’Carroll, D., Rea, S., Mechtler, K., and Jenuwein, T. (2001). Methylation of histone H3 lysine 9 creates a binding site for HP1 proteins. *Nature* 410, 116–120.
- Lehner, B., Tischler, J., and Fraser, A.G. (2006). RNAi screens in *Caenorhabditis elegans* in a 96-well liquid format and their application to the systematic identification of genetic interactions. *Nat. Protoc.* 1, 1617–1620.
- Liu, T., Rechtsteiner, A., Egelhofer, T.A., Vielle, A., Latorre, I., Cheung, M.-S., Ercan, S., Ikegami, K., Jensen, M., Kolasinska-Zwierz, P., et al. (2011). Broad chromosomal domains of histone modification patterns in *C. elegans*. *Genome Res.* 21, 227–236.
- Loyola, A., Bonaldi, T., Roche, D., Imhof, A., and Almouzni, G. (2006). PTMs on H3 variants before chromatin assembly potentiate their final epigenetic state. *Mol. Cell* 24, 309–316.
- Loyola, A., Tagami, H., Bonaldi, T., Roche, D., Quivy, J.P., Imhof, A., Nakatani, Y., Dent, S.Y.R., and Almouzni, G. (2009). The HP1 α -CAF1-SetDB1-containing complex provides H3K9me1 for Suv39-mediated K9me3 in pericentric heterochromatin. *EMBO Rep.* 10, 769–775.
- Luo, L., Gassman, K.L., Petell, L.M., Wilson, C.L., Bewersdorf, J., and Shopland, L.S. (2009). The nuclear periphery of embryonic stem cells is a transcriptionally permissive and repressive compartment. *J. Cell Sci.* 122, 3729–3737.
- Maison, C., and Almouzni, G. (2004). HP1 and the dynamics of heterochromatin maintenance. *Nat. Rev. Mol. Cell Biol.* 5, 296–304.
- Margalit, A., Brachner, A., Gotzmann, J., Foisner, R., and Gruenbaum, Y. (2007). Barrier-to-autointegration factor—a BAFfling little protein. *Trends Cell Biol.* 17, 202–208.
- Martin, D.I.K., and Whitelaw, E. (1996). The vagaries of variegating transgenes. *Bioessays* 18, 919–923.
- Mattout, A., Pike, B.L., Towbin, B.D., Bank, E.M., Gonzalez-Sandoval, A., Stadler, M.B., Meister, P., Gruenbaum, Y., and Gasser, S.M. (2011). An EDMD mutation in *C. elegans* lamin blocks muscle-specific gene relocation and compromises muscle integrity. *Curr. Biol.* 21, 1603–1614.
- Meister, P., Towbin, B.D., Pike, B.L., Ponti, A., and Gasser, S.M. (2010). The spatial dynamics of tissue-specific promoters during *C. elegans* development. *Genes Dev.* 24, 766–782.
- Peric-Hupkes, D., Meuleman, W., Pagie, L., Bruggeman, S.W.M., Solovei, I., Brugman, W., Gräf, S., Flicek, P., Kerkhoven, R.M., van Lohuizen, M., et al. (2010). Molecular maps of the reorganization of genome-nuclear lamina interactions during differentiation. *Mol. Cell* 38, 603–613.

- Peters, A.H.F.M., O'Carroll, D., Scherthan, H., Mechtler, K., Sauer, S., Schöfer, C., Weipoltshammer, K., Pagani, M., Lachner, M., Kohlmaier, A., et al. (2001). Loss of the Suv39h histone methyltransferases impairs mammalian heterochromatin and genome stability. *Cell* 107, 323–337.
- Peters, A.H.F.M., Kubicek, S., Mechtler, K., O'Sullivan, R.J., Derijck, A.A.H.A., Perez-Burgos, L., Kohlmaier, A., Opravil, S., Tachibana, M., Shinkai, Y., et al. (2003). Partitioning and plasticity of repressive histone methylation states in mammalian chromatin. *Mol. Cell* 12, 1577–1589.
- Pickersgill, H., Kalverda, B., de Wit, E., Talhout, W., Fornerod, M., and van Steensel, B. (2006). Characterization of the *Drosophila melanogaster* genome at the nuclear lamina. *Nat. Genet.* 38, 1005–1014.
- Pinheiro, I., Margueron, R., Shukeir, N., Eisold, M., Fritzsch, C., Richter, F.M., Mittler, G., Genoud, C., Goyama, S., Kurokawa, M., et al. (2012). Prdm3 and Prdm16 are H3K9me1 Methyltransferases Required for Mammalian Heterochromatin Integrity. *Cell* 150, this issue, 948–960.
- Rea, S., Eisenhaber, F., O'Carroll, D., Strahl, B.D., Sun, Z.-W., Schmid, M., Opravil, S., Mechtler, K., Ponting, C.P., Allis, C.D., and Jenuwein, T. (2000). Regulation of chromatin structure by site-specific histone H3 methyltransferases. *Nature* 406, 593–599.
- Sassi, H.E., Renihan, S., Spence, A.M., and Cooperstock, R.L. (2005). Gene CATCHR—gene cloning and tagging for *Caenorhabditis elegans* using yeast homologous recombination: a novel approach for the analysis of gene expression. *Nucleic Acids Res.* 33, e163.
- Schott, S., Coustham, V., Simonet, T., Bedet, C., and Palladino, F. (2006). Unique and redundant functions of *C. elegans* HP1 proteins in post-embryonic development. *Dev. Biol.* 298, 176–187.
- Shevelyov, Y.Y., Lavrov, S.A., Mikhaylova, L.M., Nurminsky, I.D., Kulathinal, R.J., Egorova, K.S., Rozovsky, Y.M., and Nurminsky, D.I. (2009). The B-type lamin is required for somatic repression of testis-specific gene clusters. *Proc. Natl. Acad. Sci. USA* 106, 3282–3287.
- Tachibana, M., Sugimoto, K., Nozaki, M., Ueda, J., Ohta, T., Ohki, M., Fukuda, M., Takeda, N., Niida, H., Kato, H., and Shinkai, Y. (2002). G9a histone methyltransferase plays a dominant role in euchromatic histone H3 lysine 9 methylation and is essential for early embryogenesis. *Genes Dev.* 16, 1779–1791.
- Timmons, L., Court, D.L., and Fire, A. (2001). Ingestion of bacterially expressed dsRNAs can produce specific and potent genetic interference in *Caenorhabditis elegans*. *Gene* 263, 103–112.
- Wen, B., Wu, H., Shinkai, Y., Irizarry, R.A., and Feinberg, A.P. (2009). Large histone H3 lysine 9 dimethylated chromatin blocks distinguish differentiated from embryonic stem cells. *Nat. Genet.* 41, 246–250.
- Ye, Q., and Worman, H.J. (1996). Interaction between an integral protein of the nuclear envelope inner membrane and human chromodomain proteins homologous to *Drosophila* HP1. *J. Biol. Chem.* 271, 14653–14656.
- Yuzyuk, T., Fakhouri, T.H.I., Kiefer, J., and Mango, S.E. (2009). The polycomb complex protein *mes-2/E(z)* promotes the transition from developmental plasticity to differentiation in *C. elegans* embryos. *Dev. Cell* 16, 699–710.
- Zhang, K., Mosch, K., Fischle, W., and Grewal, S.I.S. (2008). Roles of the Ctr4 methyltransferase complex in nucleation, spreading and maintenance of heterochromatin. *Nat. Struct. Mol. Biol.* 15, 381–388.

Supplemental Information

EXTENDED EXPERIMENTAL PROCEDURES

RNAi Library Screen

For the genome-wide screen RNAi was performed in liquid by using a protocol adapted from (Lehner et al., 2006). L1 larvae of strain NL2507 were synchronized by hatching in the absence of food, pelleted, and resuspended in S-basal (supplemented with 1 mM Carbenicillin and 4 mM IPTG). One hundred microliters worm suspension, containing approximately 20 larvae were dispensed in 96 well plates, where each well contained pelleted bacteria expressing dsRNA from a genome-wide RNAi library (Kamath et al., 2003). Worms were grown for 4 days at 22.5°C under agitation (150 rpm) and subsequently anesthetized with 1 mM Levamisol. Embryonic F1 progeny within the uterus of the P0 worms manually checked within the 96 well plates for increased GFP expression on an inverted fluorescent microscope (Zeiss Axiovert, 10× air objective). Positive hits were reproduced three times, and clone identity was verified by sequencing.

Antibodies

Antibodies used for IF were as follows. Figure 3: anti-H3K9me3, (gift from T. Jenuwein, #4861), anti H3K27me3 (Upstate 07-449), anti-H3K36me3 (Abcam, ab9050), anti-H3K4me3 (Upstate 07-473), anti-GFP (Roche, 11 814 460 001). Figures 5 and S5: anti-H3K9me1 (gift from T. Jenuwein, #4858), anti-H3K9me2 (Abcam, ab1220), anti-H3K9me3 (Cell Signaling Technology, #9754S, Lot 1), anti-H3 (Abcam, ab1791), anti-nuclear pore/Mab414 (Abcam, ab24609), anti-LMN-1 (gift from Y. Gruenbaum).

Quantitative IF

sams-3 and control RNAi were performed for two generations separately with strains that do (NL2507) and do not (JM50) express GFP. Embryos from both strains were mixed prior to staining and imaged at same illumination conditions. GFP signal was used to classify embryos, and maximum intensity projections were quantified by using ImageJ.

Isolation of Histones from *C. Elegans* Embryos and Mass Spectrometry

Early embryo populations were obtained by bleaching from young adults grown for 53 to 58 hr at 22.5°C on peptone enriched plates starting with synchronized L1 larvae, and histones were isolated for mass spectroscopic analysis. For each replica, embryos were extracted from approximately 300,000 worms per strain, frozen as droplets in liquid N₂, and ground to powder by using a ball mill (30 s, 30 Hz). The frozen powder was resuspended in lysis buffer (LB) (100 mM HEPES pH7.5, 50 mM NaCl, 1% Triton X-100, 0.1% DOC, 1 mM EDTA, Protease inhibitors). To remove soluble proteins the suspension was centrifuged at high speed (10 min, 16,000 g) and the supernatant was discarded. The insoluble pellet was resuspended in LB and sonicated to shear DNA and solubilize chromatin. Aliquots of the soluble chromatin fraction were separated by SDS-PAGE and the Coomassie-blue stained band containing histone H3 was cut from gel. The bands were processed twice by propionylation of free, as well as monomethylated amino groups prior trypsin digestion as adapted from Garcia et al. (2007) and Peters et al. (2003). The eluted peptides were analyzed on an Agilent 1100 nanoLC system coupled to an AB SCIEX 4000 QTRAP by LC-MRM. For unambiguous assignment of the signals two transitions per peptide were measured (see Table S4). Peak areas of both MRM transitions per peptide were integrated within Analyst 1.4.2 and averaged. Samples were normalized by using five transitions of three H3 peptides which were considered as not modified. The peak area ratios were calculated relative to the corresponding wild-type histone H3 peptides.

Lamin-DamID

Strains and Plasmid

Strains used for DamID experiments were made by using the MosSCI technique (Frøkjær-Jensen et al., 2008) leading to single-copy insertion of Dam-fusion constructs in chromosome II. Strains BN195 (*bqSi195[pBN65(unc-119(+)) hsp16.41p::dam::myc::lmn-1]* II) and BN196 (*bqSi196[pBN67(unc-119(+)) hsp16.41p::gfp::myc::dam]* II), were constructed injecting the plasmids pBN65 and pBN67, respectively, together with transformation markers (pJL43.1, pCFJ90, pCFJ104 and pBN1) in strain EG4322 (*ttT5605* II, *unc-119(ed3)* III) (Frøkjær-Jensen et al., 2008). Strains carrying the integrations were outcrossed twice with N2. Strains BN239 (*set-25(n5021) met-2(n4256) bqSi195[pBN65(unc-119(+)) hsp16.41p::dam::myc::lmn-1]* II) and BN241 (*set-25(n5021), met-2(n4256) bqSi196[pBN67(unc-119(+)) hsp16.41p::gfp::myc::dam]* II) were constructed crossing BN195 and BN196 with GW638, respectively.

Amplification of Methylated DNA

Wild-type and *set-25 met-2* strains carrying identical single-copy LMN-1-Dam or GFP-Dam constructs were grown in parallel and in three independent biological replicates. For each of the twelve cultures, 35,000 L1 larvae were grown synchronously to adults in 50 ml S-medium containing *dam*- GM119 *E. coli* strain as food source under continuous agitation (180 rpm) at 20°C for 66 hr. Embryonic progeny was harvested from adult worms by using hypochlorite treatment and genomic DNA (gDNA) was purified from 30 mg of embryos. Methylated fragments were amplified from 5 µg of gDNA by sequential DpnI / DpnII digest, adaptor ligation, and PCR by using adaptor-specific primers as described (Greil et al., 2006) with minor modifications. 1 µg of PCR product of LMN-1-Dam and GFP-Dam samples were fluorescently labeled and competitively hybridized on NimbleGen *C. elegans* whole-genome-tiling arrays (NimbleGen_Celegans_2.1M array). For each condition, a dye-swap experiment was done for one of the three replicates.

Normalization of the DamID Tiling Array Data

The probe sequences of the NimbleGen_Celegans_2.1M array were remapped to ce6 (genome.ucsc.edu) by extracting the actual probe sequences from the file 100718_Celegans180_ChIP_HX1.ndf provided by NimbleGen and mapping the probes to ce6 by using Bowtie (Langmead et al., 2009). Only uniquely mappable probes were used for the downstream analysis (97.4%). All tiling arrays were processed in R (Ihaka and Gentleman, 1996; Development core team, 2004) by using bioconductor (Gentleman et al., 2004) and the package Ringo (Toedling et al., 2007). The arrays were normalized by using the following command: `normalizeWithinArrays (RG, method = "loess")`. Due to substantial variability in the data, we smoothed the enrichment values by using a window size of 2,000 probes. All depicted genome tracks are based on this resolution.

Reanalysis of H3K9 Data from modENCODE

We downloaded ChIP-chip data for H3K9me1 (GSM562776), H3K9me2 (GSM562756) and H3K9me3 (GSM562716) from GEO (<http://www.ncbi.nlm.nih.gov/geo/>) and remapped the probe sequences extracted from GPL8647_080922_modEncode_CE_chip_HX1.ndf to ce6 by using Bowtie (Langmead et al., 2009). Enrichment values were loess normalized by using the package Ringo (Langmead et al., 2009) and smoothed based on a window size of 2,000 probes.

The DamID microarray raw data are deposited at GEO (www.ncbi.nlm.nih.gov/geo/, accession number GSE37226).

SUPPLEMENTAL REFERENCES

- Andersen, E.C., and Horvitz, H.R. (2007). Two *C. elegans* histone methyltransferases repress *lin-3* EGF transcription to inhibit vulval development. *Development* 134, 2991–2999.
- Azzaria, M., Goszczynski, B., Chung, M.A., Kalb, J.M., and McGhee, J.D. (1996). A fork head/HNF-3 homolog expressed in the pharynx and intestine of the *Caenorhabditis elegans* embryo. *Dev. Biol.* 178, 289–303.
- Bessler, J.B., Andersen, E.C., and Villeneuve, A.M. (2010). Differential localization and independent acquisition of the H3K9me2 and H3K9me3 chromatin modifications in the *Caenorhabditis elegans* adult germ line. *PLoS Genet.* 6, e1000830.
- Development Core Team (2004). R: A language and environment for statistical computing. R foundation for statistical computing (Vienna, Austria). <http://www.r-project.org>.
- Frøkjær-Jensen, C., Davis, M.W., Hopkins, C.E., Newman, B.J., Thummel, J.M., Olesen, S.-P., Grunnet, M., and Jorgensen, E.M. (2008). Single-copy insertion of transgenes in *Caenorhabditis elegans*. *Nat. Genet.* 40, 1375–1383.
- Garcia, B.A., Mollah, S., Ueberheide, B.M., Busby, S.A., Muratore, T.L., Shabanowitz, J., and Hunt, D.F. (2007). Chemical derivatization of histones for facilitated analysis by mass spectrometry. *Nat. Protoc.* 2, 933–938.
- Gentleman, R.C., Carey, V.J., Bates, D.M., Bolstad, B., Dettling, M., Dudoit, S., Ellis, B., Gautier, L., Ge, Y., Gentry, J., et al. (2004). Bioconductor: open software development for computational biology and bioinformatics. *Genome Biol.* 5, R80.
- Greil, F., Moorman, C., van Steensel, B. (2006). DamID: mapping of in vivo protein-genome interactions using tethered DNA adenine methyltransferase. *Methods Enzymol.* 410, 342–359.
- Ihaka, R., and Gentleman, R. (1996). R: A Language for Data Analysis and Graphics. *J. Comput. Graph. Statist.* 5, 299–314.
- Kamath, R.S., Fraser, A.G., Dong, Y., Poulin, G., Durbin, R., Gotta, M., Kanapin, A., Le Bot, N., Moreno, S., Sohrmann, M., et al. (2003). Systematic functional analysis of the *Caenorhabditis elegans* genome using RNAi. *Nature* 421, 231–237.
- Langmead, B., Trapnell, C., Pop, M., and Salzberg, S.L. (2009). Ultrafast and memory-efficient alignment of short DNA sequences to the human genome. *Genome Biol.* 10, R25.
- Lehner, B., Tischler, J., and Fraser, A.G. (2006). RNAi screens in *Caenorhabditis elegans* in a 96-well liquid format and their application to the systematic identification of genetic interactions. *Nat. Protoc.* 1, 1617–1620.
- Meister, P., Towbin, B.D., Pike, B.L., Ponti, A., and Gasser, S.M. (2010). The spatial dynamics of tissue-specific promoters during *C. elegans* development. *Genes Dev.* 24, 766–782.
- Peters, A.H.F.M., Kubicek, S., Mechtler, K., O'Sullivan, R.J., Derijck, A.A.H.A., Perez-Burgos, L., Kohlmaier, A., Opravil, S., Tachibana, M., Shinkai, Y., et al. (2003). Partitioning and plasticity of repressive histone methylation states in mammalian chromatin. *Mol. Cell* 12, 1577–1589.
- Tijsterman, M., May, R.C., Simmer, F., Okihara, K.L., and Plasterk, R.H.A. (2004). Genes required for systemic RNA interference in *Caenorhabditis elegans*. *Curr. Biol.* 14, 111–116.
- Toedling, J., Sklyar, O., Krueger, T., Fischer, J.J., Sperling, S., and Huber, W. (2007). Ringo—an R/Bioconductor package for analyzing ChIP-chip readouts. *BMC Bioinformatics* 8, 221.

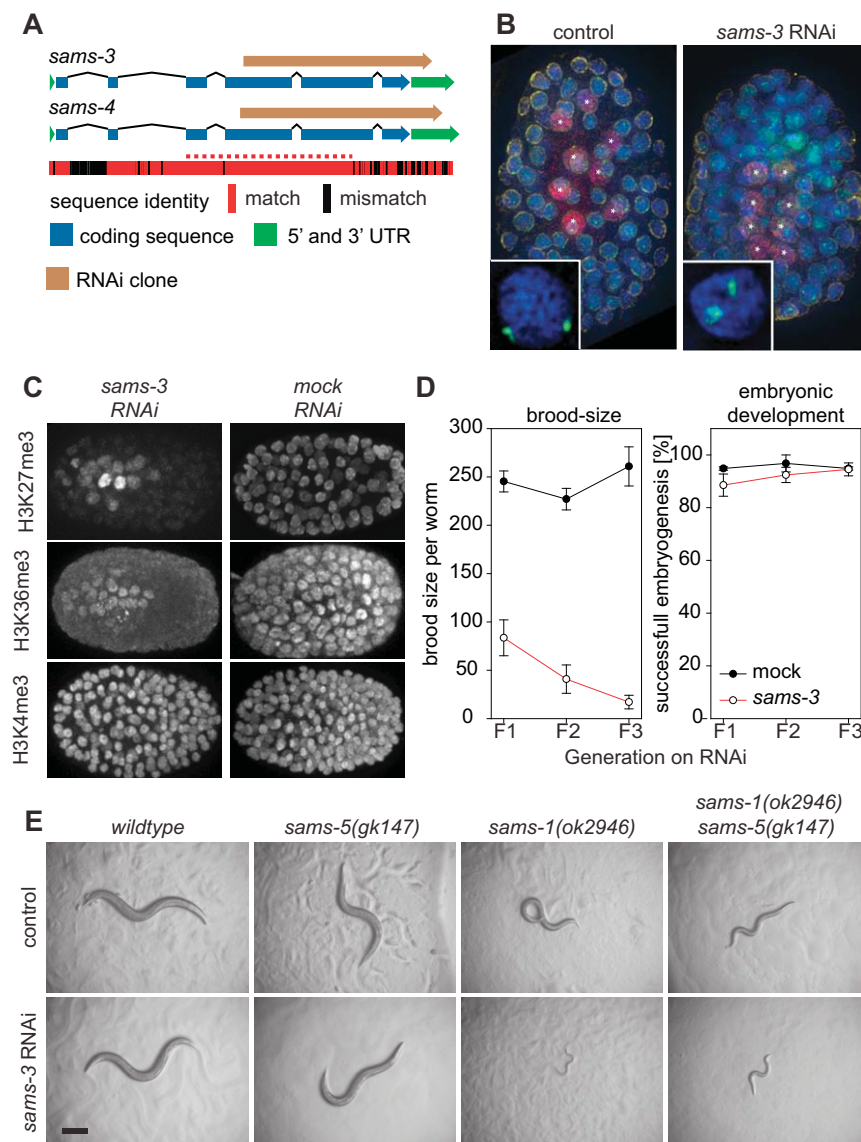


Figure S1. Redundant Function of Four *C. elegans* SAM Synthetases, Related to Figure 2

(A) Schematic drawing of *sams-3* and *sams-4* coding regions (blue), and *sams-3/4* RNAi clones (brown). Both genes and RNAi clones are highly similar (100% sequence identity over 665 nucleotides coding region, red dotted line), and are therefore both are equally downregulated by available RNAi clones that target either gene.

(B) Immunofluorescence staining for GFP-LacI (green), lamin (yellow), and LacZ (red) of strain GW471 treated with *sams-3* RNAi and control. DNA was counterstained with Hoechst (blue). The strain GW471 carries a *cal3[pha-4::LacZ; rol-6(su1006)]* gene array, and expresses GFP-LacI from an independent source to monitor transgene position. The array is found internal in the nucleus after *sams-3* RNAi, but LacZ expression remains restricted to the 8 intestinal precursor cells present at this developmental stage, in both mutant and control animals (white asterisk).

(C) Images of *sams-3* and control RNAi treated embryos stained for indicated histone methyl marks by immunofluorescence. H3K27me3 and H3K36me3, but not H3K4me3 are strongly reduced upon *sams-3* RNAi.

(D) Downregulation of *sams-3* does not increase embryonic lethality, but reduces brood-size. Wild-type worms were subjected to *sams-3* RNAi for the indicated numbers of generations (up to 3) and the number of progeny per worm and embryonic survival rate were counted at each generation. Error bars = SEM.

(E) SAMS-3 and SAMS-4 act redundantly with SAMS-1. L1 larvae of the indicated genotypes were subjected to *sams-3/4* or control RNAi and imaged after 2 days. The *sams-1* and the *sams-1/5* double mutant had a slight growth delay, but developed into fertile adults on control RNAi. In contrast to wild-type and *sams-5* mutant animals, *sams-1* and *sams-1/5* mutants arrested at larval stages on *sams-3/4* RNAi with high penetrance. Scale bar, 200 μ m.

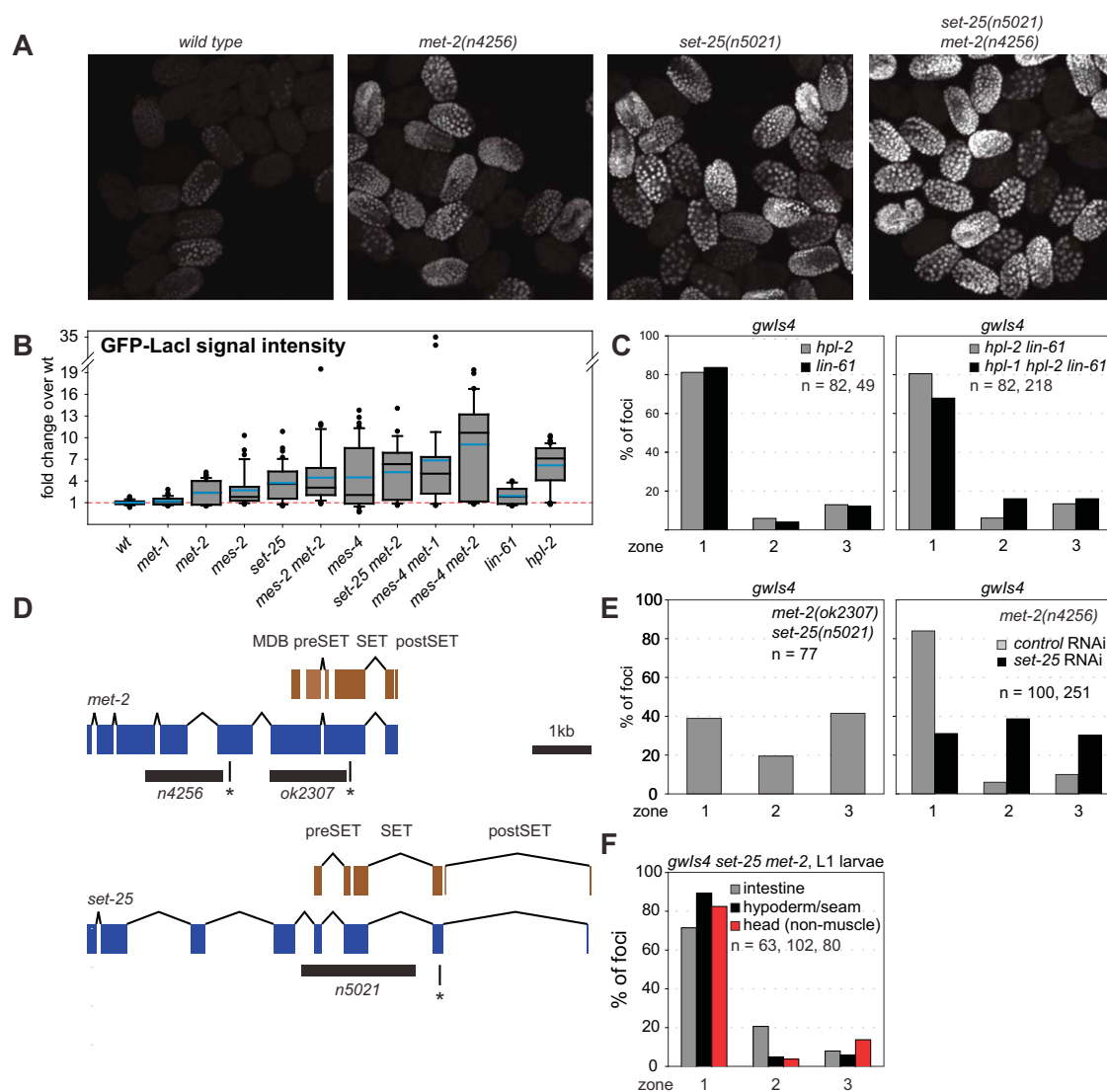


Figure S2. Array Derepression Is Not Sufficient for Array Detachment, Related to Figure 3

(A) Embryos carrying the repetitive array *gwlS4[baf-1::GFP-LacI;myo-3::RFP]* and indicated genotypes were imaged at identical exposure conditions. Shown is a maximum intensity projection of the GFP signal of 3D focal stacks of images. All panels are adjusted to identical contrast settings.

(B) Quantification of GFP intensity in embryos of indicated genotypes from images equivalent as shown in A. Whiskers: 10th and 90th percentile; black dots: outliers; black line: median; blue line: mean. See Table S2 for number of embryos scored.

(C) The H3K9me3 binding proteins LIN-61 and HPL-1/2 are not required for array anchoring. Three-zone scoring of the *gwlS4* array in 50–100 cell embryos in *lin-61* and *hpl-1/2* single, double, and triple mutants. The *gwlS4* array is strongly derepressed in the *hpl-2* mutant (see B), but remains peripheral.

(D) Schematic representation of *set-25* and *met-2* coding sequences (blue) and domain structure (brown). Deletion alleles used in this study are marked in black. All three alleles induce a frame-shift that causes a premature STOP codon shortly downstream of the deletion (asterisk).

(E) Quantification of *gwlS4* array position in *met-2(ok2307) set-25(n5021)* and *met-2(n4256) set-25(RNAi)* embryos by three-zone scoring assay as described in Figure 2.

(F) Mutation of *set-25* and *met-2* does not abolish perinuclear anchoring of the *gwlS4* array in L1 larvae. (left) L1 larvae of strain GW712 carrying the *gwlS4[baf-1::GFP-LacI;myo-3::RFP]* array, a LMN-1-GFP transgene, and the *set-25(n5021) met-2(n4256)* mutation were imaged, and array position was quantified as described in Figure 2 in indicated tissues. In contrast to embryonic cells, the array is at the nuclear periphery in differentiated tissues. Nuclei of muscle cells were excluded from this analysis, since in muscle cells the array is central independent of the genetic background, due to the presence of the muscle-specific *myo-3* promoter on the *gwlS4* array (Meister et al., 2010).

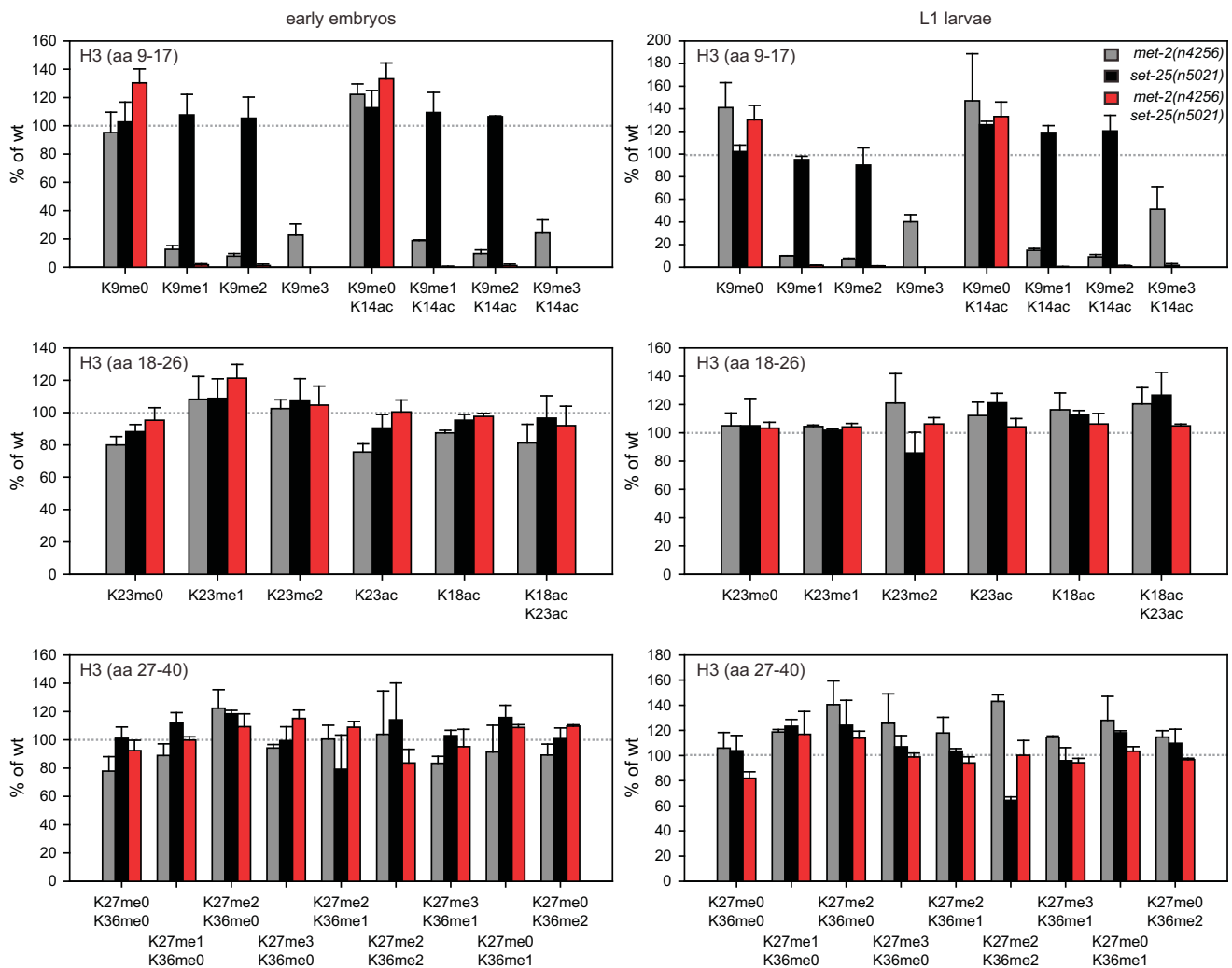


Figure S3. Mutation of *met-2* and *set-25* Strongly and Specifically Reduces Methylation of Histone H3K9 in Embryos and in L1 Larvae, Related to Figure 3

Histone H3 was extracted from early embryos and L1 larvae mutated for *met-2*, *set-25* or both genes. The abundance of the indicated peptides was measured by quantitative mass spectrometry and is shown relative to levels in wild-type extracts (gray dotted line, 100%). H3K9 methylation is strongly reduced in early embryos and L1 larvae, but no systematic changes are seen in either developmental stage for H3K23, 27, and 36. Error bars indicate the SEM in positive direction from 3 (embryos) or 2 (larvae) independent biological replica.

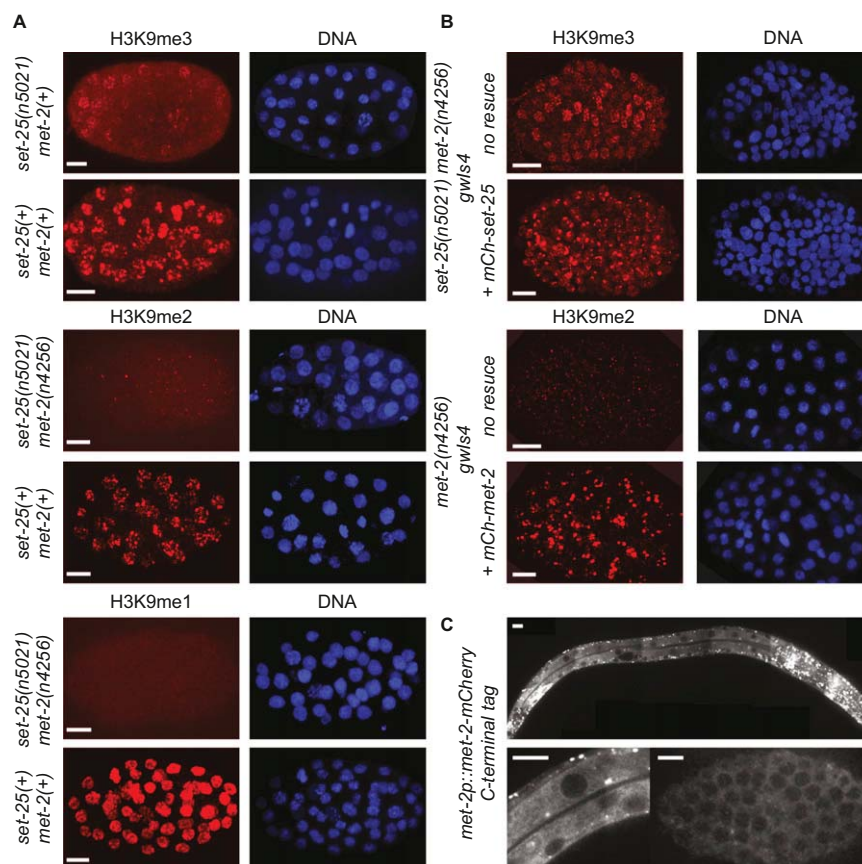


Figure S4. Validation of Antibodies and Fusion Proteins Used in This Study, Related to Figure 4

(A) Validation of H3K9me antibodies. Embryos of indicated genotypes were stained with indicated antibodies. H3K9 methylation signal was strongly reduced upon mutation of *set-25* and *met-2* demonstrating the specificity of the antibodies. The minor remaining signal for H3K9me3 in the *set-25(n5021)* mutant suggests that this antibody has a minor cross-reactivity to another modification or to unmodified histones. In agreement with previous reports (Bessler et al., 2010), H3K9me2 levels were also below detection levels in the *met-2(n4256)* single mutant (data not shown).

(B) mCh-SSET-25 and mCh-MET-2 have H3K9 methylase activity. Fusion proteins were expressed in embryos carrying the transgene array *gwl4* and the indicated deletion alleles. Both transgenes rescue the severe reduction of H3K9 methylation in the relevant mutant.

(C) MET-2-mCh localizes to the cytoplasm independent on the position of the fluorescent tag. MET-2 was C terminally tagged with mCherry and expressed under the control of its endogenous promoter. In worms as in embryos, MET-2 is localized in the cytoplasm. Top: MET-2-mCh in L1 larvae. Bottom left: magnified view of an intestinal cell. Bottom right: single focal plane of an embryo.

Scale bars, 5 μ m.

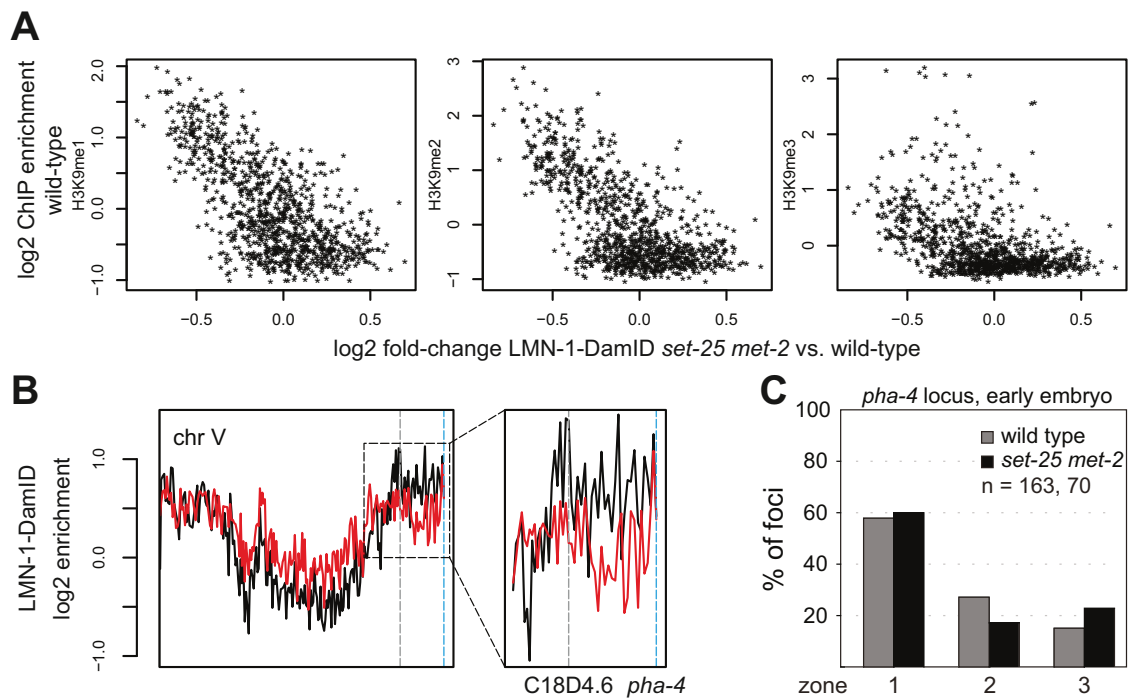


Figure S5. Reduced LMN-1 Interaction Found in Sites of High H3K9 Methylation, Related to Figure 5

(A) Changes in LMN-1-Dam methylation between wild-type and *set-25 met-2* mutant correlate with high levels of H3K9 methylation. Scatter plots of H3K9me1, me2, and, me3 against the differential of LMN-1-Dam methylation between wild-type and *set-25 met-2* mutant is shown.

(B) Magnified view of LMN-1-DamID signal on Chr V. The dotted lines mark the position of the C18D4.6 locus (gray) and the *pha-4* locus (blue).

(C) 256 *lacO* sites were integrated next to the endogenous *pha-4* locus on Chr V by transposon replacement. By expression of GFP-LacI in this strain the locus position was identified by fluorescence microscopy and quantified by three-zone scoring. Consistent with DamID data (see B) the peripheral localization of the endogenous *pha-4* locus is not affected by mutation of *set-25* and *met-2*. n = number of foci scored per condition.

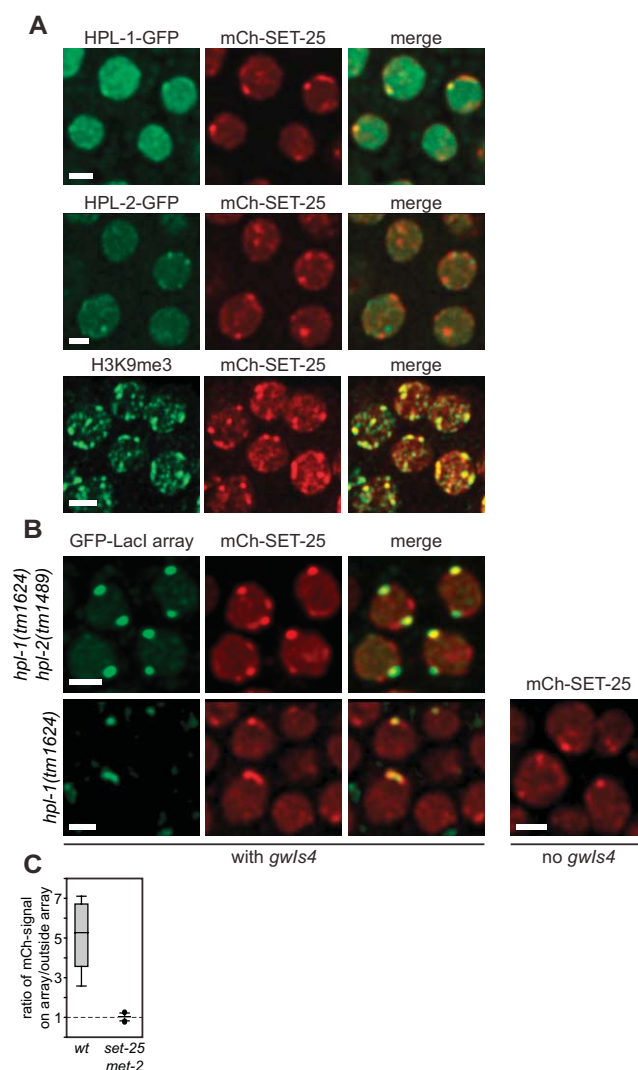


Figure S6. SET-25 Colocalizes with HPL-1, but Not HPL-2 and Associates with Arrays Independently of HPL-1/2, Related to Figure 6

(A) Representative nuclei of embryos expressing mCh-SET-25 and HPL-1/2-GFP and embryo expressing mCh-SET-25 stained for H3K9me3. Scale bar, 2 μ m. (B) mCh-SET-25 is enriched on repetitive gene arrays and in perinuclear foci in *hpl-1(tm1624)* and *hpl-1(tm1624) hpl-2(tm1489)* double mutant. Embryos with and without the repetitive transgene *gwls4* and expressing mCh-SET-25 are shown. Scale bar, 2 μ m.

(C) mCh-SET-25 Δ SET is not enriched on the *gwls4* array in a *set-25 met-2* double mutant. mCh-SET-25 levels was quantified in individual nuclei of *wild-type* and *set-25 met-2* embryos. For each nucleus, the mCherry intensity in the nuclear volume occupied by the array was measured and divided by the mCherry intensity in an equivalent region outside the array. SET-25-mCh is significantly enriched on arrays in wild-type embryos ($p < 0.001$), but not in *set-25 met-2* mutants ($p = 0.552$). Number of array foci measured: $n = 9$ (*wild-type*), 20 (*set-25 met-2*). Whiskers indicate 10th and 90th percentiles.

Table S1. Hits of Primary Screen for *let-858::GFP* Array Derepression, Related to Figure 1

Chromatin	
<i>mes-3</i>	PRC2 complex
<i>mes-6</i>	PRC2 complex
<i>mes-4</i>	NSD1 homolog
<i>set-25</i>	putative histone methyl transferase (G9a/Suv39h-like)
<i>mrg-1</i>	MRG15 homolog
<i>hpl-2</i>	HP1 homolog
<i>lin-61</i>	MBT domain protein
ZK1127.3	NuA4 complex
<i>his-37</i>	Histone H4
splicing factors	
<i>gut-2</i>	snRNP protein
<i>lsm-5</i>	snRNP protein
<i>lsm-6</i>	snRNP protein
<i>sap-1</i>	Spliceosome-associated Protein
K04G7.11	SYF2 splicing factor
metabolism	
<i>sams-3</i>	S-adenosylmethionine (SAM) synthetase
<i>sams-4</i>	S-adenosylmethionine (SAM) synthetase
other	
<i>emb-4</i>	helicase domain protein
<i>mel-46</i>	DEAD-like helicase
<i>ubl-5</i>	Ubiquitin-like family
F52C6.12	Ubiquitin-conjugating enzyme, E2
F25H5.5	Claspin homolog
Y65B4A.1	Transcription elongation factor TAT-SF1
Y57A10A.31	zinc-finger, RING type
<i>mrp-5</i>	multi drug resistance protein (ABC transporter)
<i>spe-15</i>	special myosin
<i>gsp-3</i>	Serine/threonine specific protein phosphatase
C35D10.7	unknown function
F33H1.3	unknown function
F54D10.5	unknown function

Table S2. List of HMT Mutants Tested for *gwIs4* Array Detachment, Related to Figure 3

Strain	genotype	GFP	sem	n	zone 1 [%]	n
GW76	<i>wild-type</i>	1.0	0.05	39	91	75
GW469	<i>mes-4(bn23)</i>	4.5	0.66	43	92	96
GW468	<i>mes-2(bn11)</i>	2.7	0.41	32	96	82
GW639	<i>met-2(n4256)</i>	2.4	0.24	37	83	90
GW640	<i>set-25(n5021)</i>	3.7	0.35	49	71	188
GW637	<i>set-25(n5021) met-2(n4256)</i>	5.2	0.69	29	20	181
GW650	<i>set-25(n5021) met-2(ok2307)</i>	n.d.	-	-	39	77
GW556	<i>mes-4(bn23) met-2(n4256)</i>	9.1	1.08	30	88	33
GW554	<i>mes-4(bn23) met-1(n4337)</i>	6.9	1.57	29	90	31
GW553	<i>mes-2(bn11) met-1(n4337)</i>	n.d.	n.d.	-	91	33
GW555	<i>mes-2(bn11) met-2(n4256)</i>	4.5	0.63	39	94	35
GW524	<i>met-1(n4337) met-2(n4256)</i>	n.d.	-	-	n.q.*	-
GW516	<i>met-1(n4337)</i>	1.2	0.09	35	n.q.*	-
GW631	<i>lin-61(n3809)</i>	1.9	0.17	44	84	49
GW214	<i>hpl-2(tm1489)</i>	6.2	0.40	51	81	85

GFP: mean GFP intensity

sem: standard error of the mean

zone 1 [%]: % of foci in zone 1

n: number of embryos/foci scored

n.d. not determined

n.q.* not quantified, but no detachment was apparent by gross visual inspection

Table S3. Strains Used in This Study, Related to the Experimental Procedures

Strain	genotype	Reference
N2	<i>wild-type, Bristol isolate</i>	
GW76	<i>gwls4 [baf-1::GFP-lacI::let-858; myo-3::RFP] X.</i>	(Meister et al., 2010)
NL2507	<i>pkIs1582[let-858::GFP; rol-6(su1006)]</i>	(Tijsterman et al., 2004)
GW566	<i>gwls4[myo-3::RFP; baf-1::GFP-lacI::let-858] X.; gwls39[baf-1::GFP-lacI::let-858 3'UTR; vit-5::GFP] III.</i>	this study
GW471	<i>cals3[pha-4::lacZ; rol-6(su1006)]; gwls39[baf-1::GFP-LacI::let-858 3'UTR; vit-5::GFP] III.</i>	(Meister et al., 2010)
JM50	<i>cals3[pha-4::lacZ; rol-6(su1006)]</i>	(Azzaria et al., 1996)
GW639	<i>met-2(n4256) III.; gwls4 [baf-1::GFP-lacI::let-858; myo-3::RFP] X.</i>	this study
GW640	<i>set-25(n5021) III.; gwls4 [baf-1::GFP-lacI::let-858; myo-3::RFP] X.</i>	this study
GW637	<i>set-25(n5021) III.; met-2(n4256) III.; gwls4 [baf-1::GFP-lacI::let-858 myo-3::RFP] X.</i>	this study
GW650	<i>set-25(n5021) III.; met-2(ok2307) III.; gwls4 [baf-1::GFP-lacI::let-858 myo-3::RFP] X.</i>	this study
GW516	<i>met-1(n4337) I.; gwls4 [baf-1::GFP-lacI::let-858; myo-3::RFP] X.</i>	this study
GW468	<i>mes-2(bn11) unc-4(e120)/mnC1[dpy-10(e128) unc-52(e444) II.]; gwls4[myo-3::RFP; baf-1::GFP-lacI::let-858] X.</i>	this study
GW469	<i>dpy-11(e224) mes-4(bn23) unc-76(e911)V/nT1[unc(n754) let](IV;V); gwls4[baf-1::GFP-LacI;myo-3::RFP]</i>	this study
GW553	<i>met-1(n4337) I.; mes-2(bn11) unc-4(e120)/mnC1[dpy-10(e128) unc-52(e444) II.]; gwls4 [baf-1::GFP-lacI::let858; myo-3::RFP] X.;</i>	this study
GW554	<i>dpy-11(e224) mes-4(bn23) unc-76(e911)V/nT1[unc(n754) let](IV;V); met-1(n4337);gwls4 [baf-1::GFP-lacI::let-858; myo-3::RFP] X.</i>	this study
GW555	<i>met-2(n4256) III.; mes-2(bn11) unc-4(e120)/mnC1[dpy-10(e128) unc-52(e444) II.]; gwls4 [baf-1::GFP-lacI::let-858; myo-3::RFP] X.</i>	this study
GW556	<i>dpy-11(e224) mes-4(bn23) unc-76(e911)V/nT1[unc(n754) let](IV;V); met-2(n4256) III.; gwls4 [baf-1::GFP-lacI::let-858; myo-3::RFP] X.</i>	this study
GW524	<i>met-1(n4337) I./hT2[bli-4(e937) let(q782) qIs48] (I;III); met-2(n4256) III./hT2[bli-4(e937) let(q782) qIs48] (I;III).; gwls4 [baf-1::GFP-lacI::let-858; myo-3::RFP] X.</i>	this study
GW712	<i>set-25(n5021) III.; met-2(n4256) III.; gwls4 [baf-1::GFP-lacI::let-858; myo-3::RFP] X.; ls[Imn-1::GFP-LMN-1::lmn-1]</i>	this study
GW638	<i>set-25(n5021) III.; met-2(n4256) III.</i>	this study
GW641	<i>set-25(n5021) III.</i>	this study
MT13293	<i>met-2(n4256) III.</i>	(Andersen and Horvitz, 2007)
GW694	<i>gwls85[his-72p::mcherry-set-25::his-72 3'UTR; unc-119(+)];unc-119(ed3);ttTi5605 II.</i>	this study
GW699	<i>gwls90[his-72p::mcherry-met-2::his-72 3'UTR; unc-119(+)];unc-119(ed3);ttTi5605 II.</i>	this study
GW697	<i>gwls85[his-72p::mcherry-set-25::his-72 3'UTR; unc-119(+)]; gwls4 [baf-1::GFP-lacI::let-858; myo-3::RFP] X.; unc-119(?); ttTi5605 II ?</i>	this study

GW761	<i>set-25(n5021) III.; met-2(n4256) III.; gwEx71[his-72::mcherry-set-25-c645a::his-72 3' UTR; unc-122::GFP; hpl-1::GFP]</i>	this study
GW765	<i>gwEx75[his-72::mcherry-set-25-c645a::his-72 3' UTR; unc-122::GFP; hpl-1::GFP]</i>	this study
GW756	<i>gwEx66[his-72::mcherry-set-25ΔSET::his-72 3' UTR; vit-5::GFP]; gwls4 [baf-1::GFP-lacI::let-858; myo-3::RFP] X.</i>	this study
GW759	<i>gwEx69[his-72::mcherry-set-25ΔSET::his-72 3' UTR; vit-5::GFP]; gwls4 [baf-1::GFP-lacI::let-858 myo-3::RFP] X.; set-25(n5021) III.; met-2(n4256) III.</i>	this study
GW719	<i>gwls85[his-72p::mcherry-set-25::his-72 3'UTR; cb-unc-119(+)]; unc-119(?); ttTi5605 II ?; ls[hpl-1::GFP; rol-6]</i>	this study
GW725	<i>gwls85[his-72p::mcherry-set-25::his-72 3'UTR; cb-unc-119(+)]; unc-119(?); ttTi5605 II. ?; ls[hpl-2::GFP; rol-6(su1006)]</i>	this study
GW767	<i>gwls85[his-72p::mcherry-set-25::his-72 3'UTR; unc-119(+)]; hpl-1(tm1624)X.; unc-119(?); ttTi5605 II. ?</i>	this study
GW766	<i>gwls4[myo-3::RFP; baf1::GFP-lacI::let-858] X.; gwls85[his-72p::mcherry-set-25::his-72 3'UTR; unc-119(+)]; hpl-1(tm1624)X.; unc-119(?); ttTi5605 II. ?</i>	this study
VC2428	<i>sams-1(ok2946) X.</i>	obtained from CGC
VC239	<i>sams-5(gk147) IV.</i>	obtained from CGC
GW642	<i>sams-1(ok2946) X.; sams-5(gk147) IV.</i>	this study
BN195	<i>bqSi195[pBN65(unc-119(+); hsp16.41p::dam::myc::lmn-1)] II.</i>	this study
BN196	<i>bqSi196[pBN67(unc-119(+); hsp16.41p::gfp::myc::dam)] II.</i>	this study
BN239	<i>set-25(n5021)III; met-2(n4256) bqSi195[pBN65(unc-119(+); hsp16.41p::dam::myc::lmn-1)] II.</i>	this study
BN241	<i>set-25(n5021)III; met-2(n4256) bqSi196[pBN67(unc-119(+); hsp16.41p::gfp::myc::dam)]II.</i>	this study

Alleles marked with a question mark (?) were not genotyped after genetic crosses.

Table S3 References

- Andersen, E.C., and Horvitz, H.R. (2007). Two *C. elegans* histone methyltransferases repress lin-3 EGF transcription to inhibit vulval development. *Development* 134, 2991–2999.
- Azzaria, M., Goszczynski, B., Chung, M.A., Kalb, J.M., and McGhee, J.D. (1996). A fork head/HNF-3 homolog expressed in the pharynx and intestine of the *Caenorhabditis elegans* embryo. *Dev. Biol.* 178, 289–303.
- Meister, P., Towbin, B.D., Pike, B.L., Ponti, A., and Gasser, S.M. (2010). The spatial dynamics of tissue-specific promoters during *C. elegans* development. *Genes Dev.* 24, 766–782.
- Tijsterman, M., May, R.C., Simmer, F., Okihara, K.L., and Plasterk, R.H.A. (2004). Genes required for systemic RNA interference in *Caenorhabditis elegans*. *Curr. Biol.* 14, 111–116.

Table S4. MRM Transition List for Selected, Differently Methylated Histone H3 Peptides,
Related to Figure 3

Sequence	Modification		Precursor m/z	Fragment m/z	Fragment ion	CE V
Peptide H3(9-17)						
KSTGGKAPR			535.3	241.2	b1+	33.3
KSTGGKAPR			535.3	829.5	y8+	33.3
KSTGGKAPR	K9me1		542.3	255.2	b1+	33.6
KSTGGKAPR	K9me1		542.3	829.5	y8+	33.6
KSTGGKAPR	K9me2		521.3	829.5	y8+	32.6
KSTGGKAPR	K9me2		521.3	770.4	b7+	32.6
KSTGGKAPR	K9me3		528.3	784.5	b7+	32.9
KSTGGKAPR	K9me3		528.3	641.3	y6+	32.9
Peptide H3(18-26)						
KQLATKAAR			577.9	914.5	y8+	35.4
KQLATKAAR			577.9	241.2	b1+	35.4
KQLATKAAR		K23me1	584.9	928.6	y8+	35.7
KQLATKAAR		K23me1	584.9	241.2	b1+	35.7
KQLATKAAR		K23me2	563.9	886.5	y8+	34.7
KQLATKAAR		K23me2	563.9	241.2	b1+	34.7
KQLATKAAR		K23ac	570.8	900.6	y8+	35.0
KQLATKAAR		K23ac	570.8	241.2	b1+	35.0
KQLATKAAR	K18ac		570.9	914.5	y8+	35.0
KQLATKAAR	K18ac		570.9	227.1	b1+	35.0
KQLATKAAR	K18ac	K23ac	563.8	900.6	y8+	34.7
KQLATKAAR	K18ac	K23ac	563.8	227.1	b1+	34.7
Peptide H3(27-40)						
KSAPASGGVKKPHR			822.5	623.4	y11++	47.6
KSAPASGGVKKPHR			822.5	702.4	y13++	47.6
KSAPASGGVKKPHR	K27me1		829.5	702.4	y11++	48.0
KSAPASGGVKKPHR	K27me1		829.5	623.4	y13++	48.0
KSAPASGGVKKPHR	K27me2		539.3	409.2	y3+	28.2
KSAPASGGVKKPHR	K27me2		539.3	777.5	y5+	28.2
KSAPASGGVKKPHR	K27me3		544.0	409.2	y3+	28.4
KSAPASGGVKKPHR	K27me3		544.0	777.5	y5+	28.4
KSAPASGGVKKPHR	K27me2	K36me1	544.0	371.2	b3+	28.4
KSAPASGGVKKPHR	K27me2	K36me1	544.0	409.2	y3+	28.4
KSAPASGGVKKPHR	K27me2	K36me2	530.0	371.2	b3+	27.8
KSAPASGGVKKPHR	K27me2	K36me2	530.0	609.4	y11++	27.8
KSAPASGGVKKPHR	K27me3	K36me1	548.7	409.2	y3+	28.6
KSAPASGGVKKPHR	K27me3	K36me1	548.7	791.5	y5+	28.6
KSAPASGGVKKPHR		K36me1	829.5	709.4	y13++	48.0

KSAPASGGVKKPHR	K36me1	829.5	630.4	y11++	48.0
KSAPASGGVKKPHR	K36me2	539.3	609.4	y11++	28.2
KSAPASGGVKKPHR	K36me2	539.3	688.4	y13++	28.2

For normalization

EIAQDFKTDLR	H3(73-83)	724.4	288.2	y2	42.7
EIAQDFKTDLR	H3(73-83)	724.4	950.5	y7+	42.7
YQKSTELLIR	H3(54-63)	681.9	832	y7+	40.6
YQKSTELLIR	H3(54-63)	681.9	744.9	y6+	40.6
YRPGTVALR	H3(41-49)	544.3	713.4	y7+	33.7

Chapter 5: Concluding remarks and future prospects

In this thesis I have investigated mechanisms that generate the spatial organization of the genome and the dynamics of chromatin organization during development. Using transgene-based reporters in *C. elegans*, we characterized *cis*, as well as *trans* acting factors required for the recruitment of chromatin to the nuclear envelope. Importantly, we could confirm that our findings based on transgenes were relevant for endogenous loci, using FISH and DamID methods. Two major conclusions can be drawn from this study:

i. Subnuclear chromatin organization is subject to developmental control

In several instances we found pronounced differences in the subnuclear organization of chromatin between embryonic and differentiated tissues. Namely, there was no specific subnuclear position apparent for transgenes carrying developmentally regulated promoters when present in low copy number (<50 copies) in embryos up to the 50-100 cell stage. In contrast, we observed a pronounced non-random organization for the same transgene insertions in differentiated cell types of first larval stage worms. Transgenes carrying tissue specific promoters were localized to the nuclear periphery in cells where the promoters were silent, but were positioned internally when active (Meister et al., 2011; Towbin et al., 2011).

The molecular mechanisms underlying these differences between embryonic and differentiated tissues remain unclear. Given that repetitive promoter arrays with larger copy number (>250 copies) were positioned peripherally in embryos as well as in larvae, the nuclear envelope appears to contain all the components required to bind chromatin throughout development. This suggests that changes in chromatin status, rather than in the composition of the nuclear envelope control the developmentally regulated remodeling of gene position.

Interestingly, chromatin has been described to be more dynamic in human and mouse embryonic stem (ES) cells than in differentiated tissues (reviewed in Gaspar-Maia et al., 2011). Chromatin associated proteins, such as HP1 have lower residence times in ES cells than differentiated neuronal lineages (Meshorer et al., 2006), and dense staining heterochromatic structures are less pronounced in ES cells (Efroni et al., 2008). These characteristics of ES cells are hypothesized to contribute to their pluripotency (Gaspar-Maia et al., 2011). The lower spatial constraints of chromatin positioning that we observed in early *C. elegans* embryos may functionally relate to the more dynamic chromatin state in ES cells. If so, this system would offer an experimental tool to address the functional relationship between large-scale chromatin characteristics and cell fate potential.

ii. Two enzymes that deposit H3K9 methylation are required to maintain perinuclear chromatin anchoring in C. elegans embryos

Our studies revealed a role for two SET domain proteins, MET-2 and SET-25, in perinuclear chromatin anchoring. We provide evidence that the two enzymes act consecutively, depositing H3K9me1/2 and H3K9me3 in a step-wise manner. MET-2 appears able to deposit only the former and does not catalyze H3K9 tri-methylation. In contrast, SET-25 can carry out all three modifications, albeit at low efficiency. Importantly, H3K9 tri-methylation by SET-25 is greatly enhanced when H3K9me1/2 is provided by MET-2.

In embryos lacking both enzymes, no H3K9 methylation is detectable by mass spectroscopy and repetitive transgene arrays, as well as repeat-rich chromosome arms are displaced from the nuclear periphery. Although this finding implies causality between the action of MET-2 and SET-25 and subnuclear chromatin organization, we cannot entirely exclude that substrates other than H3K9 methylation are involved. However, correlative data strongly supports the simplest model where H3K9 methylation targets chromatin to the nuclear envelope.

In agreement with a function of H3K9 methylation in perinuclear chromatin targeting, we show an enrichment of this mark at the nuclear periphery by immuno-fluorescent staining. Similarly, using genome-wide ChIP assays, it was shown that H3K9 methylation strongly correlates with nuclear envelope association (Ikegami et al., 2010; Liu et al., 2011), which predominantly occurs on repeat-rich chromosome arms. We confirm this data by DamID and show that H3K9 methylated regions are enriched for contacts with the nuclear lamin protein LMN-1. Importantly, lamin association was compromised in strains lacking MET-2 and SET-25 and the reduction in LMN-1 contacts was most pronounced in regions that normally carry high levels of H3K9 methylation under wild-type conditions. Finally, we find that SET-25 is strongly enriched in H3K9me3 foci at the nuclear periphery, indicating that histones are its major target.

Formally excluding a role for other potential SET-25 targets would require mutating K9 on H3, an experiment that is technically not feasible given the many genomic copies of histone genes in *C. elegans*. Instead, we are currently screening for additional genetic mutants with perturbed perinuclear chromatin anchoring. Our initial efforts suggest an important role for a previously uncharacterized protein with a chromodomain and homology to mammalian H3K9me binding proteins (data not shown). Characterization of this protein will undoubtedly reveal important insights into the mechanism of perinuclear chromatin anchoring. Moreover, single point mutations that specifically disrupt H3K9me binding of this protein will allow us to evaluate our proposal of a direct function for this modification in chromatin anchoring.

Future directions

An important question that is not answered in this thesis concerns the functional implications of perinuclear chromatin anchoring on gene regulation and development. Intriguingly, *set-25 met-2* double mutants are viable and display only minor phenotypes, even though they lack all detectable H3K9 methylation and have severely impaired subnuclear chromatin organization. Should one conclude that subnuclear chromatin organization and H3K9me have no or little biological relevance? Given the conservation of perinuclear chromatin localization from yeast (Steglich et al., 2012; Taddei et al., 2010) to man (Guelen et al., 2008) this seems unlikely. Instead, a selective fitness advantage resulting from subnuclear chromatin organization may not be apparent under laboratory conditions. Alternatively, the peripheral localization of chromatin may act redundantly with other pathways of gene regulation. Existing data provides evidence for both of these possibilities. In a search for subtle phenotypes of the *set-25 met-2* mutant, we found that DNA transposons are desilenced in the absence of H3K9 methylation. Furthermore, transcriptome data shows a marked upregulation of genes located on the X-chromosome in *set-25 met-2* double mutants and we also detect a slightly elevated number of males, which is indicative of defects in chromosome segregation (data not shown). Arguing for redundant functions of H3K9me with other pathways, mutation of *met-2* in a sensitized background causes ectopic vulva formation (Andersen and Horvitz, 2007). Synthetic RNAi screens may be used to identify genetic interactors of *met-2* and *set-25*. These may characterize pathways that function redundantly with H3K9 methylation and reveal developmental functions of subnuclear chromatin organization.

More generally, the genetic toolbox offered by the experimental system described here may be applied to study numerous important questions on the role of nuclear organization in gene regulation. A particularly attractive focus concerns the emerging post-mitotic functions of cohesin in guiding chromatin architecture. Cohesin depletion experiments are typically difficult to design, due to the dual function of this complex in S-phase and G1. Since all somatic cells of adult worms are post-mitotic, this issue is alleviated in *C. elegans*. Moreover, available temperature sensitive alleles offer simple tools for time resolved cohesin inactivation (Baudrimont et al., 2011).

Conversely, it will be interesting to study the importance of chromatin attachment to nuclear landmarks, such as the nuclear lamina, on global chromatin folding. The mutants described here, as well as direct depletion of nuclear landmark proteins offer simple means of genetic interference.

Although never applied in the worm, there is no apparent reason why chromosome conformation capture methods should not be applicable to *C. elegans*. The comparatively small size of the worm genome may even facilitate data analysis and allow one to map DNA contacts at a higher resolution than is possible in mammalian systems. An important technical obstacle, however, will be the large scale purification of material from a single tissue.

In brief, this thesis has validated the importance of histone modification in the subnuclear positioning of chromatin in *C. elegans*. Moreover, it has established a robust genetic system which will provide powerful means for further assessment of the function of subnuclear chromatin organization in gene regulation and the molecular machinery involved. Still unclear is to what extent the higher-order organization of genes contributes to the determination of cell fate. The interplay between developmental gene expression, chromatin modifications, chromatin folding, and gene attachment to nuclear landmarks remains a challenge, for which *C. elegans* has been shown to be a powerful model system.

References

- Andersen, E.C., and Horvitz, H.R. (2007). Two *C. elegans* histone methyltransferases repress *lin-3* EGF transcription to inhibit vulval development. *Development* 134, 2991-2999.
- Baudrimont, A., Penkner, A., Woglar, A., Mammun, Y.M., Hulek, M., Struck, C., Schnabel, R., Loidl, J., and Jantsch, V. (2011). A New Thermosensitive *smc-3* Allele Reveals Involvement of Cohesin in Homologous Recombination in *C. elegans*. *PLoS ONE* 6, e24799.
- Efroni, S., Duttagupta, R., Cheng, J., Dehghani, H., Hoepfner, D.J., Dash, C., Bazett-Jones, D.P., Le Grice, S., McKay, R.D.G., Buetow, K.H., *et al.* (2008). Global Transcription in Pluripotent Embryonic Stem Cells. *Cell Stem Cell* 2, 437-447.
- Gaspar-Maia, A., Alajem, A., Meshorer, E., and Ramalho-Santos, M. (2011). Open chromatin in pluripotency and reprogramming. *Nat Rev Mol Cell Biol* 12, 36-47.
- Guelen, L., Pagie, L., Brasset, E., Meuleman, W., Faza, M.B., Talhout, W., Eussen, B.H., de Klein, A., Wessels, L., de Laat, W., *et al.* (2008). Domain organization of human chromosomes revealed by mapping of nuclear lamina interactions. *Nature* 453, 948-951.
- Ikegami, K., Egelhofer, T., Strome, S., and Lieb, J. (2010). *Caenorhabditis elegans* chromosome arms are anchored to the nuclear membrane via discontinuous association with LEM-2. *Genome Biology* 11, R120.
- Liu, T., Rechtsteiner, A., Egelhofer, T.A., Vielle, A., Latorre, I., Cheung, M.-S., Ercan, S., Ikegami, K., Jensen, M., Kolasinska-Zwierz, P., *et al.* (2011). Broad chromosomal domains of histone modification patterns in *C. elegans*. *Genome Research* 21, 227-236.
- Meister, P., Mango, S.E., and Gasser, S.M. (2011). Locking the genome: nuclear organization and cell fate. *Current Opinion in Genetics & Development* 21, 167-174.
- Meshorer, E., Yellajoshula, D., George, E., Scambler, P.J., Brown, D.T., and Misteli, T. (2006). Hyperdynamic Plasticity of Chromatin Proteins in Pluripotent Embryonic Stem Cells. *Developmental Cell* 10, 105-116.
- Steglich, B., Filion, G., van Steensel, B., and Ekwall, K. (2012). The inner nuclear membrane proteins Man1 and Ima1 link to two different types of chromatin at the nuclear periphery in *S. pombe*. *Nucleus* 3.
- Taddei, A., Schober, H., and Gasser, S.M. (2010). The Budding Yeast Nucleus. *Cold Spring Harbor Perspectives in Biology* 2.
- Towbin, B.D., Meister, P., Pike, B.L., and Gasser, S.M. (2011). Repetitive Transgenes in *C. elegans* Accumulate Heterochromatic Marks and Are Sequestered at the Nuclear Envelope in a Copy-Number- and Lamin-Dependent Manner. *Cold Spring Harbor Symposia on Quantitative Biology*.

List of abbreviations

3C	Chromosome Conformation Capture
4C	Chromosome Conformation Capture on Chip
5C	Chromosome Conformation Capture Carbon Copy
ac	acetylation
ChIA-PET	Chromatin Interaction Analysis using Paired End Tag sequencing
ChIP	chromatin immunoprecipitation
CT	chromosome territory
CTCF	CCCTC-binding factor
DamID	DNA adenine methyltransferase identification
DNA	deoxyribonucleic acid
ES cells	embryonic stem cells
FISH	fluorescence <i>in situ</i> hybridization
HMT	histone methyltransferase
HP1	heterochromatin protein 1
HxKx	lysine residue at position x on histone x
INM	inner nuclear membrane
Jmj	Jumonji
KDM	lysine demethylase
LAD	lamin associated domain
LAP2	lamin associated protein 2
LBR	lamin B receptor
MBT	malignant brain tumor
me (1,2,3)	methylation (mono-, di-, tri-)
NPC	nuclear pore complex
PHD	plant homeo domain
PRC	polycomb repressive complex
PTM	posttranslational modification
RNA	ribonucleic acid
SAM	S-adenosylmethionine
SAMS	S-adenosylmethionine synthetase
TF	transcription factor

Acknowledgements

I am grateful to Susan Gasser for mentoring and continuous support, as well as to Dirk Schübeler and Peter Askjaer for helpful discussions during and outside of thesis committee meetings. Special thanks also go to Peter Meister for sharing and teaching his enthusiasm on science and microscopy, as well as extensive experimental training and helpful discussions.

During the course of this thesis I have learnt to appreciate the importance of a highly communicative and supportive lab atmosphere. I am thankful to Susan Gasser for her great efforts to maintain this state within and across generations of students and post-doc. Similarly, I thank Monika Tsai and Razel Arpagaus for organizing the laboratory in a way that avoids conflicts on shared reagents and equipment and fosters a productive communication among lab members.

Important insights and technical help came from numerous lab members. In particular, I would like to thank Véronique Kalck and Monique Thomas for help with experiments and worm maintenance, Leslie Hoerner for microarray hybridization, Helder Ferreira for help in proof-reading numerous abstracts and conference applications, as well as this thesis, Stephanie Kueng for critical evaluation of faulty conclusions, Mariano Oppikofer for help with protein purification and Lutz Gehlen for support in theoretical and statistical questions.

Research at FMI is greatly supported by the enormous efforts of the technical platforms. Among them, special thanks go to Laurent Gelman for coordination and continuous maintenance of the microscopy facility together with Steven Bourke. I am also thankful to Aaron Ponti and Patrick Schwarb for help with image analysis and Iskra Katic for support in *C. elegans* transgenesis. Similarly, Ragna Sack, Tim Roloff and Dimos Gaidatzis from mass-spec and genomics/computational biology were instrumental for this thesis.

Finally, I am thankful to Peter Askjaer and Cristina Gonzalez, as well as Yosef Gruenbaum and Anna Mattout for fruitful and enjoyable research collaboration.

Acknowledgements to family and friends outside the scientific community are equally appropriate, but will be communicated elsewhere.

Curriculum Vitae

Home address

Jungstrasse 2
CH-4056 Basel
Switzerland

Tel.: +41 61 69 75583
Nationality: Swiss

Institute address

Friedrich Miescher Institute for Biomedical Research
Maulbeerstrasse 66
CH-4058 Basel
Switzerland

Date of birth: 7 September 1982
email: benjamin.towbin@fmi.ch

Research experience and education

Since Dec 2007 **PhD studies at the Friedlicher Miescher Institute (FMI), Basel (CH)**

Project title: Step-wise methylation of histone H3K9 positions heterochromatin at the nuclear envelope in *C. elegans* embryos

Supervisor: Prof. Dr. Susan Gasser.

Repressed and active genes are spatially separated within the nucleus. Silent heterochromatin is located peripherally, whereas active loci reside in the nuclear center. In this project we aimed at identifying factors that are involved in the repression and perinuclear sequestration of heterochromatin. To this end, I have setup a genome-wide RNAi screen using a GFP reporter system, which has identified the H3K9 methylation pathway to be involved.

2005-2007 **Masters in Cancer genomics and Developmental Biology at the University of Utrecht (NL)**

final grade: 8.9 (scale: 1-10), GPA: 4.00, top 5%

Project 1 (9 months): Silencing of Tc1 DNA transposons in somatic cells of *C. elegans* requires the polymerase β nucleotidyl transferase RDE-3

Supervisor: Prof. Dr. R. Plasterk/ Dr. M. Tijsterman

Project 2 (5 months): The efficiency of DNA double strand break repair by homologous recombination is limited by recombination template concentration in budding yeast.

Supervisor: Prof. Dr. S. Gasser/Dr. H. Van Attikum

2002 - 2005 **Bachelor in Molecular Biology at the University of Basel (CH)**

final grade: 5.9 (scale: 1-6)

2001 - 2002 Internships in Molecular Biology laboratories at the University of California Davis (3 months, Supervisor: Prof. Dr. Paul FitzGerald) and at the FMI (5 months, Supervisor: Dr. Ruth Chiquet)

First author publications

Step-wise methylation of histone H3K9 positions heterochromatin at the nuclear envelope in *C. elegans* embryos, Towbin BD, Gonzalez C, Meister P, Gaidatzis D, Kalck V, Sack R, Askjaer P, Gasser SM, *under revision at Cell*

Repetitive transgenes in *C. elegans* accumulate heterochromatic marks and are sequestered at the nuclear envelope in a copy-number- and lamin-dependent manner, Towbin BD, Meister P, Pike BL, Gasser SM., *Cold Spring Harb Symp Quant Biol.* 2010;75:555-65. (conference paper)

The nuclear envelope - a scaffold for silencing? Towbin BD, Meister P, Gasser SM., *Curr Opin Genet Dev.* 2009 Apr;19(2):180-6. (review)

Co-author publications

The spatial dynamics of tissue-specific promoters during *C. elegans* development, Meister P, Towbin BD, Pike BL, Ponti A, Gasser SM, *Genes Dev.* 2010 Apr 15;24(8):766-82.

An EDMD mutation in *C. elegans* lamin blocks muscle-specific gene relocation and compromises muscle integrity, Mattout A, Pike BL, Towbin BD, Bank EM, Gonzalez-Sandoval A, Stadler MB, Meister P, Gruenbaum Y, Gasser SM, *Curr Biol.* 2011 Oct 11;21(19):1603-14

Talks at conferences and workshops

1. Heterochromatin anchoring at the nuclear envelope: a role for H3K9 methylation, Towbin BD, Gonzalez C, Meister P, Gaidatzis D, Kalck V, Sack R, Gasser SM, InteGeR Workshop Nuclear Structure and Gene Expression in Utrecht, NL (invited speaker)
2. Tethering of heterochromatin at the nuclear envelope requires step-wise methylation of histone H3K9 in *C. elegans* embryos, Towbin BD, Meister P, Kalck V, Sack R, Gasser SM, EMBO conference on Nuclear Structure and Dynamics in L'Isle sur la Sorgue (selected talk)
3. Stepwise assembly of perinuclear heterochromatin by H3K9 methylation, Towbin BD, Meister P, Gasser SM, EMBO Workshop on Chromatin structure, organization and dynamics in Prague (selected talk)
4. A genome-wide screen for factors required for perinuclear heterochromatin anchoring in *C. elegans*, Towbin BD, Meister P, Gasser SM, 6th course on epigenetics 2010, Institut Curie, Paris (selected talk)
5. Differentiation associated spatial separation of active and silent loci, Towbin BD, Meister P, Pike BL, Gasser SM, International worm meeting 2009, Los Angeles (selected talk)